Technoeconomic Analysis of Air Based Solar Assisted Heat Pump Water Heaters for Canadian and American Cities

by

Calene Treichel

A thesis submitted to the Faculty of Graduate and Postdoctoral Affairs in partial fulfillment of the requirements for the degree of

Master of Applied Science

in

Sustainable Energy Engineering and Policy

Carleton University

Ottawa, Ontario

Abstract

Heat pump water heaters (HPWHs) have limited market share in Canada and the United States largely due to their space cooling effect which increases heating costs throughout winters in these countries. Coupling a HPWH with solar collectors lessens the space cooling effect during cold-climate heating seasons while also improving HPWH performance year-round in cold and moderate climates. This study experimentally and numerically examined air-based solar collectors and their impact on HPWHs with the objective of determining the feasibility of solar assisted HPWHs in residential detached dwellings in Canada and the United States. An air-based solar collector was added to an experimentally validated HPWH model, and different configurations of solar-assisted HPWH (SAHPWH) were analyzed to determine their energy performance, greenhouse gas emissions (GHGs), and various economic parameters. The results indicate that the space cooling effect of HPWHs can be mitigated by coupling the HPWH with a solar collector in all configurations studied. The three configurations of SAHPWHs were analyzed to minimize water heating electricity consumption for each Canadian and American city, and a correlation was found between climate zone and the configuration with minimum electricity consumption. The maximum electricity reductions from an electric water to a SAHPWH were realized near the Canada and US border, and with a 5% transition to SAHPWHs, Canadian residential energy for water heating can be decreased by 3.1%. The HPWHs and SAHPWHs were compared against electric water heaters (EWHs) and natural gas water heaters (NGWHs). The greatest GHG reductions were found to occur in locations

with clean electricity grids for a NGWH to HPWH or SAHPWH transition, and in locations with fossil fuel dominant grids for an EWH to HPWH or SAHPWH transition. In the economic analysis, the payback period (PBP) was found to be correlated to climate zone; in colder climate locations there were greater benefits from reducing the space cooling caused by HPWHs, so the SAHPWH had the lowest PBP and in warmer locations which benefitted from space cooling throughout more of the year, the HPWH had the lowest PBP. When comparing a HPWH or SAHPWH to a NGWH, the low cost of natural gas caused the HPWH and SAHPWH to have long PBPs that were greater than the predicted lifetime in many locations. Subsidies which could be implemented by governments to increase the economic viability of HPWH and SAHPWHs were also considered and were found to significantly decrease when a price was put on the GHGs emitted by a NGWH.

Acknowledgements

I would like to thank my supervisor, Cynthia Cruickshank, for her continued support and guidance throughout this project.

I would like to acknowledge my colleagues in the Solar Energy Systems Laboratory for their encouragement, friendship, and discussion throughout this research. This includes Brock Conley, Chris Baldwin, Chris Campbell, Jordan McNally, Tyler Ulmer, Kayla Lewry, Belal Daouk, and Ben Beauchamp.

I would like to acknowledge the generous financial support provided by the National Science and Engineering Research Council (NSERC) and the Canadian Federation for Innovation (CFI). This research could not have been done without these contributions.

I would finally like to thank my family and my partner Jeffrey Baylis for the unceasing love, support, and reassurance they have given me.

Table of Contents

List of Figures

List of Tables

Abbreviations

COP	Coefficient of performance
DHW	Domestic hot water
EF	Energy factor
GHGs	Greenhouse gas emissions ($kgCO_2e$)
HPWH	Heat pump water heater
LCC	Lifecycle cost ($)
PBP	Payback period (years)
SAHPWH	Solar assisted heat pump water heater
UEF	Uniform energy factor

Nomenclature

A_c	Cross sectional area (m^2)
A_s	Surface area (m^2)
c	Fuel cost for conditioning system ($/kWh)
C	Capital cost of a water heating system including installation ($)
C_{BE}	Breakeven capital cost of a water heating system ($)
CJC	Cold junction compensation temperature (°C)
C_p	Specific heat capacity (kJ/kgK)
CP	Carbon price ($/kg$CO_2$e)
d	Discount rate
E	Energy (kJ)
GHG_{offset}	Greenhouse gas emissions offset (kgCO_2e)
h	Enthalpy (kJ/kg)
HR	Heat rejection to storage tank (kJ/h or W)
i	Inflation rate
I	GHG intensity (kgCO_2e/kWh)
k	Thermal conductivity (W/mK)
$\dot{m}$	Mass flow rate (kg/h)
m	Mass (kg)
M	Annual water heater maintenance costs ($)

n	Lifetime (years)
N	Number of samples
p	Pressure (kPa)
P	Power (kJ/h or W)
ρ	Density (kg/m^3)
Q	Heat transfer rate from air (kJ/h or W)
r	Interest rate
R	Leakage rate of refrigerant (%/year)
s_{x}	Standard deviation
$s_{\bar{\mathrm{x}}}$	Standard deviation of the means
S	Impact of HPWH on space conditioning system (kJ or kWh)
t	Time (h)
$t_{\nu,95\%}$	Coverage factor with 95% confidence interval
T	Temperature (°C or K)
u	Uncertainty
U	Heat loss coefficient (W/m^{2}K)
V	Volume (L or m^3)
V	Voltage (V)
ν	Degrees of freedom
x	Experimental sample value
$\bar{x}$	Sample mean value
Δx	Distance (m)

X	Total annual operating cost of a water heater, including space heating and cooling impacts ($)
W	Water heating energy cost ($)
ω	Humidity ratio ($kg_{water}/kg_{dry\ air}$)
η	Efficiency of a system

Subscripts

air	Applies to air
atm	Atmospheric
bias	Bias uncertainty
compressor	Applies to compressor of HPWH system
cooling	Space cooling
CS	Cooling season
dp	Dewpoint
delivered	Delivery to water storage tank
element	Applies to element of HPWH system
fuel	Applies to a fuel source
heating	Space heating
HPWH	Applies to HPWH system
HS	Heating season
i	Storage tank node i
$i + 1$	Storage tank node above node i
$i - 1$	Storage tank node below node i
in	Inlet condition
out	Outlet condition
prec	Precision uncertainty

PV	Present value
r	Applies to HPWH refrigerant
ref	Reference value
sat	At saturation
sens	Sensible heat transfer
system	Applies to alternative water heating system
t	Value at timestep t
$t-1$	Value at previous timestep
total	Total of all values
vapour	Applies to water vapour

Chapter 1: Introduction

The motivation, relevant background information, and objectives for this research are described in this chapter. This includes a description of the existing landscape of water heating within Canada, the importance of decarbonizing the residential water heating sector, and potential technological and policy options available to achieve this.

1.1 Motivation

In Canada, 8786 PJ of secondary energy was consumed in 2016. As Figure 1.1 illustrates, 17% of this energy was attributed to the residential sector [1]. Energy consumed by the residential sector is largely used for space heating and domestic hot water (DHW), both of which are dominated by natural gas-burning technologies. As such, a significant reduction in national fossil fuel consumption can be achieved via cleaner technologies for space and water heating in the residential sector.

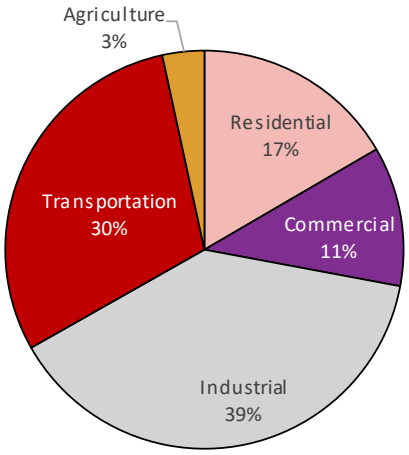

Figure 1.1: Breakdown of energy end uses in Canada

The energy consumed by the residential sector contributes approximately 61.1 Mt of CO_2e to the atmosphere annually [1]. By lowering the energy consumption of water heating

technologies and shifting the fuel used for water heating away from natural gas to electricity-driven heat pump water heaters (HPWHs), this number could be significantly reduced. This reduction in greenhouse gases will allow Canada to work towards climate change mitigation in alignment with Paris Agreement goals [2].

1.2 Background

Water heating accounts for almost 19% of secondary residential energy use in Canada, as shown in Figure 1.2. Although water heating consumes 19% of the residential energy, it produces 21% of the residential greenhouse gas emissions (GHGs). The high percentage of GHGs from water heaters is indicative of the dependence on natural gas for water heating, as Figure 1.2 also illustrates.

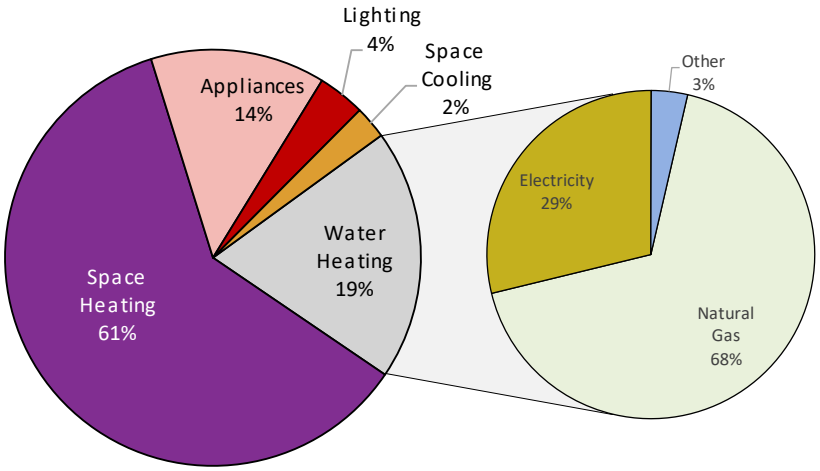

Figure 1.2: Breakdown of energy consumed for water heating in Canada

A transition away from natural gas water heaters (NGWHs) and electric resistance water heaters (EWHs) would significantly reduce the GHGs and energy consumed for water heating and, by extension, in the residential sector as a whole. The other existing options

for water heating include heat pump water heaters (HPWHs), solar water heaters (SWHs), and solar-assisted heat pump water heaters (SAHPWHs).

Water heaters can be compared based on their daily performance using energy factors (EFs – energy delivered to the tap per unit of energy input). The EF metric was replaced in 2017 by the uniform energy factor (UEF) which is a modified daily performance metric that categorizes water heaters based on the anticipated draw volume and attempts to make comparison between water heating methods easier. Currently, Energy Star certifies products based on either the EF or the UEF metrics [3].

NGWHs have energy factors between 0.6 and 0.8, EWHs have EFs approaching 1, and HPWHs achieve EFs between 2 and 3. Electric water heaters shown in the breakdown in Figure 1.2, include traditional EWHs, as well as electricity-driven HPWHs. Although HPWHs consume 30% to 50% less electricity than EWHs, they account for a limited fraction of the electric water heating market share, and an even smaller fraction of the overall water heating market share. If significant energy savings are to be realized, a transition must be made to HPWHs or SWHs [4].

1.2.1 Water heating technology options

Several water heating technology options exist in current markets for DHW, most of which include a water storage tank in which the water is stored until a hot water demand event. The storage tanks have a temperature setpoint to which the water inside is heated using various fuel sources and technologies. Setting a cooler hot water tank setpoint would decrease energy consumption and reduce the risk of scalding. This comes with the drawback that lower temperatures facilitate the development of legionella, a waterborne

bacterium which can cause serious health risks particularly to those with already weakened immune systems. To prevent legionella growth, the Canadian government recommends that residential DHW systems have a hot water tank setpoint of 60ºC, with a delivery temperature of 49ºC to reduce the risk of burns [5].

Water heating is presently dominated by traditional water heating methods, which are energy-intensive NGWHs and EWHs. NGWHs heat water using an always-on pilot light which ignites a burner to combust the natural gas when needed. Heat generated through the combustion process is used to warm the water, and the combustion products are ducted out of the home. EWHs operate using electric elements within the water tank that convert electric energy to thermal for water heating. EWHs typically have two heating elements: an upper element used to quickly heat water when little hot water remains in the storage tank, and a lower element which heats water slowly over a longer period.

HPWHs are an emerging technology which heat water using a vapour compression refrigeration cycle. In the refrigeration cycle, energy is removed from an air source by the evaporator and is rejected to the water storage tank by the condenser. The condenser coils are typically either wrapped around or submersed in the storage tank. A schematic of an air source HPWH is shown in Figure 1.3.

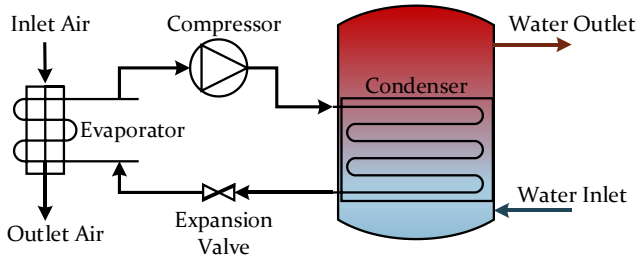

Figure 1.3: Schematic of a heat pump water heater

HPHW performance is measured using a coefficient of performance (COP), which is the ratio of the heat delivered to the water storage tank to the input compressor power. It is similar to the EF in that both measure a performance ratio. However, the COP measures the instantaneous ratio of the energy input and output of the refrigeration cycle and is used only for refrigeration and heat pump cycles, whereas the EF measures the daily ratio of energy input and energy delivered to the tap, and can be used for all water heaters.

Air source HPWHs remove energy from surrounding air and reject the energy to the water storage tank while exhausting air at a cooler temperature. HPWHs are often located in a house, thus causing space cooling in the conditioned environment as a by-product of their operation. Although this space cooling effect decreases cooling loads in warm and moderate climates, in Canada and other locations with long heating seasons, it has been shown to increase annual space heating costs [6].

One method that has been suggested to mitigate the space cooling effect in cold climate locations is using outdoor air as the supply and return for the HPWH. However, for the refrigeration cycle to efficiently heat water, the inlet air temperature must be above approximately 5°C [7]. Outdoor air temperatures are below 5°C for significant portions of the year across much of Canada and the United States, so it is infeasible to use outdoor air as a source for the HPWH in these locations. In the southern United States or other warm climates, HPWHs could use outdoor air for most or all of the year, but this is not commonly done because the warm southern locations benefit from the secondary space cooling effect of the refrigeration cycle which decreases annual space cooling costs for the home. As

such, in most locations, a conditioned space is typically used to supply air to and exhaust air from the HPWH.

Despite the benefits of HPWHs in lowering energy consumption for water heating, the combination of the space cooling effect and their relatively high capital costs have prevented them from obtaining a significant share of the water heating market. A potential solution to address the space cooling effect of HPWHs is to couple a HPWH with a solar collector to reduce the space cooling throughout the heating season and allow the electricity reductions of HPWHs to be realized.

Solar collectors are commonly coupled with HPWHs in either direct- or indirect-expansion configurations which are shown in Figure 1.4. In the direct expansion configuration, the solar collector is the evaporator in the refrigeration cycle, so the HPWH refrigerant is the working fluid in the collector. In the indirect configuration, the collector and refrigeration cycle are connected via a heat exchanger, one side of which is the HPWH evaporator. Because a heat exchanger separates the solar collector system from the HPWH, the collector may have water, a glycol solution, or air as a working fluid rather than refrigerant. The indirect expansion configuration is easier and less expensive to couple with a commercially available HPWH because no modifications to the refrigeration cycle are required. Although solar collectors decrease the space cooling effect caused by HPWHs and improve HPWH performance, solar collectors have the drawback of exacerbating capital cost of HPWHs even further.

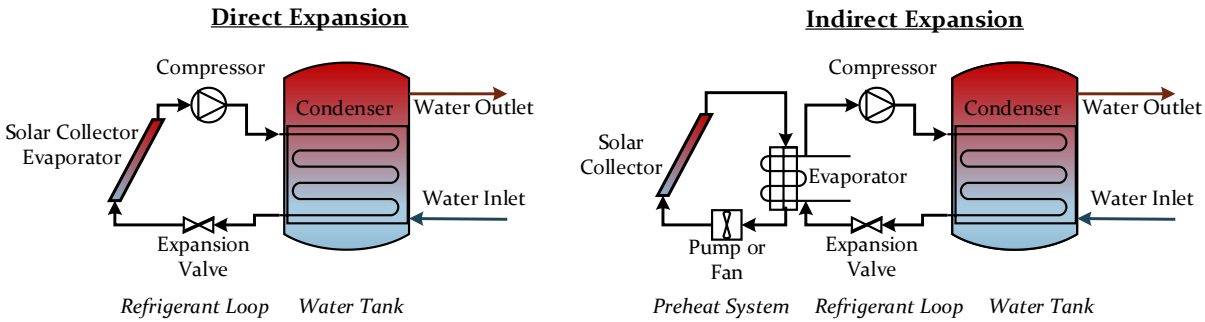

Figure 1.4: Solar assisted HPWHs in direct (left) and indirect (right) expansion configurations

When using an air-based indirect expansion configuration of SAHPWH, there are several possible configurations that could be used, as shown in Figure 1.5. The configurations differ in the location from which inlet solar collector air is drawn: the first draws air from and exhausts to a conditioned space, the second recirculates air in a closed loop between the solar collector and HPWH, and the third draws air from and exhausts to outdoors. The closed loop and outdoor air configurations eliminate the space cooling issue associated with HPWHs because they have no impact on air in the conditioned space. The conditioned configuration, like the HPWH, impacts space heating and cooling loads. However, advantages of the conditioned configuration are that it could reduce the space cooling effect of a standalone HPWH and provide space heating to offset a portion of the heating load.

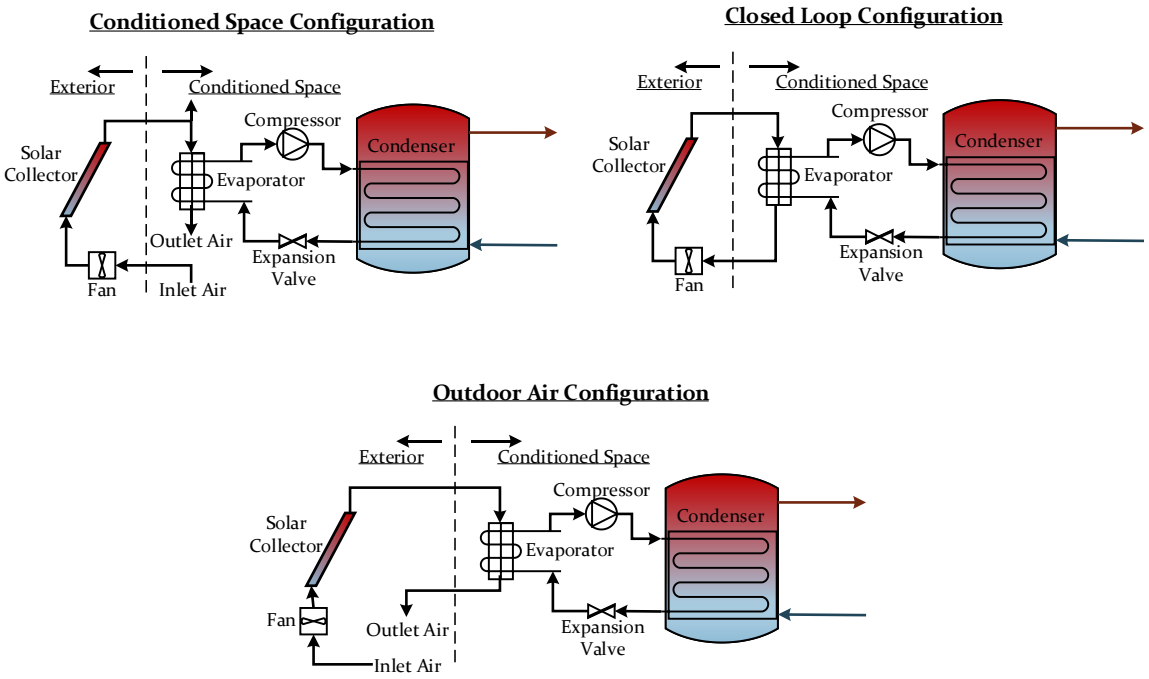

Figure 1.5: Possible configurations for air based indirect expansion SAHPWHs

All water heating options – NGWHs, EWHs, HPWHs, and SAHPWHs – come with inherent benefits and drawbacks. A summary of the benefits and drawbacks of each is summarized in Table 1.1. Although HPWHs and SAHPWHs have a higher capital cost than the electric and natural gas water heaters, the energy and GHG reductions achievable with HPWHs and SAHPWHs may offset the high capital cost and render these lower carbon options more feasible than the traditional water heating methods.

Table 1.1: Comparison of select water heating methods

	Benefits	Drawbacks
EWH	• Electricity can be clean energy	• Energy intensive
NGWH	• Often cheaper fuel prices than electricity	• High GHGs produced • Energy intensive
HPWH	• Less energy for water heating • Space cooling in cooling season	• High capital costs • Space cooling in heating season
SAHPWH	• Less energy for water heating • Space heating and cooling	• Very high capital costs

1.2.2 Regulatory framework

Many national and international locations have set goals for reduction of GHGs but few have implemented policies to address efficient water heating technologies as a method to achieve them. Potential options to increase the uptake of HPWHs and reduce GHGs and energy consumption for water heating include regulation mandating the use of HPWHs, incentives, or public education, among others. There has been past analysis on effective methods to increase uptake of an efficient technology, such as a HPWH, and research indicates that mandating efficient water heating standards is the most effective method to increase uptake of the technology as opposed to introducing incentives [8]. Part of the reason standards have been more effective than incentives is that when past incentives for HPWHs have been introduced, they have typically been programs with unpredictable and short durations due to government changes. As such, consumers have been hesitant to rely on financial incentives, and research has shown that higher uptake of a technology is achieved when incentive programs are implemented in the longer term [8]. Although there are past and present incentives for HPWH systems in some locations, there has yet to be any implemented for SAHPWHs despite the possible benefits as compared to HPWHs.

China and the United States are examples of two countries that introduced policy to encourage uptake of HPWHs. In China, a subsidy for 10% of the HPWH capital cost was introduced in 2012, and between the years of 2013 and 2015, residential HPWH sales increased by 46%, with a compound annual growth rate of over 25% [9]. Despite this growth, the total market share remained at 3% in 2014. In the United States, a policy was introduced in 2015 requiring that new water heaters have energy factors of at least 1.97 for electricity-driven water heaters with volumes of 208 L (55 gallons) and above [10].

Because EWHs cannot achieve energy factors above one, this mandates the use of HPWHs [1]. With almost one third of new residential homes installing HPWHs since introduction of the regulation, the market share in the US has reached almost 9%.

Canada plans to follow suit with the US and mandate that all electricity-driven water heaters for sale by 2030 will have an energy factor above one [11]. Some provinces within Canada, such as British Columbia, New Brunswick, Nova Scotia, and Prince Edward Island, have implemented incentive programs to encourage residential HPWH usage. Similarly, Ontario had a brief pilot program, which offered rebates to both contractors and homeowners but was it unsuccessful in significantly increase HPWH market shares due to its short duration and the reluctance to rely on rebates with uncertain durations [12].

1.3 Thesis Objective

The objective of this research was to assess the feasibility of an indirect expansion HPWH coupled with an air-based solar thermal collector system for single detached dwellings in Canada and the United States via experiments and simulation. With an air-based solar thermal collector to preheat inlet air for the HPWH, it may be possible to realize electricity and life cycle cost reduction of HPWH and SAHPWH systems as compared to EWHs, without increasing space heating loads throughout Canadian and American winters. Additionally, coupling a solar collector with a HPWH may increase year-round operating performance compared to a HPWH alone in all climates within these countries. The goal was to assess performance of HPWHs and SAHPWHs in various configurations to make comparisons in terms of energy consumption and reduction, economic factors such as

payback period (PBP) and lifecycle cost (LCC), and GHG reduction across Canada and the United States.

The scope of this thesis includes analyzing three configurations of SAHPWH and a HPWH to determine a preferred configuration in various cities across Canada and the United States. Preferred configurations were recommended based upon water heating energy reduction, space heating and cooling reductions, GHG reduction based on natural gas emissions and local electricity grids, and PBP and LCC based on local energy prices. The SAHPWH and HPWHs were compared against EWHs and NGWHs for all the above parameters. All water heater options compared within this thesis were storage tank water heating options, while tankless water heaters were outside the scope of this research.

1.4 Thesis Layout and Methodology

This thesis includes seven chapters to describe the completed research. The breakdown of chapters is as follows:

- Chapter 1 Introduction: provides the background information and grounds for this research, in addition to the research objectives,
- Chapter 2 Literature Review: explains the existing research in the field of SAHPWHs, including the most relevant publications and research gaps,
- Chapter 3 Experimental Methodology: describes the experimental apparatus used for this research, including the limitations and assumptions employed,
- Chapter 4 System Modelling Approach: describes the modelling methodology and analysis used to calculate the results throughout the simulation study,

- Chapter 5 Results: presents the data obtained within this study, including comparisons of SAHPWH and HPWH configurations, and differences in performance for various locations,
- Chapter 6 Discussion: analyzes the results and discusses the associated implications of the results, and
- Chapter 7 Conclusions and Future Work: summarizes the main conclusions of this research and identifies potential areas of future research in the field.

The process followed throughout this research is shown in Figure 1.6.

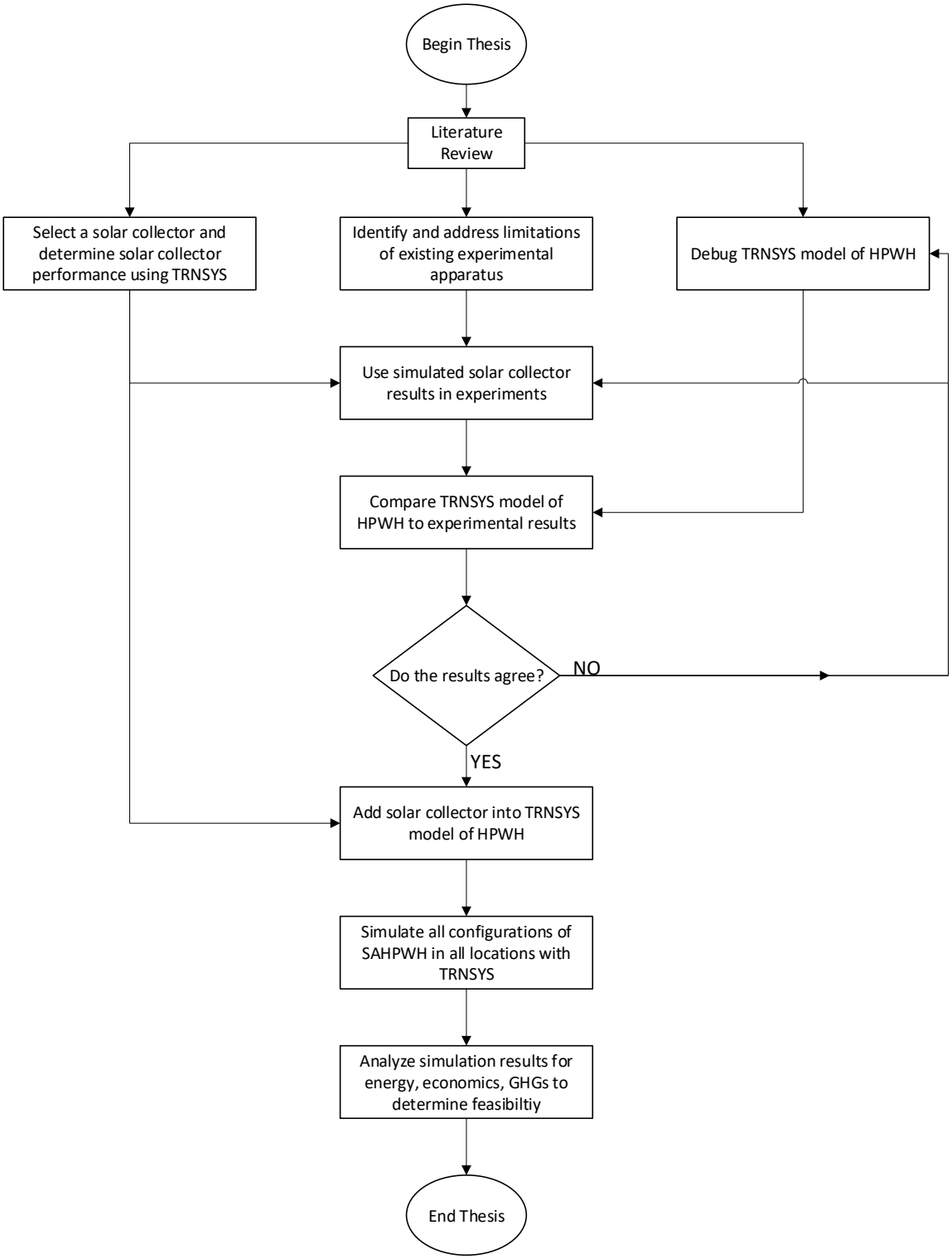

Figure 1.6: Research methodology and process

Chapter 2: Literature Review

HPWHs have been studied in various locations worldwide to determine their feasibility and benefits or costs due to their inherent space cooling. The HPWH research has included coupling the HPWH with solar collectors having various working fluids, varying different operating parameters to improve HPWH energy performance, and analyzing the effects of different ambient conditions on the systems. An overview of the research on HPWHs, SAHPWHs, past economic analysis on these systems, modelling and simulation used for HPWHs, and research gaps are presented in this section.

2.1 Heat Pump Water Heaters

Heat pumps have been used for decades for applications such as refrigeration, manufacturing, and industrial applications. In a review of heat pumps, Chua et al. [13] described maturation of the technology through more recent advancements such as improved compressor performance, multistage cycles, ejector systems, and new refrigerants, but indicated that one application of heat pumps that has yet to be utilized to its full potential despite various advancements in heat pump technology is water heating. Despite the benefit of lower electricity consumption, market penetration of HPWHs remains limited since becoming commercially available in the 1950s [14].

A study by Bursill et al. [15] analyzed the effects of preheater water tank and HPWH temperature set points on the overall energy consumption of the system, and found that total energy consumption could be minimized when the HPWH temperature set point was equal to the preheater tank set point. These results could represent HPWH performance trends when coupled with a water-based solar collector to preheat the inlet water if the

electric source in the study were replaced with a solar collector. The research by Bursill et al. also showed an increase in performance of HPWH systems as the HPWH water temperature set point decreases, which is representative of other research in the field [16]. However, a lower limit on the storage tank temperature of 49ºC is required by the Canadian government to prevent growth of legionella bacteria. Lei et al. [16] conducted experiments on an instantaneous HPWH and found that instantaneous HPWHs could achieve a COP as high as 12.6. This is because instantaneous water heaters are tankless which mitigates the risk of legionella, allowing low temperature setpoints to be used thus eliminating the energy consumption that tank water heaters use to reach higher temperatures. COPs as high as the study by Lei et al. are not observed in conventional HPWHs with a storage tank; conventional HPWHs however are able to provide hot water for longer, larger draw periods, and have lower capital costs than their instantaneous counterparts.

The significant energy reductions achievable with HPWHs can be increased further in warm climate locations when space cooling is considered, as shown in an experimental study by Ji et al. [17]. In this study, HPWHs were analyzed in a tropical climate where they provide significant space conditioning benefits year-round. However, HPWH performance varies in different climate zones around the globe, but have been shown to provide net energy benefits in many locations. Hudon et al. [18] simulated HPWHs in various American locations and determined that HPWHs were beneficial in most climates, providing cost savings over 38% and 10% as compared to EWHs and NGWHs when space heating and cooling effects were considered. This is a representative study of others in the industry: Maguire et al. [19] also determined that despite variations in HPWH performance in different climate regions in the US, HPWHs always resulted in net energy savings.

Khalaf [6] studied a HPWH across Canada and observed an increase in space heating costs with the HPWH during Canadian winters, which is common when using HPWHs in cooler climates. Sparn et al. [20] came to similar conclusions to Khalaf. After experimentally replicating HPWH operation in various climates in the United States, Sparn et al. recommended HPWHs not be used in conditioned spaces in cold regions with long heating seasons.

Despite the apprehension about HPWH success in cold climates, studies have shown net electricity reduction in Canadian locations. Amirirad et al. [21] studied HPWHs in cold climate conditions, including changes to annual electricity consumption due to the HWPH and its space cooling and heating effects. It was found that annual electricity consumption decreased by 22% when using a HPWH in Toronto. This study was limited, however, like many others in the field, as it did not analyze PBP, or consider the relatively high HPWH capital costs as compared to the capital cost of NGWHs in its cost analysis for the two.

Smith [22] compared a HPWH operating in a basement to a HPWH with a heat recovery ventilator (HRV) using outdoor air. The HRV ducted system was analyzed as a potential mitigation strategy for the HPWH space cooling effect. The conclusion of this study was that both systems reduced utility costs, but the additional ducting and additional cost of the HRV caused the HPWH operating with basement air to be a more economically viable option. Although the HPWH in the basement was more economically viable than an HRV ducted HPWH, Smith agreed with other research in the recommendation to not use HPWHs in some Canadian climates.

In addition to the space cooling effect which hinders their use in Canada, HPWHs also have the unique challenge of frost buildup on the evaporator coils when used in cold, humid ambient conditions, which decreases the system effectiveness. Song et al. [23] summarized several defrosting methods to mitigate this issue including reversing the cycle, jet defrosting, and preheating the inlet air. Although Song et al. indicated that reverse cycle defrosting is most widely evaluated, no single defrosting technique is highly recommended amongst leading researchers. In addition to the suggested defrosting solutions, coupling a HPWH with an air-based solar collector may sufficiently preheat inlet HPWH air and significantly reduce or prevent frosting on the evaporator coils in the system.

Kwak and Bai [24] coupled an electric air preheater with a heat pump system and saw a COP increase of 57% for 1-2ºC air as compared to the system at that temperature without a preheater. Although Kwak and Bai determined that an electric air preheater has the potential to be an economical solution to the frosting issue in cold climates, there exist other lower-electricity preheating methods such as using solar to preheat the air, which could further increase cost savings and system effectiveness, while allowing the electricity savings of HPWHs to be realized.

The issues due to cold climate operation discussed in this section included decreased HPWH performance, space cooling which increases space heating costs, and frosting issues in high-humidity and low temperature environments. It may be possible to mitigate all of these issues and realize additional energy reductions for DHW and space heating by coupling the HPWH with a solar collector.

2.2 Solar-assisted heat pump water heaters

The SAHPWH systems offer the potential of lower-cost water heating, and, in locations such as Canada with long heating seasons, harnessing solar energy reduces the supplementary space conditioning required to offset the cooling caused by the traditional HPWH. Significant research has been conducted to date on direct-expansion SAHPWH systems. A study by Kong et al. [25] on a direct-expansion SAHPWH system in China concluded that the site-specific conditions of insolation and ambient temperatures had a significant effect on the overall system COP and heating time. Deng and Yu [26] went further to show that ambient temperature had a large effect on SAHPWHs when solar insolation was low, but little effect when insolation was high. Vieira et al. [27], however, concluded that HPWHs in warmer climates were not highly influenced by site-specific conditions, thus achieving a high COP at a wide range of temperature and insolation values. The variance between the effect of insolation, temperature, and other site-specific parameters between the aforementioned studies can be explained using findings in a review by Poppi et al. [28], which indicated that existing studies are difficult to compare due to the wide variety of boundaries, geometries, locations, and assumptions. This means detailed analysis of the systems is required for each configuration and location in which they are implemented to improve and optimize performance.

Despite the considerable research effort which has been spent on direct-expansion SAHPWH systems, Kamel et al. [29] explained that direct-expansion photovoltaic-coupled SAHPWHs are inefficient, because additional controls are required for the mass flow rate to prevent refrigerant from pooling at the evaporator outlet. In addition, direct-expansion SAHPWHs are complex to fabricate from commercially available HPWHs because they

require redesign of the refrigerant cycle, so indirect-expansion SAHPWHs are often preferred for aftermarket coupling of solar collectors with HPWHs.

Several studies agree that SAHPWHs improved performance compared to HPWHs alone in all climates, and most notable improvements occurred in cold climate regions. Carbonell et al. [30] simulated solar thermal HPWHs and saw large electricity savings when using an air-source heat pump system, particularly in cold climates with high insolation values. This is because energy consumption for space and water heating is greater in cold climates, and systems with a higher energy demand are operational for a greater proportion of time, therefore realizing larger absolute electricity savings than those with low energy demand. Cai et al. [31] also determined that a dual source multi-functional solar HPWH system was particularly beneficial in cold climate conditions, with significant COP increases in an optimized cold climate system, as compared to other climates. Chu [32] studied a dual tank indirect expansion solar assisted heat pump for the combined use of water heating, space heating, and space cooling, and quantified the reduction in energy consumption in a Canadian climate, concluding that energy savings of about 30% could be realized.

Li et al. [33] simulated and optimized the solar collector area and storage factor for domestic hot water and space heating in Beijing and was able to increase the COP by 1.4 times compared to the non-optimized system. It is likely that this optimized system would not necessarily be the optimal configuration in other locations, however, due to the significant influence of climate and on-site conditions and due to the variations in DHW and space heating loads in other climates.

Kegel et al. [34] compared an air-source solar collector coupled with an air-source HPWH to a water-source solar collector with a ground-source heat pump system for space and water heating in Montreal. This study concluded that the air-source solar collector and heat pump system configuration was more efficient than the water-source configuration. Despite the benefit of air-based collectors with HPWHs, a review by Kamel et al. [29] highlighted that there is limited research on air-based solar collectors coupled indirectly with HPWHs. Past research has shown reduced performance of HPWH-only and combined HPWH-solar systems in cold climates compared to moderate climates, so new strategies and configurations of SAHPWH which prevent or reduce impact on space conditioning loads should be developed to increase feasibility of SAHPWHs in these harsher climate conditions.

2.3 Economics of heat pump water heaters

Although HPWHs have been available commercially for several decades, their uptake remains limited, largely due to high capital and lifecycle costs [8], [35]. However, the increased efficiency of HPWHs and SAHPWHs compared to electric or natural gas water heaters translates to lower operating and fuel costs [36]. Further, it has been shown that there is little room for water heating efficiency increases to be realized with traditional electric and natural gas water heater technology, so if significant efficiency and operating savings are to be realized, solar water heaters, HPWHs, or SAHPWHs must be used [4]. In order to justify the purchase of a more expensive HPWH, the efficiency increases over the lifetime must be accounted for, using parameters such as LCC and PBP which encompass not only capital costs but also operating and fuel cost savings.

Khalaf [6] studied HPWHs in various Canadian locations, finding that the PBP for HPWH systems doubled in Ontario from 4 years to 8 years when the increased space heating load was considered for a new HPWH installation. The study found that the low cost of NGWHs has hindered market penetration of HPWHs in locations such as Ontario, while the low cost of electricity in Quebec and BC makes the reduction in electricity cost insignificant as compared to EWHs due to the large capital costs for HPWH systems.

Amirirad et al. [37] studied heat pumps across Canada, and showed that there were energy cost savings to be realized with HPWHs, with the maximum savings realized in Vancouver and minimum in Edmonton. Kegel et al. [34] encompassed capital costs, as well, in an analysis of a solar assisted air source heat pump and determined that although it was more efficient than a solar assisted water source heat pump, the high capital costs could not be overcome in Quebec. This is in part due to low electricity costs in Quebec which limit the operating cost savings attainable with HPWHs or SAHPWHs. Maguire et al. [19] also conducted an analysis of HPWHs in various locations which included breakeven points and agreed that the breakeven point occurs quicker in locations with high electricity costs, because it is these locations that realize higher operating cost savings.

PBP has been one of the more common economic parameters used to encompass capital and operating costs in past research. Kegel et al. [38] calculated PBP of HPWHs in various Canadian locations and determined that the PBP was greater than the assumed lifetime in a large number of locations. Poppi et al. [28] also indicated that there are long PBPs for HPWHs in Canadian locations, because PBP increases in more northern locations which have significant space cooling externalities of the HPWH. Buker and Riffat [39] analyzed

trends of solar assisted heat pumps and determined that although PBP is high for solar assisted heat pumps, it has decreased in recent years, but indicated that more research is needed on the economics of solar assisted heat pumps. Marinelli et al. [40] reviewed residential heat pump usage with a life cycle thinking approach. The study agreed that economic analysis has been limited in research of heat pump systems, went further to indicate that studies including social aspects of heat pump systems such as air quality improvements via GHG reductions are even more limited.

2.4 Modelling and simulation of heat pump water heaters

Studies that compare the same water heater configuration in different locations are necessary to determine variations in water heater performance due to climate but are difficult or impossible to achieve without modelling and simulation. This is true for all types of water heating, including HPWHs. To develop these water heating models, it is important to determine the level of detail necessary to accurately represent the water heater while reducing computational effort.

Baldwin and Cruickshank [41] modelled three storage tank subroutines using TRNSYS to determine differences in their performance, and also conducted a sensitivity study on the number of nodes used within a 270 L storage tank for cold thermal storage. The sensitivity study used between 12 and 100 nodes to model the storage tank, and it was observed that increasing the number of nodes increased the rate of temperature change at any given point. When comparing the results with 50 and 100 nodes, it was concluded that although an improvement existed for the 100-node model, the improvement was small and thus the 50-node storage tank was deemed sufficient for the cold thermal storage analysis.

Cruickshank [42] studied a solar water heater and analyzed the common assumptions in modelling of solar storage systems, including the assumption of one-dimensional temperature changes only in the vertical direction. This analysis was done using an experimental water tank with two sets of ten equally spaced thermocouples in the horizontal direction and nine thermocouples equally spaced in the vertical direction. A cool-down test was run to determine the uniformity of the horizontal temperature gradients and it was concluded that these gradients were nearly zero. This conclusion can be applied to various water heating systems with storage tanks in both experimental and simulated models, because it indicates the validity of the one-dimensional assumption.

In TRNSYS, two HPWH models exist in the TESS library – Type 938 and Type 1237. Type 938 is a simplified HPWH which models the refrigerant to water exchange similar to that of a counterflow heat exchanger. For many physical, commercially available HPWHs such as those with wrap-around condenser coils, modelling the heat exchange as a counterflow heat exchanger does not capture the behavior to a sufficient degree of detail. Type 1237 uses a wrap-around coil heat exchanger to model the refrigerant to water heat exchange but does not accurately model phase change materials like certain refrigerants. To account for the lack of accurate modelling capability with existing TRNSYS models, Khalaf [6] used the FORTRAN Compiler to develop Type 240. Type 240 models a wrap-around condenser coil with capability to determine performance of phase change materials. Khalaf used an experimental HPWH to develop a performance map for Type 240 and validate the model.

2.5 Areas of limited research

Among the research on HPWHs and SAHPWHs, there exist a few areas of limited knowledge. Although there is research on the effects and benefits of preheating inlet HPWH air to increase performance, there is little research to date on preheating that inlet air using solar thermal. Most of the strategies that exist to improve cold climate performance of HPWHs and mitigate their space cooling effect use water- or other liquid-based solar collectors as opposed to air-based.

Review studies have attempted to compare performance between several SAHPWHs in different configurations and locations, but it is difficult to draw conclusions about performance between studies when the research employs vastly different boundary conditions, configurations, and assumptions. In addition, there are few studies which analyze and compare solar assisted heat pump water heaters across Canadian and American locations, and even fewer that include an analysis of economics or GHG reduction. A summary of the notable findings from the literature review, as well as the research gaps is provided in Table 2.1.

Table 2.1: Summary of literature review and research gaps

Study	Important Findings
Khalaf	Experimental and numerical simulation of HPWH determined that space heating costs increase when HPWHs are used in Canadian climates, rendering the technology uneconomical in many locations
Poppi et al.	It is difficult to compare HPWHs in various locations between studies due to different assumptions and configurations – to compare performance in different locations, the same systems must be used.
Marinelli et al.	Social aspects of HPWHs are infrequently discussed, including economics and GHGs, and their ability to increase overall social satisfaction
Kamel et al.	Research on air-based solar collectors coupled with HPWHs is lacking, despite the benefits of the system
Kawk and Bai	HPWH performance can be increased with preheated air

Chapter 3: Experimental Methodology

The experimental apparatus used within this study included an instrumented and controlled air source HPWH, air-handling unit, water draw system, and mains water cooling system. The details of all components used, including the instrumentation and data acquisition are described in this section, beginning with an overview of the full apparatus.

3.1 Overview of experimental apparatus

The experimental setup was designed with the capability to test a commercially available HPWH under various water temperature, air temperature, air humidity, and flow rate conditions. The setup can be divided into five major systems: the HPWH, the hot water draw system, the mains water cooling system, the air-handling unit, and the data acquisition system. Figure 3.1 shows some components of these systems in the experimental apparatus.

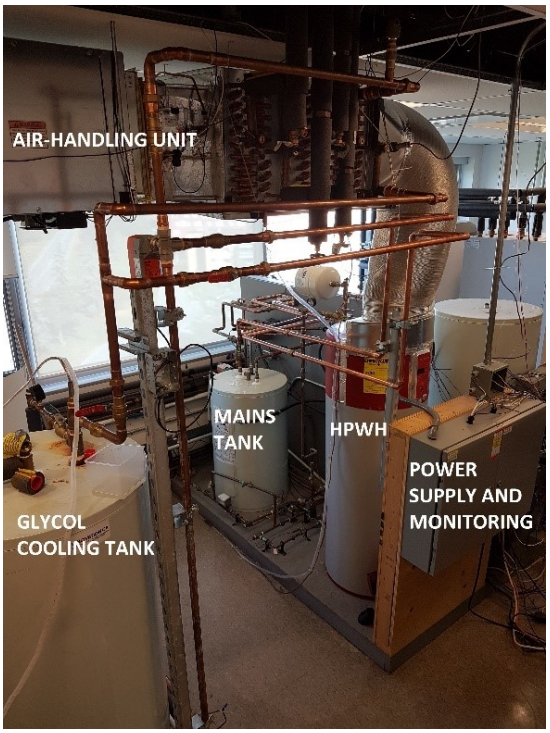

Figure 3.1: Experimental apparatus and layout

The experimental apparatus was designed to operate as follows. The water was heated in the HPWH storage tank, and during designated hot water draw events, the water draw system operated to remove water from the HPWH tank. Water from the mains tank simultaneously entered the HPWH tank to replenish the volume drawn. The mains tank stored water that was cooled to temperatures representative of those occurring throughout winters in Canadian locations. The mains tank was cooled via a heat exchanger that was connected to the glycol cooling tank. The glycol cooling tank was a glycol storage tank that was cooled to near zero or sub-zero temperatures using a chiller. A schematic of the experimental apparatus is shown in Figure 3.2. The glycol cooling tank also fed chilled glycol to a supercooling coil in the air handling unit. This coil was one of three coils used to temper the inlet HPWH air. The air in the air-handling unit was conditioned to temperature, humidity, and flow rates setpoints and heat was removed from the air by the HPWH to heat the water. A schematic diagram of the air-handling unit used in the experimental apparatus is shown in Figure 3.3.

As the experimental apparatus was operated, temperatures, humidity values, flow rates, and power values were monitored and controlled using a data acquisition system. Additional details of all components used in the experimental system are provided in the following sections.

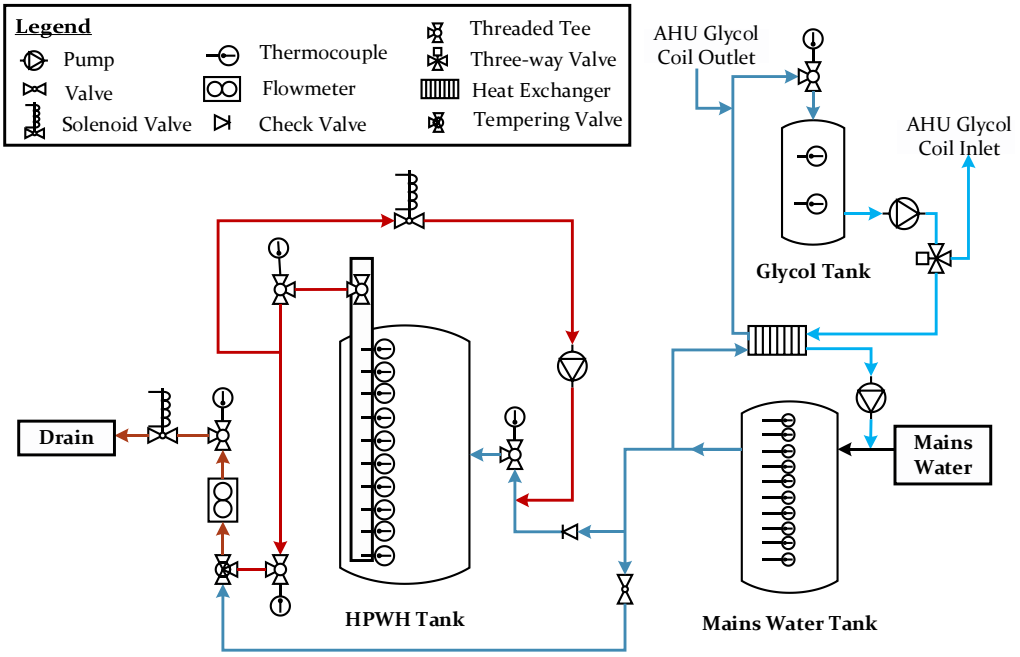

Figure 3.2: Schematic diagram of experimental apparatus

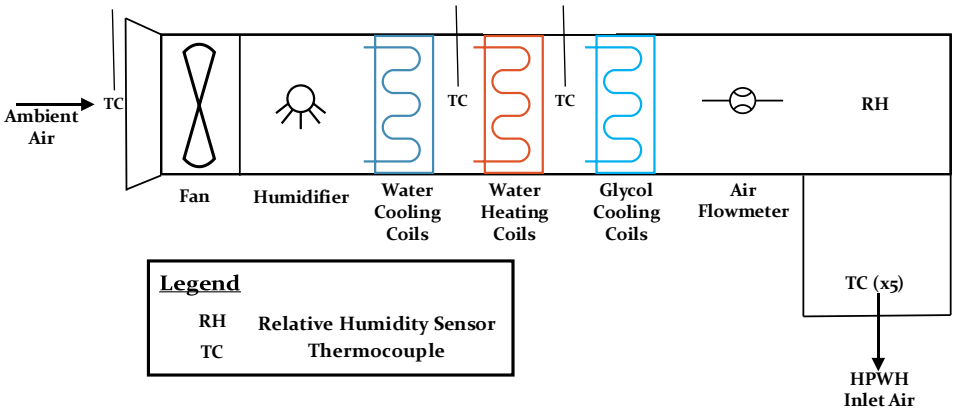

Figure 3.3: Schematic diagram of air-handling unit

3.2 Heat pump water heater

The HPWH used in the experiments was a commercially available 189 L Geospring model with wrap-around condenser coils. The refrigeration loop and water storage tank were one packaged unit. The evaporator, which removed energy from the air, was located on top of the storage tank with a fan to force air across the evaporator and promote energy exchange.

The HPWH also included two heating elements: an upper element for rapid water heating during high draw events and a lower element for slower water heating over longer periods. The HPWH tank temperature setpoint was set at 60°C. The specifications of the HPWH are provided in Table 3.1.

Table 3.1: Specifications for HPWH used in experimental apparatus [7]

HPWH Parameter		Value
Power Output	Heat Pump Power (W)	550
	Upper Element Power (W)	4500
	Lower Element Power (W)	4000
Refrigerant Details	Refrigerant Type	R-134a
	Refrigerant Charge (kg)	0.78
Temperature Settings	Water Temperature Setting (°C)	38-60
	Air Temperature Range (°C)	7-49
Electrical Requirements	Required Voltage (V)	208/240
	Required Current (A)	30 (min)
	Required Electrical Frequency (Hz)	60
Dimensions	Tank Height (m)	1.5
	Tank Diameter (m)	0.5
	Tank Volume (L)	189

The HPWH could be operated in one of four water heating mode settings: HPWH-only, hybrid, high demand, and electric. HPWH-only mode allowed only the refrigeration cycle to heat the water. Hybrid mode combined the refrigeration cycle with an electric element during periods of high draws. This allowed the HPWH to increase tank temperatures more quickly, but operation of the electric resistance element increased the energy required to heat the water thus decreasing the COP. High demand mode was similar to hybrid mode but operated by cycling the upper and lower heating elements to satisfy hot water demand

during periods of unusually high demand. Due to the increased use of electric elements, high demand mode consumed more electricity and had a higher COP than either HPWH or hybrid mode. Electric mode prevented operation of the refrigeration cycle. It used the upper or lower heating element to heat water similar to an EWH and therefore consumed more energy than the other modes. The HPWH was instrumented and controlled using thermocouples, relative humidity sensors, relays, and power monitoring equipment. A summary of the HPWH instrumentation is provided in Table 3.2.

Table 3.2: Instrumentation used to monitor HPWH

HPWH Instrument	Type/Model	Quantity and Location
Thermocouples	T	10 – water tank 5 – outlet air 5 – inlet air (also shown in Table 3.5) 8 – refrigerant lines
Omega Relative Humidity Sensor	HX94A	1 – outlet air 1 – inlet air (in AHU)
Continental Control Systems, LLC – WattNode	WNB-3Y-208-P	1 – Power Cabinet

The temperature of the hot water was measured using ten Type T thermocouples with equal vertical spacing of 0.1 m in the storage tank. The horizontal temperature gradients were not measured because they were found to be negligible in [42]. Thermocouples were also used to record air temperatures entering and leaving the HPWH. Five thermocouples were used for each the inlet and the outlet air so average temperatures could be used. The relative humidity was measured using relative humidity and temperature sensors at the inlet and outlet of the HPWH.

The HPWH, in its market ready condition, did not allow for control of the HPWH fan and compressor or upper and lower element, or allow for measurement of the power consumed.

To achieve the required level of control and monitoring of the HPWH, Khalaf [6] and Smith [22] overrode the original controls by replacing and modifying select relays. Existing relays for the compressor and heating elements were replaced with external relays which could be independently controlled, without compromising the safety features of the unit.

Power consumption was monitored with current transformers and a WattNode Pulse. The current transformers were installed on HPWH power supply wires and transformed the line current into a power. The WattNode measured the power and generated pulses in a frequency proportional to the total power consumption of the HPWH unit [43]. The pulses were read in by the data acquisition system to provide a power readout. The power cabinet containing the current transformers, relays and WattNode are shown in Figure 3.4.

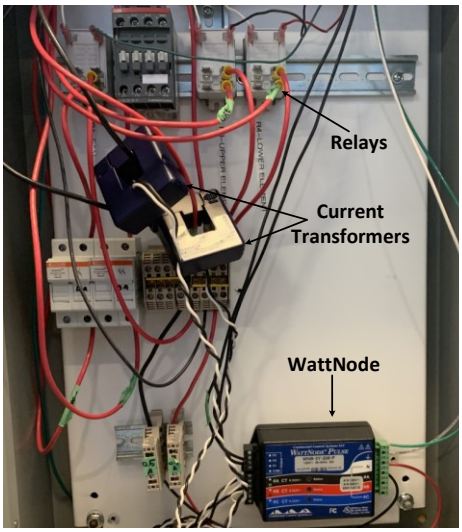

Figure 3.4: HPWH power control and monitoring cabinet

3.3 Water draw and supply systems

The water draw and supply systems removed water from and replenished water to the storage tank, respectively. The water draw system connected the HPWH to the drain, while the water supply system connected the water mains to the HPWH.

3.3.1 Water draw system

The hot water draw system included solenoid and tempering valve to control the temperature, time, and duration of the draws. The solenoid valve was controlled via the data acquisition system to open or close to achieve the desired draw times and volumes. The water draw volumes and schedules were based on CSA-F379.1 standard draw profiles which represent various levels of occupancy. The solenoid valve would open at a set time based upon the standard draw profile and remain open until a flow meter indicated that the draw volume requirement had been met. During draws, a throttling valve was used in line with the solenoid valve to set the desired flow rate of 11.5 L/min in accordance with CSA-F379.1 [44]. When water was drawn from the HPWH tank at 60°C, it was cooled to 55°C using the tempering valve to reduce the risks of scalding and of legionella formation [45]. An image of the water draw system is shown in Figure 3.5.

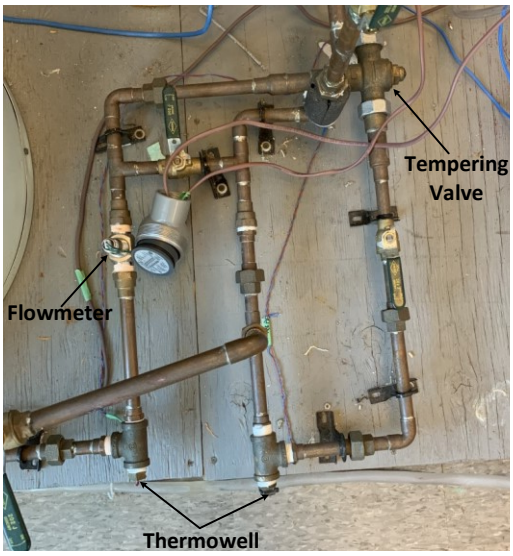

Figure 3.5: Water draw system components

The water draw system instrumentation included a flow meter and thermocouples in a thermowell. A summary of the water draw instrumentation is shown in Table 3.3.

Table 3.3: Instrumentation used in water draw system

Water Draw Instrument	Type/Model	Quantity and Location
Themowell	Type T Thermocouple	1 – hot water from storage tank 1 – hot water after tempering valve
Flow Meter	Blancett B220-886	1 – hot water drawn from tank
Tempering Valve	Heatguard HG110-HX	1 – mixing hot water and mains water
Solenoid Valve	Schneider AG13A020	1 – hot water draw line 1 – HPWH recirculation loop

A recirculation loop was also used in the experimental apparatus to reduce stratification of the HPWH tank. The recirculation loop consisted of a pump and a solenoid valve which drew water from the HPWH outlet and returned it to the inlet. Recirculation was used to precondition the HPWH tank to a uniform temperature prior to a draw test.

3.3.2 Water supply system

The water supply system was used to cool inlet water to the HPWH tank which was supplied during hot water draws. The existing mains water lines supplied water at 20°C, which is greater than winter mains water temperatures in Canada. To replicate winter water temperatures, a system for cooling the mains water entering the HPWH was implemented.

The water supply system consisted of a chilled water storage tank, heat exchanger, glycol cooling tank and chiller, and three-way valve. Water in the mains water tank could be cooled below 10°C which allowed the HPWH to be tested in response to lower water temperatures to expand the existing HPWH performance map and test the HPWH under conditions representative of Canadian winters. The water mains temperatures were determined based on the algorithm developed by Burch and Christensen [46]. Water in the mains water tank was cooled using a recirculation loop connected via a heat exchanger to

the chilled glycol system, which had a 50/50 glycol/water mixture by volume. Water was removed from the water tank, circulated through the counterflow heat exchanger, and pumped back into the tank through the return line, as shown in Figure 3.6. When water was drawn from the HPWH and therefore from the mains water tank, the mains water tank was refilled with the building supply water at around 20°C.

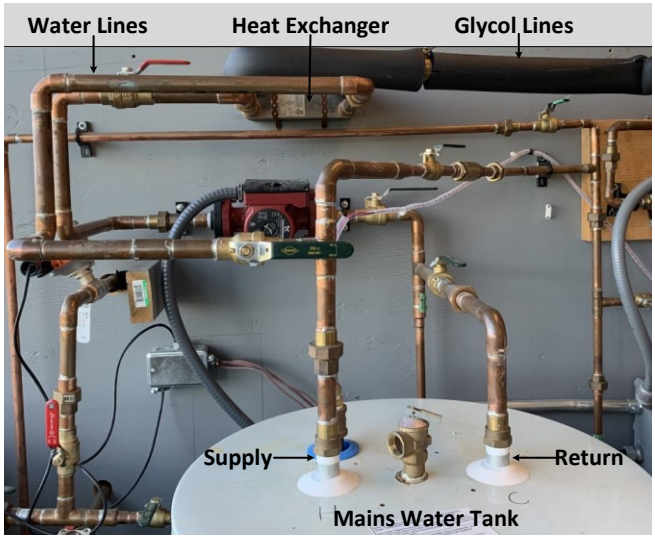

Figure 3.6: Mains water cooling system

The chilled glycol was fed to the heat exchanger from a glycol storage tank. The glycol was cooled to around 0°C using a chiller and was stored in the glycol storage tank to be used to cool the mains water and air in the AHU. A three-way valve was controlled and used to proportion the amount of glycol used for chilling the water and the air throughout tests. The instrumentation for the water supply system is shown in Table 3.4.

Table 3.4: Instrumentation used in water supply and water-cooling system

Water Supply Instrument	Type/Model	Quantity and Location
Thermocouples	T	10 – mains water tank 2 – chilled glycol tank
Three-way valve	Belimo TFRB24-SR	1 – selector Between water cooling and air cooling system

3.4 Air handling unit

The air-handling unit (AHU) was used to condition the inlet HPWH air to various temperature, flowrate, and humidity conditions. The air-handling unit had a humidifier, humidification filter, fan, and three sets of tempering coils. The specifications of the AHU components are provided in Table 3.5 and an image of the AHU is shown in Figure 3.7.

Table 3.5: Components used in air-handling unit

AHU Component	Type/Model	Quantity and Location
Thermocouples	T	1 – AHU inlet air 1 – after cooling coils 1 – after heating coils 5 – AHU outlet (HPWH inlet shown in Table 3.2)
Omega Relative Humidity Sensor	HX94A	1 – AHU outlet (HPWH inlet shown in Table 3.2)
Humidifier	Skuttle 529	1 – before tempering coils
Humidifier Filter	GeneralAire FBA_HUGEN1099	1 – after humidifier
Water Cooling Coil	CW12C06S12-12.5x14-RH	1 – after humidifier filter
Water Heating Coil	HW12C02A11-12.5x14-RH	1 – after cooling coil
Glycol Supercooling Coil	CW12C06S12-12.5x14-RH	1 – after heating coil

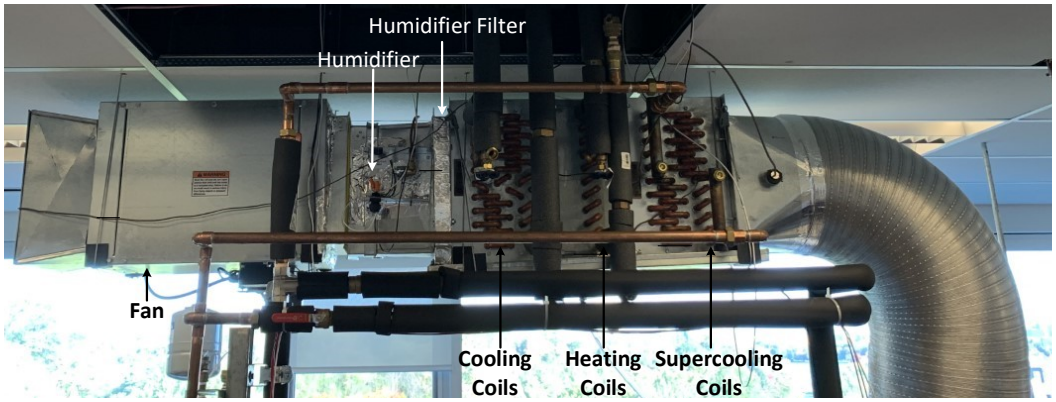

Figure 3.7: Air-handling unit in experimental apparatus

The fan was used to control the flow rate of air over the HPWH. Khalaf [6] determined that variations in air flow rate had little impact on the performance of the system, so the flow rate was typically set at 260 m^3/h, which was the normal flow rate over the HPWH due to the built-in HPWH fan [22].

The humidification system included a humidifier and a filter. After the studies conducted in [4] and [20], it was suggested that a humidification filter be added to facilitate further humidification. The filter served the purpose of holding moisture from the humidifier to promote evaporation as the air passed through.

The three tempering coils were used to temper and dehumidify the air entering the HPWH. The air passed over the water-fed cooling coil, then the water-fed heating coil, and finally over the chilled glycol-fed supercooling coil. The flow rates of the water and glycol within the coils were controlled using variable flow control valves that were operated through the control program.

3.5 Data acquisition and control program

The readings obtained from the experimental apparatus were measured and recorded using a National Instruments CompactDAQ with a digital input, digital output, analog input, and analog output card, as well as three thermocouple cards. The data was collected using the input and thermocouple cards, while the signals were sent using the output cards. A summary of the cards used is provided in Table 3.6.

Table 3.6: Data acquisition and control system details

Card Type	Model	Use	
Analog Input	NI9207	Recording Data	• AHU flowmeter flow rate • Heating and cooling coil valves • RH sensor humidity and temperatures
Analog Output	NI9263	Control Signals	• AHU fan • Heating, cooling, and supercooling coil
Digital Output	NI9476	Control Signals	• Fan, compressor, heating element relays • Recirculation pump relays • Solenoid valve relays • HPWH power • Humidifier
Digital Input	NI9422	Recording Data	• Total power consumption • Flow meter
Thermocouple Input	2 x NI9213 1 x NI9214	Recording Data	• HPWH, mains water, glycol tank temperatures • AHU air temperature • Inlet and outlet HPWH water temperatures

A Laboratory Virtual Instrument Engineering Workbench (LabVIEW) [47] program was used to control the outputs and collect data from the inputs of the experimental apparatus. The LabVIEW program monitored the operating conditions and compared them to the setpoints for air temperature, velocity, and humidity, and tank temperatures and adjusted the output controls to achieve the setpoints. Simultaneously, the LabVIEW program recorded details about the operating conditions at 60-second intervals.

3.6 Experimental testing

The experimental apparatus was run in different tests to expand the performance map used in [4] and [20] and test system performance under daily draw trials, with the additional capability provided by the chilled glycol for cooling water and supercooling air. The HPWH was run under draw and charge tests, and the LabVIEW program was developed to toggle between the two. In charge tests, the water in the HPWH was cooled to a uniform

temperature of 10°C, then the refrigeration cycle was turned on and performance was monitored using heat rejection to the water tank, compressor power, sensible heat transfer from the air, and total heat transfer from the air during the heating process to the setpoint of 60°C. A charge test was run for each set of different air temperature and relative humidity conditions. Air temperatures between 10°C and 40°C at 10°C increments were used to test the full range within which the HPWH can operate. Relative humidity levels of 20% and 30% were the relative humidity levels achievable for the full temperature range with the experimental setup and, as such, were used to test HPWH performance at each of the tested air temperatures. The charge tests for each of the temperature and humidity pairs were used to create the experimental performance map. During a charge test, the performance of the HPWH in terms of the compressor power, heat rejection, and air cooling capacity were calculated between 10°C and 60°C water temperatures at 10°C increments. The results for the performance map are shown in Appendix A. Linear interpolation was used to determine heat rejection to the storage tank, compressor power, and sensible and total heat transfer from the air at temperatures, relative humidity levels, and storage tank temperatures between the tested values within the operating range.

Draw tests began with the water in the HPWH storage tank at a uniform 60°C temperature. Water draws then occurred at each hour throughout the experiments to correspond to CSA-F379.1 Schedule A 150 L daily draw profile. During the draw tests, water in the HPWH storage tank was replaced with chilled mains water. The draw test was conducted with inlet HPWH air conditions that simulated solar collector outlet temperatures. Solar collector outlet temperatures for Ottawa, Canada in January are shown in Figure 3.8 along with the hourly draw volumes for a 150 L daily draw.

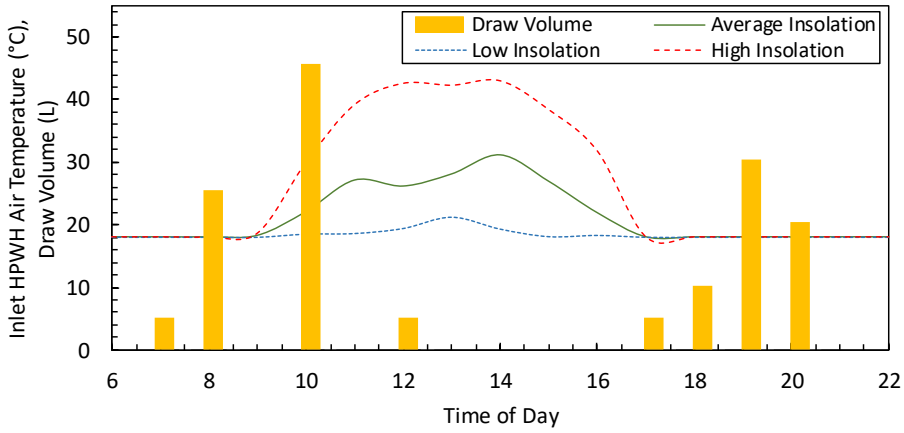

Figure 3.8: HPWH draw test input conditions

3.7 Experimental calculation methodology

The experimental analysis included calculation of the HPWH storage tank heat rejection, compressor power, and sensible and total heat transfer of the air across the HPWH. To calculate heat rejection, the storage tank was treated as a ten-node system with equal vertical spacing of 10 cm throughout the storage tank. The nodal heat rejection was the difference in energy of the current and previous timesteps, in Equation (3.1).

$$HR_t = \frac{E_{\mathrm{t}} - E_{\mathrm{t-1}}}{t} \tag{3.1}$$

In Equation (3.1), the subscript denotes the timestep considered, either the present or previous timestep, while E is the energy of the node in kJ and t is the timestep duration in hours. The nodal energy for each of the ten tank nodes at a given timestep was calculated from Equation (3.2), based on nodal volume, V in m^2, a temperature-dependent density parameter, ρ in kg/m^2, and specific heat capacity C_{p}.

$$E_{\mathrm{t}} = V\rho C_{\mathrm{p,water}}(T_{\mathrm{t}} - T_{\mathrm{ref}}) \tag{3.2}$$

Nodal energy was added together at each timestep to get the total energy delivered, $E_{\text{delivered}}$ in kJ. The COP was calculated as the ratio of the sum of the energy delivered to the sum of the energy consumed by the compressor, $E_{\text{compressor}}$, in kJ over the full test.

$$COP = \frac{\sum E_{\text{delivered}}}{\sum E_{\text{compressor}}} \quad \textbf{(3.3)}$$

The sensible cooling of the air, Q_{sens}, due to the temperature difference and total air cooling, Q_{total}, due to temperature and humidity differences between the inlet and outlet air were calculated from Equations (3.4) and (3.5), respectively.

$$Q_{\text{sens}} = \dot{m} C_{\text{p,air}} (T_{\text{in}} - T_{\text{out}}) \quad \textbf{(3.4)}$$

$$Q_{\text{total}} = \dot{m} (h_{\text{in}} - h_{\text{out}}) \quad \textbf{(3.5)}$$

In Equations (3.4) and (3.5), $\dot{m}$ is the mass flow rate of the air over the HPWH in kg/h. The subscripts in and out denote the air entering or leaving the HPWH, respectively. The enthalpy, h in kJ/kg, was calculated using the combined enthalpies of the dry air, h_{air}, and vapour, h_{vapour}, along with the humidity ratio, ω, as shown in Equation (3.6) [48].

$$h = h_{\text{air}} + \omega h_{\text{vapour}} \quad \textbf{(3.6)}$$

With constant specific heat capacities, the enthalpy of the dry air can be calculated as the product of the temperature and heat capacity, C_{p} in kJ/kg°C. The enthalpy of the vapour can be calculated from Equation (3.7).

$$h_{\text{vapour}} = h_{\text{sat}} + C_{\text{p,vapour}} T \quad \textbf{(3.7)}$$

Combining Equation (3.7), Equation (3.6) gives:

$$h = C_{\text{p,air}} T + \omega (h_{\text{sat}} + C_{\text{p,vapour}} T) \quad \textbf{(3.8)}$$

where $C_{\mathrm{p,air}}$, $C_{\mathrm{p,vapour}}$, and h_{sat} are 1.006 kJ/kg°C, 1.806 kJ/kg°C, and 2501 kJ/kg, respectively, as shown in Equation (3.9).

$$h = 1.006T + \omega(2501 + 1.805T) \tag{3.9}$$

To calculate the humidity ratio, the atmospheric pressure, p_{atm}, partial pressure of the air, p_{air}, and partial pressure of the vapour, p_{vapour}, all in kPa were used in Equation (3.10).

$$\omega = 0.6219\ \frac{p_{\mathrm{vapour}}}{p_{\mathrm{air}}} = 0.6219 \frac{p_{\mathrm{vapour}}}{p_{\mathrm{atm}} - p_{\mathrm{vapour}}} \tag{3.10}$$

The partial pressure due to the water vapour, which is equal to the partial pressure at the dewpoint temperature, T_{dp}, was determined experimentally through the procedure in [22] to follow the relationship shown in Equation (3.11).

$$p_{\mathrm{vapour}} = 6.1164\ x\ 10^{\frac{7.5914 * T_{\mathrm{dp}}}{T_{\mathrm{dp}} + 240.726}} \tag{3.11}$$

Calculation of the dewpoint temperature allows for the partial pressure of the vapour, humidity ratio, and therefore enthalpy and total heat transfer to be calculated.

3.8 Uncertainty analysis

In experimental analysis, there exist two main types of uncertainty which must be quantified to demonstrate the validity of the analysis. These uncertainties are bias uncertainties which occur as a result of uncertainty within the equipment, details of which are often provided by the manufacturer, and precision uncertainties which occur as a result of scatter in measured data. Precision uncertainty for this analysis was obtained based on the procedure in [49] from a data set having finite size. The calculation began with

determining the sample mean value, $\bar{x}$ based on the number of measurements, N, and the value of each measurement, x_{i}, as shown in Equation (3.12).

$$\bar{x} = \frac{1}{N}\sum_{i=1}^{N} x_{\mathrm{i}} \tag{3.12}$$

From the sample mean value, the sample variance s_{x}^2 and therefore the sample standard deviation s_{x} could be calculated using Equations (3.13) and (3.14), respectively.

$$s_{\mathrm{x}}^2 = \frac{1}{N-1}\sum_{i=1}^{N}(x_{\mathrm{i}} - \bar{x})^2 \tag{3.13}$$

$$s_{\mathrm{x}} = \left(\frac{1}{N-1}\sum_{i=1}^{N}(x_{\mathrm{i}} - \bar{x})^2\right)^{\frac{1}{2}} \tag{3.14}$$

The standard deviation of the means, $s_{\bar{\mathrm{x}}}$, was a function of the standard deviation of the sample, as well as the number of measurements, using Equation (3.15).

$$s_{\bar{\mathrm{x}}} = \frac{s_{\mathrm{x}}}{\sqrt{N}} \tag{3.15}$$

When a normal distribution was assumed with a 95% confidence interval, 95% of the measured values should be within a certain number of standard deviations from the mean, then the following was true:

$$x_{\mathrm{i}} = \bar{x} \pm t_{\nu,95\%}\, s_{\mathrm{x}} \tag{3.16}$$

where $t_{\nu,95\%}$ is the coverage factor that was determined based on the coverage factor table in [49], as a function of the confidence interval, in this case 95%, and the degrees of freedom, ν. The number of degrees of freedom was defined as one less than the number of measurements, as shown in Equation (3.17).

$$\nu = N - 1 \tag{3.17}$$

The precision uncertainty, u_{prec}, could be calculated from the coverage factor and the standard deviation of the means from Equation (3.18).

$$u_{\text{prec}} = t_{\nu,95\%}\, s_{\bar{x}} \tag{3.18}$$

The total uncertainty, u_{total}, was then calculated as a factor of the precision and bias uncertainty, u_{bias}, values. The total uncertainty was calculated from Equation (3.19).

$$u_{\text{total}} = \sqrt{u_{\text{prec}}^2 + u_{\text{bias}}^2} \tag{3.19}$$

3.8.1 Thermocouple uncertainty

Thermocouples are a temperature measurement device with two wires of dissimilar alloys (copper and constantan) coupled together. When a temperature difference occurs, the thermocouple produces a proportional voltage due to the dissimilar material properties. Using the voltage, and a known temperature of a reference junction called the cold-junction compensation (CJC) temperature, the temperature measured by the thermocouple can be determined. The relationship between the voltage and temperature can either be determined using tables by the National Institute of Standards and Technology (NIST) or using an equation obtained by thermocouple calibration [50]. The NIST thermocouple tables provide readings accurate to 0.5°C and do not include uncertainty due to the cold junction, therefore the uncertainty of the thermocouples in this research was obtained via more precise experimental calibration.

In the experimental apparatus, 30-gauge and 24-gauge thermocouple wire were used and both were calibrated based on the procedure described in [50]. In the calibration experiments, the thermocouple wire was placed in a uniform temperature bath with a temperature setting accurate to ±0.02°C. The temperature of the bath was brought to 5°C to begin the test and was slowly increased to 95°C in 2°C intervals, for a total of 46 temperature tests. Throughout the test, the temperatures were measured using a resistance temperature detector (RTD) with an accuracy of ±0.02°C. Simultaneously, the voltage readings from both gauges of thermocouple wire were recorded and a relationship between the voltage and the temperature difference was established for each. The relationships between voltage, V, and temperature, T, for the thermocouple wires were fitted based on a sixth order polynomial for 30-gauge and 24-gauge wire, as shown in Equations (3.20) and (3.21), respectively. The CJC temperature was measured on the NI 9214 thermocouple card using a built-in thermistor having an accuracy of ±0.25°C within the range of 23±5°C [51].

$$T_{30-\text{gauge}} = 0.00109 * \mathrm{V}^6 + 0.00615 * \mathrm{V}^5 - 0.0799 * \mathrm{V}^4 + 0.212 * \mathrm{V}^3 - 0.708 * \mathrm{V}^2 + 24.65 * \mathrm{V} - 0.186 + CJC \quad \textbf{(3.20)}$$

$$T_{24-\text{gauge}} = 0.00258 * \mathrm{V}^6 - 0.00374 * \mathrm{V}^5 - 0.0633 * \mathrm{V}^4 + 0.227 * \mathrm{V}^3 - 0.741 * \mathrm{V}^2 + 24.68 * \mathrm{V} + 0.091 + CJC \quad \textbf{(3.21)}$$

Uncertainty also occurred due to the voltage reading of the thermocouple card and resistance reading of the RTD, which were calculated in [50] to be 0.18°C and 0.04°C, respectively. The total uncertainty values for the 24-gauge and 30-gauge thermocouple

wires were calculated as 0.46°C and 0.49°C, respectively, by taking the square root of the sum of the squares of the values shown in Table 3.7.

Table 3.7: Uncertainty values for thermocouples used in experimental apparatus

Source of Uncertainty	30-Gauge (°C)	24-Gauge (°C)
Bath temperature homogeneity	0.02	0.02
Bath RTD reading	0.02	0.02
Resistance reading error	0.04	0.04
Voltage reading error - calibration	0.18	0.18
Voltage reading error - experimental	0.18	0.18
Regression prediction error	0.24	0.16
Cold junction temperature - calibration	0.25	0.25
Cold junction temperature - experimental	0.25	0.25
Total uncertainty	0.49	0.46

3.8.2 Draw volume uncertainty

The water flowmeter used in this experiment was a positive displacement flowmeter that operated by sending pulses to the data acquisition system corresponding to flow drawn. The flowmeter generated 282.8 pulses per litre of water and had a bias uncertainty of 1%. In the CSA-F379.1 Schedule A draw profile, draw volumes between 5 L and 45 L were drawn from the storage tank at various times throughout the day. When a water draw event occurred, the LabVIEW program sent a signal to open the water draw solenoid. Throughout all draws, the flowmeter measured the draw volumes via pulses, and the LabVIEW program sent a signal to close the solenoid valve when the draw volume was met.

The total uncertainty values for each water draw volume, all of which were less than the uncertainty limit of 0.14 L set by the CSA standard, were calculated from the procedure shown in Equations (3.12) through (3.19), and are shown in Table 3.8.

Table 3.8: Uncertainty values for each water draw volume

Water Draw Volume (L)	Uncertainty (L)	Uncertainty (%)
5	0.0626	1.25%
10	0.1091	1.09%
20	0.1107	0.55%
25	0.1046	0.42%
30	0.1187	0.40%
45	0.1105	0.25%

3.8.3 Coefficient of performance uncertainty

The coefficient of performance (COP) of the HPWH was used as a comparison mechanism between the experimental and simulated systems to validate the simulated model. As such, the experimental uncertainty propagation for the COP was calculated, based on the heat rejection to the storage tank, HR, and the compressor power, $P_{\text{compressor}}$, from the generalized formula for uncertainty propagation shown in Equation (3.22), and the specific formula for COP uncertainty shown in Equation (3.23).

$$u_{\text{y}} = \left(\sum_{i=1}^{N} \left(\frac{\partial y}{\partial x_{\text{i}}} u_{\text{i}} \right)^2 \right)^{1/2} \tag{3.22}$$

$$u_{\text{COP}} = \left(\left(\frac{\partial COP}{\partial HR} u_{\text{HR}} \right)^2 + \left(\frac{\partial COP}{\partial P_{\text{compressor}}} u_{P_{\text{compressor}}} \right)^2 \right)^{1/2} \tag{3.23}$$

To calculate the heat rejection uncertainty, the variables used in the heat rejection calculation (Equation (3.1)), volume, V, and temperature, T, were used in a variation of

Equation (3.22). Because density and specific heat capacity were calculated based on temperature, the error associated with these values was assumed to be negligible. The uncertainty of the heat rejection is shown in Equation (3.24).

$$u_{\mathrm{HR}} = \left(\left(\frac{\partial HR}{\partial V} u_{\mathrm{V}} \right)^2 + \left(\frac{\partial HR}{\partial T} u_{\mathrm{T}} \right)^2 \right)^{1/2} \tag{3.24}$$

The uncertainty due to the heat rejection was calculated based on the volume and temperature to be 1.66% over a draw test from Equation (3.24).

The uncertainty due to the compressor power was also calculated using the bias and precision uncertainties associated with the measurement. The bias uncertainty was 1% for the WattNode used within this experiment [43], with a 90 W resolution on each pulse, while the precision uncertainty was calculated using the procedure from Equations (3.12) through (3.19) with a 95% confidence interval to be 2.87%. With the bias and precision uncertainty values, the total uncertainty over a draw test was calculated as the square root of the sum of the squares to be 3.03% or 14.32 W. The uncertainty of the COP was then calculated over a draw test using Equation (3.23) and the values obtained for heat rejection and compressor power. The calculated uncertainty of the COP was 3.46% or 0.092.

3.9 Limitations and assumptions

The experimental apparatus included some limitations and assumptions throughout this research. The humidifier in the AHU was incapable of humidifying the air to high relative humidities, particularly at high temperatures. As such, the tested relative humidity range was limited to between 20% and 30% RH. One solution examined in this research was adding a humidifier filter after the humidifier in the AHU to facilitate further moisture

evaporation to the air. Although the humidity slightly increased, it was insufficient to test higher relative humidity values at the full temperature range. Ultimately, the best solution to this would be to heat the air prior to humidification to increase the humidity levels achievable. If air was heated prior to passing over the humidifier, the air would be capable of holding more moisture and thus higher humidity levels could be achieved. Despite the limitation, the existing humidification was deemed suitable for this research because the main objective was to analyse HPWH performance when coupled with a solar thermal collector in winter conditions, when moisture content within the air is lowest. When using either basement air or cool outdoor air through a solar collector, the increase in temperature resulted in a decrease in relative humidity, which often left the relative humidity within the 20% to 30% RH performance map range. As such, the limited relative humidity range in the experimental apparatus was not detrimental to this research.

Another limitation of the experimental apparatus was present in the power monitoring equipment. The WattNode used to measure the power of the experimental apparatus could not measure the HPWH compressor power and the element power separately, and thus all power readings were recorded together. Although this decreased the neatness of power readings, the difference in power consumption between the compressor which drew about 400-600 W and the element which drew 4000 W, made it clear which systems were operating when nonzero power readings occur.

The mains water cooling system caused another source of error within the experimental analysis. The mains water tank used to store chilled water to supply to the HPWH during hot water draw events was 136 L compared to the HPWH tank which was 189 L. Although

the mains water tank could store over 70% of the HPWH tank volume, it was unable to maintain 10°C HPWH supply temperatures during the largest draw events and instead increased to 15°C. Although the 10°C temperature was maintained for a high percentage of the draws, particularly the draw volumes between 5 L and 20 L, the increasing temperatures entering the HPWH tank added a small source of error to the analysis.

3.10 Summary of Experimental Apparatus

The experimental apparatus used within this study was described in this section. The experimental apparatus included a commercially available HPWH with a fully instrumented and controlled AHU, hot water draw system, and air and water chilling system. Water charging tests to heat the water in the storage tank and water draw tests to determine HPWH performance during draw events were conducted as described in this section. An uncertainty analysis was performed on the experimental system components to determine the error on the experimental COP calculated for the system. The experimental apparatus and procedures described in this section were used to update a performance map for the system and validate the simulated system model.

Chapter 4: System Modelling Approach

TRaNsient SYStem simulation software (TRNSYS) [52] was used to simulate performance of the HPWH and outdoor, conditioned, and closed loop SAHPWHs, shown in Figure 1.5, in locations across Canada and the United States. An overview of the simulation methodology, experimental validation, analysis methods and parameters, and limitations and assumptions are presented in this section.

4.1 Modelling overview

The modelling portion of this study included two main steps: modelling of the solar collector to determine inlet HPWH conditions for the experimental setup and full modelling of the HPWH and SAHPWHs. The performance of the experimental system with the simulated solar collector was compared to the full HPWH model for validation. The HPWH and SAHPWH models were then used for the modelling study and analysis.

The HPWH and SAHPWH modelling included analysis of the systems in various locations across Canada and the United States in terms of energy consumption, greenhouse gas emissions, and economic factors such as LCC and PBP. The configuration with the best performance based on each of these parameters was determined for each location studied.

4.2 System configurations analyzed

The configurations analyzed within this study were the HPWH, and the closed loop, outdoor, and conditioned SAHPWHs. All configurations studied included the same TRNSYS subroutines. The SAHPWH configurations differed in the location from which inlet solar collector air was drawn and to which air was exhausted: one recirculated air in a closed loop between the solar collector and HPWH, the second drew air from and

exhausted to outdoors, and the third configuration drew air from and exhausted to a conditioned space. The HPWH, like the conditioned SAHPWH, drew from and exhausted to a conditioned space and had an impact on space conditioning that was calculated based on the temperature differential at the inlet and outlet of the HPWH. Whenever the HPWH was operating, inlet air was 20°C and outlet air was cooler so space cooling occurred.

In the closed loop configuration, the inlet to the solar collector was the outlet to the HPWH and vice versa, which led to the SAHPWH system operating independently from the space conditioning system. Similarly, the outdoor air configuration which drew air from outside, heated it in the solar collector, and exhausted it to the outdoors was also independent of the space conditioning system. During periods of low insolation in colder climates, HPWH inlet temperatures in these two configurations decreased below 5°C, which is the threshold under which the HPWH does not operate. If water draws occurred dropping the water tank temperature was below 45°C and the inlet air temperature was below 5°C, the water recharged with the backup electric element which is in commercially available HPWHs.

In the conditioned configuration, air was drawn from a conditioned space so HPWH inlet air temperatures were always at least 20°C, meaning the electric element usage was eliminated. The conditioned space configuration removed air from a conditioned room, circulated it through the solar collector to the HPWH inlet, and exhausted air to the space causing net heating or cooling, depending on the temperature differential between the inlet and exit air. During periods of high solar insolation, if the exit HPWH air temperatures to the room were greater than the 20°C room temperature, heating occurred in the space. If the HPWH exit temperatures were lower than the room temperatures, cooling occurred in

the space. In addition, when the HPWH was not in operation and it was the heating season, all solar thermal gains from the collector were used to directly heat the space.

For the conditioned SAHPWH and the HPWH alone, the impact on space heating and cooling necessitated that heating and cooling seasons be defined to quantify the impacts and benefits due to the water heating systems. The heating and cooling seasons for the cities studied were defined based on ASHRAE climate zones, as shown in Figure 4.1.

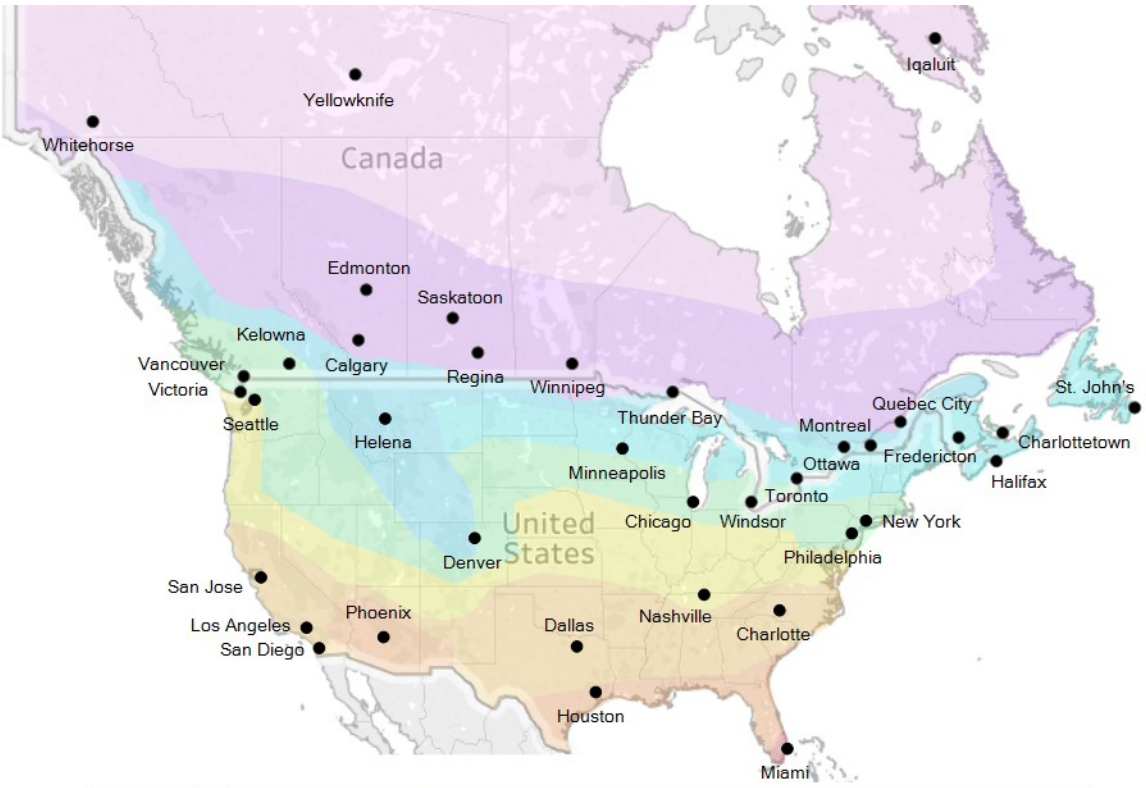

Climate Zone	Heating Season	Cooling Season
1	Jan	Feb, Mar, **Apr, May, Jun, Jul, Aug, Sept, Oct, Nov, Dec**
2	Jan	Feb, Mar, **Apr, May, Jun, Jul, Aug, Sept, Oct, Nov, Dec**
3	Dec, Jan	Feb, Mar, **Apr, May, Jun, Jul, Aug, Sept, Oct, Nov**
4	Nov, Dec, Jan, Feb	Mar, **Apr, May, Jun, Jul, Aug, Sept, Oct**
5	Nov, Dec, Jan, Feb, Mar	**Apr, May, Jun, Jul, Aug, Sept, Oct**
6	Oct, Nov, Dec, Jan, Feb, Mar	**Apr, May, Jun, Jul, Aug, Sept**
7	Oct, Nov, Dec, Jan, Feb, Mar, Apr	**May, Jun, Jul, Aug, Sept**
8	Sep, Oct, Nov, Dec, Jan, Feb, Mar, Apr, May, Jun	**Jul, Aug**

Figure 4.1: Climate zones and heating and cooling seasons for cities studied

4.3 Details of simulation modelling

The HPWH and SAHPWH configurations studied were modelled using different TRNSYS projects. The projects simulated the behavior of HPWHs and several SAHPWH configurations across Canada and the United States. The projects were systems composed of multiple common subroutines and all projects followed the same solution methodology.

4.3.1 Numerical solution methodology

In numerical simulation, solutions describe the behavior of a system over a desired time period, called the simulation runtime, that may be days, months, or years. The simulation runtime is broken into smaller periods called timesteps. At each timestep the simulation solves a set of equations, which is unique to the system analysed, under initial and boundary conditions to obtain the solution at said timestep. The solution is calculated using software-dependent numerical methods. Regardless of the numerical methods used, an iterative procedure is followed until the solution for the present timestep at the current iteration is sufficiently close to the solution at the previous iteration. When the solutions are close, as defined by the convergence criteria, convergence is said to be achieved and the simulation proceeds to the next timestep. If convergence is not achieved after a predefined number of iterations, a warning occurs before the simulation proceeds to the next timestep, and if a predefined number of warnings occur, an error aborts the simulation. This error indicates that the simulation has not converged throughout a high percentage of the simulation.

Prior to conducting a simulation, the tolerance criteria, timestep, and iterations to warning and error must be determined. Two types of tolerance criteria exist: rounding errors which are defined in TRNSYS by the tolerance integration, and truncation errors which are errors

due to the numerical methods used and are defined by the tolerance convergence in TRNSYS. In the annual simulations conducted in this study, the tolerance integration and tolerance convergence were set at 0.001 and 0.01, respectively.

To determine a timestep for this analysis, simulations were run at a range of timesteps and the maximum predicted solar collector outlet temperature in January for each simulation was recorded to illustrate variation due to different timesteps. The variation in predicted solar collector outlet temperature is shown in Table 4.1. To maintain a high timestep resolution and to match the experimental 1-minute recording frequency, 1-minute timesteps were chosen for the modelling.

Table 4.1: Effect of timestep on predicted maximum solar collector temperature

Timestep (minutes)	0.5	1	15	30	60
Mean temperature prediction (°C)	28.311	28.314	28.243	27.929	28.008
Variation between average prediction and current timestep (°C)	0.150	0.153	0.082	-0.232	-0.153

The behavior of the SAHPWH and HPWH systems through a year was used to compare the systems in various locations, so the simulation runtime for all simulations in this study was 1 year or 8760 hours. A summary of the simulation settings is shown in Table 4.2.

Table 4.2: Simulation settings used for analysis of SAHPWH and HPWH systems

Simulation Setting	Value Used
Tolerance integration	0.001
Tolerance convergence	0.01
Timestep (s)	60
Simulation runtime (h)	0-8760
Iterations before warning	50
Iterations before error	5000

In TRNSYS, subroutines have three different kinds of variables: parameters, inputs, and outputs. Parameters are constant value variables set at the beginning of the simulation. Inputs can either be set at a constant value like parameters or can be connected to a varying output from another subroutine. Outputs are the results from the solution of the equations associated with a subroutine. Because outputs from one subroutine are inputs of another, there must be a simulation order set to determine which subroutine should be solved first. The subroutine(s) solved first use inputs from the previous timestep, while subsequent subroutines use inputs that are outputs from another subroutine at the current timestep.

4.3.2 Overview of TRNSYS component interaction

The TRNSYS model used in this study simulated the behavior of HPWH and SAHPWHs using several interconnected components or subroutines or Types. Subroutines that modelled the solar collector, refrigeration cycle, water storage tank, and subroutines that read in weather files, controlled water draws, and recorded outputs were all combined to model full systems. An image of the project for the HPWH is shown in Appendix B.

A Type 15 weather file reader was used to read in typical meteorological year (TMY) and Canadian weather year for energy calculation (CWEC) files, and outputted properties such as solar insolation, ambient temperature, and mains water temperature. A Type 539 flat plate solar collector took the insolation and ambient temperature as inputs and calculated resultant outlet temperatures which were given to a refrigeration cycle. In analysis that did not include a solar collector, the inlet HWPH air temperature was a constant 20°C.

The refrigeration cycle had a wrap-around condenser coil to determine power consumption and heat rejection to the storage tank based on the inlet air conditions and an on/off control

signal. The HPWH storage tank, modelled using Type 534, took the heat rejection from the refrigeration cycle and determined the HPWH tank temperatures at each of the ten nodal positions. The tank temperatures were then fed back to the refrigeration cycle component. Based on the tank temperatures, a Type 1502 controller determined the on/off signal for the refrigeration cycle. When the refrigeration cycle could not maintain hot water temperatures, the controller turned on a Type 1226 electric element for supplemental heating to the storage tank. Hot water draws from the storage tank were imposed by a Type 1243a forcing function. During draw events, a Type 953 temperating valve determined the proportion of mains water and hot water required to achieve a distribution temperature of 55°C. The simulation data was recorded by Type 65 online plotters at each timestep.

4.3.3 Solar collector modelling

The solar collector modelling was conducted in two stages: first, as an independent unit to determine the outlet temperatures to use as inlet HPWH temperatures in the experimental setup and second, in the full SAHPWH simulations. The air-based solar collector simulated in this study was used to preheat the inlet air to the HPWH. As such, the outlet air of the solar collector was the inlet to the HPWH. Depending on the configuration of SAHPWH, the inlet air to the solar collector was either outdoor-temperature air, 20°C room air from the conditioned space, or air at the temperature of the HPWH outlet air.

The solar collector was based on the 1.26 m^2 Solar Venti SV14NS collector [53]. It was modelled using Type 539 with a flow rate of 320 kg/h which is the flowrate of the HPWH

fan during normal operation. The collector controls were set to maintain the collector flowrate while the collector was gaining energy and turn off when it was not.

The solar collector used ambient temperature and insolation from a weather TMY or CWEC weather file in the Type 15 weather data reader. The collector tilt angle was a parameter in Type 15 which calculated the incident beam, sky diffuse, and ground reflected radiation onto the collector, all of which were inputs to the collector. The collector tilt angle was set at 15° greater than latitude which is optimal for winter. The tilt angle was not varied throughout winter as Chu [32] has shown that there is little impact of varying tilt angle.

4.3.4 Water heating and thermal storage modelling

The experimental HPWH had condenser coils that wrapped around the water storage tank. Existing TRNSYS models, however, were not available to accurately predict the performance of wrap-around condenser coils. To address this, Khalaf [6] developed Type 240, which is a refrigeration cycle for a HPWH with wrap-around condenser model for use within TRNSYS. Type 240 used the storage tank temperatures at each of the ten nodal positions, the inlet air conditions, and an on/off control signal as inputs to determine the heat rejection delivered to each node and the sensible and latent heat removed from the air. When an on signal was received, the HPWH refrigeration cycle operated, and thus calculated the heat rejection to the storage tank and heat transfer from the air based on the experimental performance map. The heat rejection calculated by Type 240 for each nodal tank position was the input for the corresponding nodal position of the water storage tank.

The water storage tank took the nodal heat rejection values from the HPWH refrigeration cycle and calculated the nodal temperature throughout the tank. The nodal temperatures were fed back to the HPWH and to a Type 1502 controller.

The controller operated the HPWH refrigeration cycle and electric backup element (Type 1226) to reflect operation of the backup element in the experimental HPWH. If the storage tank temperature at node 3 was reduced to 5°C below the setpoint of 60°C and the ambient air temperature was greater than 5°C, the HPWH cycle received an ON signal to operate. If the storage tank temperature was reduced by 15°C below the setpoint or heating was called but the ambient temperatures were less than 5°C, the electric backup element would turn on and reject heat to node 3, the location of the upper heating element. The control scheme for the electric and heat pump heating systems is shown in Figure 4.2.

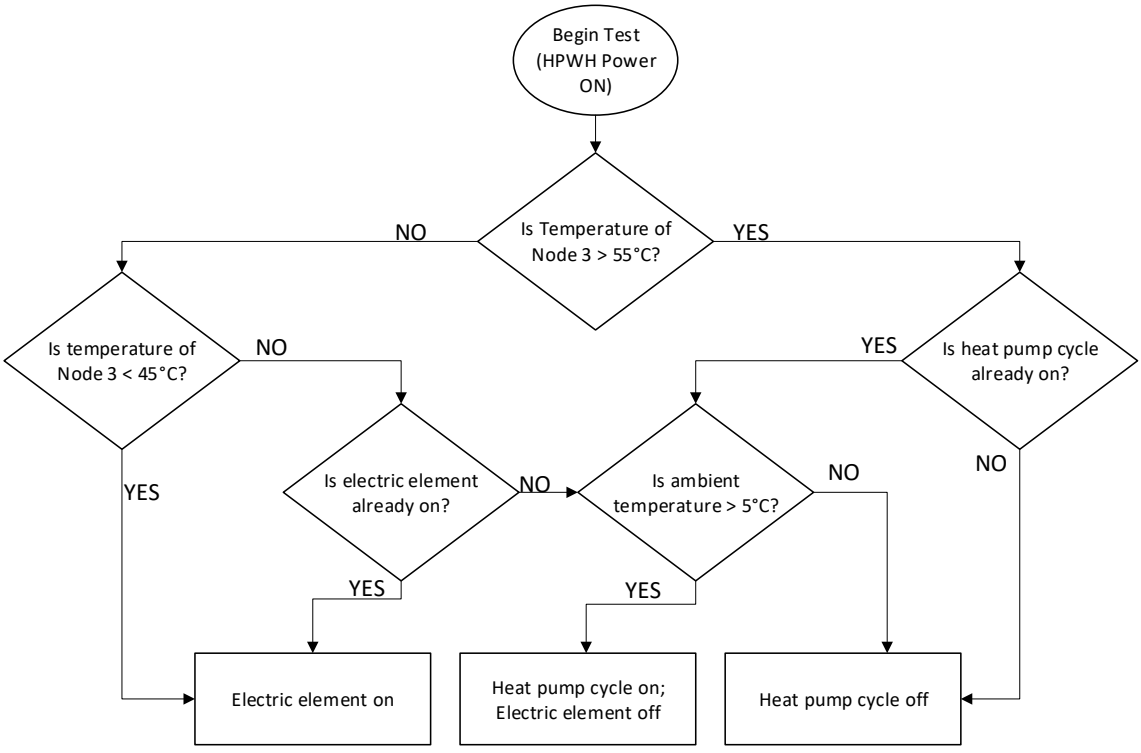

Figure 4.2: Water heating control logic

In addition to the direct heat energy input into the nodal locations from the condenser coils and electric element, heat transfer also occurred by mixing between adjacent nodes, water draws, and stand-by losses to the environment at each node of the storage tank. The heat loss due to water draws, mixing between nodes, and heat energy input were calculated during simulation of the system, but the stand-by losses were determined via experiment. Following the procedure outlined by Cruickshank [42] and Smith [22] calculated the net change in energy that occurred during cool-down tests of the tank to calculate the stand-by environmental losses of the system. In the cool-down tests, the HPWH was charged to a uniform 60°C temperature and was left to cool down, while the energy balance of each node was analyzed over time. The energy balance of the node in the i^{th} position in the tank is shown in Equation (4.1).

$$\begin{aligned}\rho_{\mathrm{i}} V_{\mathrm{i}} C_{\mathrm{p}} \frac{dT_{\mathrm{i}}}{dt} = {} & \frac{(k+\Delta k)A_{\mathrm{c,i}}}{\Delta x_{\mathrm{i+1\rightarrow i}}}(T_{\mathrm{i+1}} - T_{\mathrm{i}}) + \frac{(k+\Delta k)A_{\mathrm{c,i}}}{\Delta x_{\mathrm{i-1\rightarrow i}}}(T_{\mathrm{i-1}} - T_{\mathrm{i}}) \\ & + U_{\mathrm{i}} A_{\mathrm{s,i}}(T_{\mathrm{amb}} - T_{\mathrm{i}}) + \dot{m}_{\mathrm{down}} C_{\mathrm{p}} T_{\mathrm{i-1}} - \dot{m}_{\mathrm{up}} C_{\mathrm{p}} T_{\mathrm{i+1}} \\ & + \dot{m}_{\mathrm{in}} C_{\mathrm{p}} T_{\mathrm{in}} - \dot{m}_{\mathrm{out}} C_{\mathrm{p}} T_{\mathrm{out}} + P_{\mathrm{in}}\end{aligned} \quad \textbf{(4.1)}$$

In Equation (4.1), ρ is the fluid density in kg/m^2, V is the volume of the fluid with in the node in m^3, C_{p} is the specific heat capacity in kJ/kgK, k is the thermal conductivity of the fluid in W/mK, T is the temperature, $\Delta x_{\mathrm{i+1\rightarrow i}}$ is the distance between the centers of the node for which the energy balance is conducted and the node directly above, $A_{\mathrm{c,i}}$ is the nodal cross sectional area in m^2 which is the same for all nodes in a cylindrical tank, $A_{\mathrm{s,i}}$ is the nodal outer surface area in m^2, $\dot{m}$ is the mass flow rate in kg/h in or out of a node, or up or down within the storage tank caused by temperature gradients, P_{in} is the nodal power

input by the electrical element or heat pump cycle in kJ/h, and U is the heat loss coefficient in W/m^{2}K. A summary of the heat loss coefficients for each of the ten nodal positions in the storage tank, which are 10 cm-tall section of the storage tank, is shown in Table 4.3.

Table 4.3: Heat loss coefficients for each storage tank node

Node Number	Heat Loss Coefficient (W/m^{2}K)
1	0.956569
2	0.959190
3	0.957596
4	0.957691
5	0.961579
6	0.963551
7	0.989515
8	1.092323
9	1.277035
10	2.432742

When water draw events occurred, water was removed from the storage tank and chilled mains water replaced it. The mains water temperatures used for the storage tank inlet were mains water temperatures from the TMY or CWEC weather files, that varied based on location and time of year.

The water draw volumes in the draw profile used were set to occur at each hour at a flow rate of 11.5 L/min. A Type 14 forcing function was used to achieve these water draws. The forcing function drew water at the desired flow rate until the set volume requirement was met. When water was drawn from the storage tank, it was tempered to 55°C using a tempering valve which mixed the 60°C storage tank water with mains water to reach 55°C.

4.3.5 House model

Throughout most of this study, standalone HPWHs and SAHPWHs were used and impacts on space heating and cooling were calculated based on assumptions about heating and cooling seasons and using the outlet temperatures of the HPWH. A house model was used for a portion of this study to determine heating and cooling seasons, and to compare trends from the HPWH and SAHPWH impact on heating and cooling loads between the house model and the assumed impacts from the standalone models.

The house model was a two storey detached house developed by Baldwin [54] using TRNbuild. It had four zones: a main floor which was controlled by the thermostat at 20°C for heating and 23°C for cooling, a second floor, a basement, and an attic. Each floor had an area of 110 m^2, and the total air volume was 835 m^3. For air distribution, 20% of conditioned air went to the basement, 35% to the main floor, and 45% to the second floor. The second floor had a larger proportion of the conditioned air supply to account for the higher loads required to maintain temperatures as a result of the energy losses in the second floor to the attic. The house had four occupants and an air infiltration rate of 0.05 ACH. The windows had a U-value of 1.27 W/m^2K. The thermal resistance values for the above and below grade walls were 4.5 m^2K/W and 2.7 m^2K/W, respectively.

The impact of the HPWH or SAHPWH on the heating or cooling load was the difference in performance of the house model with and without the system in place. The impact of the HPWH or SAHPWH on the house model was compared to the assumed impact of the standalone HPWH or SAHPWH model on the space conditioning loads.

For the space conditioning impact of the standalone systems, the temperature differential of the room air and the outlet air of the HPWH or SAHPWH were used to calculate the heating or cooling load caused. If space cooling occurred during winter, it was said to increase the space heating load, whereas if space cooling occurred during summer, it was said to decrease the space cooling load.

4.4 Parameters analyzed

The HPWH and SAHPWH configurations were analyzed based on three main categories: energy consumption and reduction, greenhouse gas emissions (GHGs) reduction, and economics such as PBP, LCC, and possible financial incentives or subsidies. For each evaluation criteria, the best configuration option in each location was determined.

4.4.1 Energy consumption and reduction methodology

Energy consumption required to heat water for one household on an annual basis was calculated using TRNSYS for the HPWH and SAHPWH configurations studied. The total energy consumption was the sum of the electricity consumption by the compressor in the heat pump cycle and the electricity consumed by the electric backup element. The energy reduction or offset due to the HPWH or SAHPWH was calculated relative to an electric or natural gas water heater. The coefficient of performance of the HPWH was used, in addition to the compressor energy consumption and backup element consumption to calculate the electric or natural gas energy consumption for a water tank having similar physical characteristics to the HPWH. The energy consumed by the system to which the HPWH or SAHPWH energy consumption was compared, E_{system}, was calculated as:

$$E_{\text{system}} = \frac{E_{\text{compressor}} * COP + E_{\text{element}}}{\eta_{\text{system}}} = \frac{E_{\text{HPWH}}}{\eta_{\text{system}}} \quad \textbf{(4.2)}$$

where $E_{\text{compressor}}$ is the energy consumed by the heat pump compressor in kJ, COP is the heat pump coefficient of performance, E_{element} is the heat input to the HPWH tank from the electric backup element in kJ, and η_{system} is the efficiency of the system for which the energy calculation is conducted. $E_{\text{HPWH}}$is the total energy consumed to heat the water in the storage tank, which was considered to be constant between any system studied to represent storage tanks with the same characteristics such as size and heat loss and to capture only changes to the energy consumption due to the fuel type, rather than to variations in size or geometry. The energy offset was taken as the difference of the energy consumed by the alternative system and the HPWH or SAHPWH system.

The energy added or removed for space conditioning due to the HPWH or SAHPWH was also analyzed. Space cooling due to the HPWH or SAHPWH during the cooling season was said to decrease house space cooling loads, while space cooling during the heating season was said to increase the heating loads. Similarly, space heating due to the SAHPWH in the heating season was said to decrease space heating loads. The change in energy consumption for space heating and cooling caused by the HPWH or SAHPWH was calculated based on Equation (4.3) and (4.4), respectively.

$$E_{\text{heating}} = \frac{S_{\text{heating}\rightarrow\text{HS}} - S_{\text{cooling}\rightarrow\text{HS}}}{\eta_{\text{heating}}} \quad \textbf{(4.3)}$$

$$E_{\text{cooling}} = \frac{S_{\text{cooling}\rightarrow\text{CS}}}{\eta_{\text{cooling}}} \quad \textbf{(4.4)}$$

The term S, in kJ, represents the impact on space conditioning due to the HPWH or SAHPWH. The subscripts represent space cooling c or heating h, that occurred during the heating season HS or cooling season CS due to the HPWH or SAHPWH. $S_{c\rightarrow HS}$, for example, indicates space cooling during the heating season, thus energy for space heating increased. The heating efficiency was assumed to be 1 for electric space heating and 0.67 for natural gas, while the cooling efficiency was assumed to be 3.5.

4.4.2 Greenhouse gas emissions reduction methodology

The GHG reduction was calculated by first determining the GHGs produced from each fuel type per unit of energy consumed, or GHG intensity, of all fuel types as a carbon dioxide equivalent value. The IPCC report values for GHGs by fuel type for the 50th percentile were used [55], as shown in Table 4.4.

Table 4.4: Emissions intensity of electricity generation fuel sources used in Canada

Fuel Source	GHG Intensity (gCO_2e/kWh)
Hydro	4
Wind	12
Nuclear	16
Biomass	18
Solar	46
Natural Gas	469
Oil	840
Coal	1001

With the emissions intensity for each fuel source, the breakdown of electricity generation by fuel source for each location studied was required to calculate the GHG intensity in each location. The GHG intensity of the Canadian locations are shown in Table 4.5. The GHG intensity values used for the American locations are provided in Appendix C.

Table 4.5: GHG intensity of electricity grids in Canadian locations

Location	GHG Intensity (gCO2e/kWh)
Alberta	662.76
British Columbia	22.58
Manitoba	58.81
New Brunswick	282.03
Newfoundland	45.94
Northwest Territories	490.44
Nova Scotia	682.36
Nunavut	840.00
Ontario	35.57
Prince Edward Island	20.34
Quebec	4.46
Saskatchewan	631.10
Yukon	63.46

The electricity generation fuel sources on an annual basis were used from the National Energy Board for the Canadian provinces and territories [56]. A comparison was done for annual electricity fuel sources and fuel source variations based on seasons and on- mid- and off-peak generation, as shown in Appendix D.

To consider the GHG equivalent values of the HPWH and SAHPWH systems over their lifetimes, the refrigerant leakage over the lifetime was considered. Annual leakage rates for heat pumps typically range from 3% to 10% [57] and an average value of 6% was used for this study. The GHG offsets, GHG_{offset}, in $kgCO_2e$ were calculated as follows:

$$GHG_{\text{offset}} = E_{\text{system}} * I_{\text{fuel}} + E_{\text{heating}} * I_{\text{heating}} + E_{\text{cooling}} * I_{\text{electricity}} - (E_{\text{HPWH}} * I_{\text{electricity}} + m_{\text{r}} * I_{\text{r}} * (1 - (1 - R)^{\text{n}})) \quad \textbf{(4.5)}$$

where I is the GHG intensity of the fuel source (either electricity, natural gas, or refrigerant) in $kgCO_2e/kWh$, E_{system} is the energy consumption of the alternative water heating system

in kWh, E_{heating} is the reduction in space heating, E_{cooling} is the reduction in space cooling, m_{r} is the refrigerant charge in kg that the HPWH was charged with when manufactured and the subscript r denotes the refrigerant, R is the leakage rate of the refrigerant from the HPWH, and n is the projected lifetime of the HPWH which is 15 years.

4.4.3 Economic evaluation methodology

Economic evaluation of the HPWH and SAHPWHs included simple PBP, LCC, breakeven analyses, and potential subsidies and effects of carbon pricing. Throughout this analysis, the electricity rates for the locations studied were required, and local currency was used for all analysis. The utility rates for the Canadian provinces and territories are shown in Table 4.6. The utility rates for the American locations are provided in Appendix B.

Table 4.6: Utility rates for Canadian provinces and territories

Location	Electricity Rate ($/kWh)	Natural Gas Rate ($/kWh)
Alberta [58], [59]	0.068	0.0199
British Columbia [60], [61]	0.0945	0.0320
Manitoba [62]	0.0874	0.0406
New Brunswick [63], [64]	0.1091	0.0827
Newfoundland [65]	0.12	*
Northwest Territories [66]	0.301	*
Nova Scotia [67], [68]	Off-peak: 0.08676 On-peak: 0.15603	0.0713
Nunavut (Iqaluit) [69]	0.5856	*
Ontario [70], [71]	Off-peak: 0.065 Mid-peak:0.094 On-peak: 0.134	0.0227
Prince Edward Island [72]	0.1437	*
Quebec [73], [74]	0.0608	0.0181
Saskatchewan [75]	0.1565	0.0169
Yukon [76]	0.1214	*

*Natural gas not available in PEI, Newfoundland, or territories [77]

The natural gas rates in Table 4.6 include a carbon tax of $0.039 per cubic metre of natural gas [78]. The electricity and natural gas rates were used in the simulations to calculate the annual cost of water heating. The annual operating costs were calculated from the electricity cost of water heating, as well as the impact on space heating and cooling loads where applicable, as follows:

$$X_{\mathrm{HPWH}} = W + c_{\mathrm{fuel,h}}\left(S_{\mathrm{cooling\rightarrow HS}} - S_{\mathrm{heating\rightarrow HS}}\right) - c_{\mathrm{fuel,c}}\left(S_{\mathrm{cooling\rightarrow CS}}\right) \quad \textbf{(4.6)}$$

where X_{HPWH} is the annual operating cost of the HPWH or SAHPWH, W is the electricity cost for water heating, c_{fuel} is the cost of the space heating or cooling fuel per kWh, and S represents the impact on space conditioning due to the HPWH or SAHPWH operation which was described in Section 4.4.1.

To encompass the high capital cost and low operating cost of HPWHs and SAHPWHs and compare against other water heating systems, the PBP and LCC calculations were used. The following formulae for the economic analysis are shown for HPWHs but are applicable to SAHPWHs as well. The PBP formula used was:

$$PBP = \frac{C_{\mathrm{HPWH}} - C_{\mathrm{system}}}{(X_{\mathrm{system}} + M_{\mathrm{system}}) - (X_{\mathrm{HPWH}} + M_{\mathrm{HPWH}})} \quad \textbf{(4.7)}$$

where C is the capital cost of the HPWH or system, M is the annual maintenance costs, and X is the annual operating cost of the HPWH or other water heating system. The capital, maintenance, and installation costs used for the water heating systems are shown in Table 4.7. An exchange rate of 1.33 CAD per USD [79] and an inflation rate of 2% [80] were used.

Table 4.7: Capital and installation costs of water heating systems

	HPWH	SAHPWH	Electric water heater	Natural gas water heater
Capital Cost (CAD) [19]	1714.52	3673.18 [81]	415.06	660.00
Installation Cost (CAD) [19]	607.05	920.00 [81]	421.90	694.67
Annual Maintenance Cost (CAD) [19]	23.33	57.62	16.50	16.70

The capital, installation, and maintenance costs were also used to calculate the LCC [19] which is the sum of all costs throughout the lifetime of a system, as shown in Equation (4.8).

$$LCC = C + X_{\mathrm{PV}} + M_{\mathrm{PV}} \quad \textbf{(4.8)}$$

In the LCC calculation, X_{PV} and M_{PV} are the present value of the annual operation and annual maintenance costs throughout the lifetime of the system. The present value of each annuity was calculated as shown for the operating cost, but the same formula applies to the maintenance costs:

$$X_{\mathrm{PV}} = X * \frac{1 - (\frac{1}{1+r})^{\mathrm{n}}}{r} \quad \textbf{(4.9)}$$

where r is the percent interest rate and n is the lifetime in years. The interest rate was based on the discount rate d and the 2% inflation rate i [82] as shown in Equation (4.10). The DOE discount rate of 3% was used [83] with sensitivity at the recommended Canadian interest rate of 8% [84].

$$r = (1 + d) * (1 + i) - 1 \quad \textbf{(4.10)}$$

A variation of the LCC calculation was also used to compare the LCC of an alternative system such as an electric or natural gas water heater to the HPWH using a cost breakeven calculation [19]. The breakeven cost analysis was used to calculate the capital cost requirement for a HPWH that results in the HPWH having the same LCC as an alternative system. If the breakeven cost calculated, $C_{\mathrm{BE,HPWH}}$, was less than the actual HPWH capital cost, then the capital cost of the HPWH must decrease to be economically preferred. Alternatively, if the calculated breakeven cost was greater than the actual HPWH capital cost, the HPWH was currently economically preferred. The breakeven HPWH capital cost was calculated as:

$$C_{\mathrm{BE,HPWH}} = C_{\mathrm{system}} + \left(M_{\mathrm{PV,system}} - M_{\mathrm{PV,HPWH}}\right) + (X_{\mathrm{PV,system}} - X_{\mathrm{PV,HPWH}}) \quad \textbf{(4.11)}$$

where the subscripts denote the systems in comparison and the present value for the annual maintenance and operating costs. The breakeven cost was used to determine if a new system such as a HPWH was presently an economically viable option to replace another system such as an electric or natural gas water with. In addition, if uptake of the more expensive system was desired, a financial government subsidy could be introduced for the difference in the calculated breakeven cost and the actual capital cost to increase uptake. The subsidy, F, for a HPWH was calculated from Equation (4.12).

$$F = C_{\mathrm{HPWH}} - C_{\mathrm{BE,HPWH}} \quad \textbf{(4.12)}$$

The required subsidies when transitioning either from natural gas or electric water heating to HPWH were calculated for each location studied.

The effect of carbon pricing was also considered in the breakeven and subsidy calculations to determine the impact of a potential carbon price, CP, on the economic feasibility of switching from an electric or natural gas water heater to a HPWH or SAHPWH. If the HPWH results in a GHG offset, the carbon price increases the cost associated with an alternative system thus making the HPWH more feasible. The adjusted breakeven cost associated with the HPWH when carbon pricing is considered is shown in Equation (4.13). For this analysis a carbon price of $50 per metric ton of carbon dioxide equivalent was analyzed [85]. The subsidy calculation was also adjusted using the breakeven cost with carbon pricing to determine the impact on the required subsidy for a HPWH.

$$C_{\mathrm{BE,HPWH,CP}} = C_{\mathrm{BE,HPWH}} + GHG_{\mathrm{offset}} * CP \quad \textbf{(4.13)}$$

In addition to the calculations and values indicated within this section, sensitivity analysis was conducted to determine the impacts of the assumed inflation, discount rate, lifetime, capital costs, air conditioning COP, space heating efficiency and fuel, and carbon tax value. The calculations were conducted for each location studied and the sensitivity analysis was conducted for a location in each climate zone.

4.5 Limitations and assumptions

The simulation analysis was subjected to a number of assumptions throughout the process. For the HPWH itself, the assumptions of uniform temperature of each node of a storage tank and one-dimensional heat transfer were made, both of which are common assumptions in modelling of domestic hot water storage tanks. Additionally, it was assumed that there was no air pressure difference over the HPWH. In reality, a small pressure difference would occur but it was deemed negligible in this analysis.

When comparing the commercially available HPWH to alternative water heating systems, commercially available alternatives were not analyzed. Rather, it was assumed that the alternative systems would have the same characteristics as the HPWH, and as such, the COP and energy consumption of the HPWH were used to calculate the energy consumption of the alternatives. Although commercially available water heating alternatives would have different properties such as geometry, heat losses, and heating techniques, these differences were not considered in this analysis. Neglecting the differences allowed the HWPH to be compared to systems with storage tank characteristics that were as similar as possible to the HPWH tank itself, thus the analysis only considered variations due to fuel type and not due to variations in geometry or other parameters.

The heating and cooling seasons were verified by the house model for each climate zone, but it was assumed for the standalone HPWH and SAHPWH analyses that the heating and cooling seasons did not overlap, despite that there may be both heating and cooling during a single month, in reality. Distinct heating and cooling months were used in this analysis because overlapping the conditioning seasons would misrepresent the increases and decreases in space conditioning loads due to the HPWH and SAHPWH. For example, with the SAHPWH in the winter, the solar collector provided space heating benefits and in the summer the system provided cooling benefits. Thus, if the heating and cooling seasons overlapped for a few weeks or a month, dual benefits would be counted for that duration, so the annual benefits would be overstated. As such, distinct heating and cooling seasons were used in this analysis.

When comparing the HPWH and SAHPWH in the house model and standalone models, the same single detached house with the same insulation was used regardless of the climate zone studied. In reality, houses in warm climate zones typically require less insulation than those in cold climate zones, but this was not captured within this study. However, because only the difference in energy consumption due to the HPWH or SAHPWH was analyzed within this project rather than the full space conditioning loads, varying the insulation for each climate zone was likely to have little to no impact on the results from this study.

In the GHG analysis, the GHG emissions were assumed on an annual basis rather than an hourly basis varying with on- and off-peak hours or with heating and cooling seasons. Although there is some variation, in GHG intensity, the variance due to the HPWH or SAHPWH was small and was neglected.

It was assumed that there were no heat losses in the ducts connecting the solar collector to the HPWH. The temperature to which the air was heated in the solar collector was assumed to be the same temperature as the inlet temperature to the HPWH. In reality, the solar collector would be on a roof and the HPWH is often located in a basement, so there would be heat losses in the large physical distance between the two components.

In the cost analysis of the solar collector, it was assumed that the system was a regular contract installation rather than a single system [81]. As such, the assumption was made that the contractor installing the solar collector and duct work would have access to the required materials and would be familiar with the installation procedure, allowing them to be priced at a cheaper cost than a one-time system installation.

4.6 Summary of the modelling approach

This chapter provided the modelling methodology used within the simulations and a description of the TRNSYS subroutines used within the simulations. In addition, the calculation methodology used for the energy, GHG, and economic analyses were discussed. The modelling methodology and simulation techniques described in this chapter were used throughout this study for detailed modelling of the various configurations of SAHPWH across Canada and the United States.

Chapter 5: Results

The results obtained through this research include the experimental model validation and all simulations for which the validated model was used. The simulations included a comparison of the HPWH and SAHPWH systems in a house model and as standalone systems with assumptions about the space conditioning impacts, and the results of the energy analysis, GHG reductions, and economic analysis. The trends for all climate zones are provided in this chapter. The results are shown for sample locations within each climate zone; the purpose of this is to show trends caused by variation in climate. There may, however, be slightly different trends for different locations within each climate zone, depending on the electricity generation sources and prices in each location. The sample locations used for this study are shown in Table 5.1.

Table 5.1: City used to illustrate trends between climate zones

Climate Zone	Sample City	Local Currency
1	Miami, FL	USD
2	Phoenix, AZ	USD
3	Dallas, TX	USD
4	Nashville, TN	USD
5	Chicago, IL	USD
6	Toronto, ON	CAD
7	Winnipeg, MB	CAD
8	Whitehorse, YK	CAD

5.1 Experimental validation

The experimental validation was done by comparing the experimental results to simulations under the same inlet conditions. A solar thermal collector was simulated using TRNSYS and the output temperatures for the solar collector were the inlet experimental conditions used in the AHU. In the experimental setup, there was some variation between

the setpoint inlet HPWH air temperature and mains water temperature conditions. The actual temperatures, draw volumes, and humidity values that occurred in the experimental test were recorded and used as inputs for the simulation. The HPWH model and the experimental HPWH were run using these same conditions to compare performance.

The HPWH model was validated in [6], so the validation process in this study was conducted to analyze the performance under the lower air and water temperature capabilities of the experimental system that were added in this study. The experimental apparatus was run using inlet air and mains water temperature conditions representative of an average day in January, and the simulated HPWH model was run under the same input conditions. The hourly draw volumes and inlet HPWH temperatures throughout the test are shown in Figure 3.8. A comparison of the storage tank temperature and compressor power for the experimental and modelled systems over a single day test is shown in Figure 5.1.

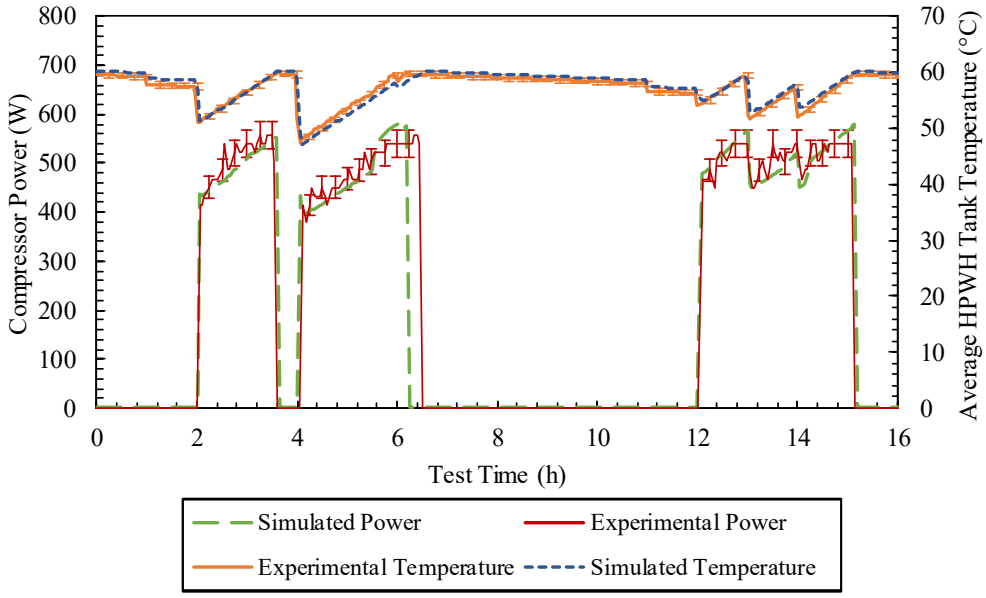

Figure 5.1: Comparison of experimental and simulated results

The offset in experimental and simulated power near the test time of 6 hours was caused by water mixing in the experimental storage tank, which did not occur in the simulations, due to the inlet water flow rate of 11.5 L/min. When nodal mixing with cold mains water occurred, experimental tank temperatures at nodes near the condenser coils decreased below that of the simulated tank temperatures in which mixing did not occur. The decrease in experimental temperatures reduced compressor power and caused charging over a greater time than the simulated system which had higher temperatures in most bottom tank nodes and therefore higher compressor power. Despite the offset, however, the total compressor energy consumption deviated by only 3.71% through the day long test.

The mean average error (MAE) was used to compare the simulated and experimental datasets. The MAE is the average difference between the experimental and simulated result at each timestep over the duration of the test. The MAE between the simulated and experimental results was 8.1 W for the compressor power and 0.40°C for tank temperature over the day-long draw test. The coefficient of performance was also calculated based on the experimental and simulated results to have a MAE of 0.042.

The heat rejection and compressor power for the day-long test are shown in Table 5.2. In the full day-long test, the experimental and simulated compressor power and heat rejection had a difference of 3.7% and 2.0%, respectively. A summary of the results obtained using the model and experimental setup is shown in Table 5.2. The differences between the simulated and experimental results were within the range of experimental error, so the model provided a sufficient degree of accuracy for comparison of results for various locations and configurations in annual simulations.

Table 5.2: Heat rejection and compressor power in day-long tests

	Model	Experimental	Difference	Percent Difference
Heat Rejection (kWh)	10.01	10.21	0.20	1.96%
Compressor Energy (kWh)	3.47	3.60	0.13	3.71%
COP	2.88	2.83	0.05	1.79%

5.2 Energy performance of configurations analyzed

The energy performance of the HPWH included the energy required to heat water and the energy impact of the HPWH on the space conditioning system. The energy required to heat the water was dependent upon the air temperatures, water temperatures, and water draw volumes, while the energy impact on space conditioning was dependent upon outlet air temperatures, and space conditioning seasons.

5.2.1 Energy for water heating

The energy consumed for water heating varied based on the location, configuration, and draw profile, which defined the solar insolation, air temperatures, water temperatures, and draw volumes used. The impacts of the parameters were analyzed in various tests with different constant air inlet temperatures, different draw profiles, and different locations with different configurations.

A simulation was run with 30°C, 20°C, and 10°C inlet air temperatures to the HPWH to quantify the impact of varying air temperatures on the energy consumed by the compressor and the heat rejection. The results are shown in Table 5.3.

Table 5.3: HPWH energy consumption and heat rejection with inlet air temperature

	Inlet Air Temperature (°C)		
	10	**20**	**30**
Compressor Energy (kWh)	4.76	4.20	3.66
Heat Rejection (kWh)	8.86	8.89	8.92
COP	1.86	2.12	2.44

When all other parameters were maintained constant in a day-long test and the air temperature varied from 10°C to 30°C, there was a 23% decrease in compressor energy consumption, less than a 1% increase in heat rejection, and a 31% increase in COP. At lower temperatures, the compressor consumed more energy to provide nearly the same amount of heating, thus reducing the COP. At the same mains water temperature conditions, the same heat rejection must be delivered to heat the water, causing the heat rejection to be maintained relatively constant. Although the mains water temperatures were constant within this test, they were greater than those in the validation test day shown in Table 5.2, which caused a greater compressor power and lower heat rejection in this test than the validation test.

The effect of different inlet air temperatures can be seen in a comparison of the annual electricity consumption between the HPWH and the conditioned space, closed loop, and outdoor air SAHPWHs in Figure 5.2. Various tank volumes and daily draw volumes were examined to illustrate trends caused by variations in system design and performance. In this analysis, all input parameters were maintained constant, except the daily draw or tank volumes studied. Annual electricity trends in Ottawa, which are representative of major

cities across Canada, and Dallas, which are representative of the southern United States are shown in Figure 5.2.

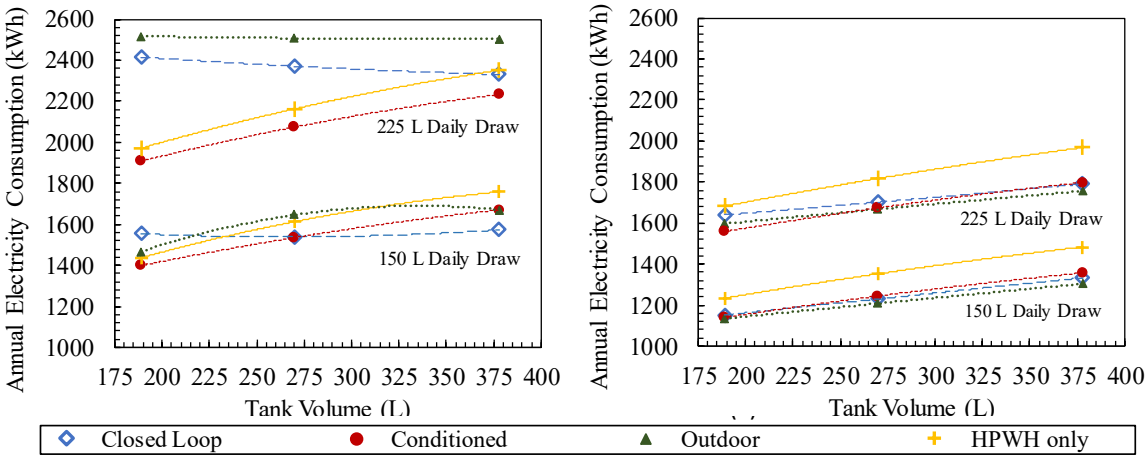

Figure 5.2: Variation in annual electricity consumption with daily draw volume, tank size, and configuration in Ottawa, Ontario (left), and Dallas, Texas (right)

In Ottawa, the conditioned configuration had lowest electricity consumption in most cases, because relatively low winter air temperatures and insolation levels limited the performance of the outdoor and closed loop configurations. In the conditioned configuration, inlet HPWH air temperatures were at least 20°C, whereas the closed loop and outdoor configurations inlet temperatures were below 5°C during periods of low insolation and temperature. Below 5°C inlet air temperatures, which were common in the closed loop and outdoor air configurations in Ottawa, an electric backup element heated the water, significantly increasing electricity consumption. The outdoor configuration had a high proportion of time during which the electric element operated and thus often had greatest annual electricity consumption. The closed loop configuration only had the least electricity consumption in Ottawa when the storage tank size was relatively large compared to the daily draw volume. This is because at larger tank volumes with relatively small draws, less variation in tank temperature occurred, limiting the fraction of time the tank

temperature was below 45°C and thus the time electric backup element operated for the closed loop configuration, therefore reducing overall electricity consumption. Further, the electric element only turned on below 45°C, and if air temperatures were below 5°C, the HPWH would not operate, thus the tank temperature was significantly lower for the closed loop case than the HPWH or conditioned cases leading to lower electricity consumption.

For all configurations in both locations, electricity consumption increased for larger tank sizes that were oversized for the draw volume, due to two main factors: greater losses from the tank occur at larger tank volumes, and more energy was consumed to heat water at higher temperatures, which occurred for a larger portion of time with larger tank sizes. This indicated the importance of properly sizing storage tanks to hot water demand in reduction of electricity. Although the closed loop configuration had lower electricity consumption in larger tank volume cases, it would be impractical to design a system with these characteristics.

In Dallas, ambient temperatures and solar insolation were high so there was more time during which the inlet temperatures to the HPWH were above 5°C in closed loop and outdoor configurations, meaning the SAHPWHs could operate without the electric backup element for significantly more time throughout the year. As such, there was little variation in electricity consumption between the three SAHPWH configurations in Dallas. The slight variations in annual electricity consumption can be partially attributed to differences in the inlet temperatures of the HPWH air, because greater inlet temperatures improve HPWH performance. The closed loop and outdoor configurations had higher inlet temperatures than the conditioned configuration for a larger portion of the year, which lead to lower

electricity consumption. In addition, the overall electricity consumption for all configurations including the HPWH-only scenario was lower in the southern United States than Canada due to warmer mains water temperatures.

Mains water temperatures were found to significantly impact water heating energy consumption across the climate zones. The sample cities in each climate zone were used to illustrate the trends in annual energy consumption for the various water heating methods. The annual electricity consumption with the SAHPWHs, HPWH, EWH, and NGWH are shown in Figure 5.3.

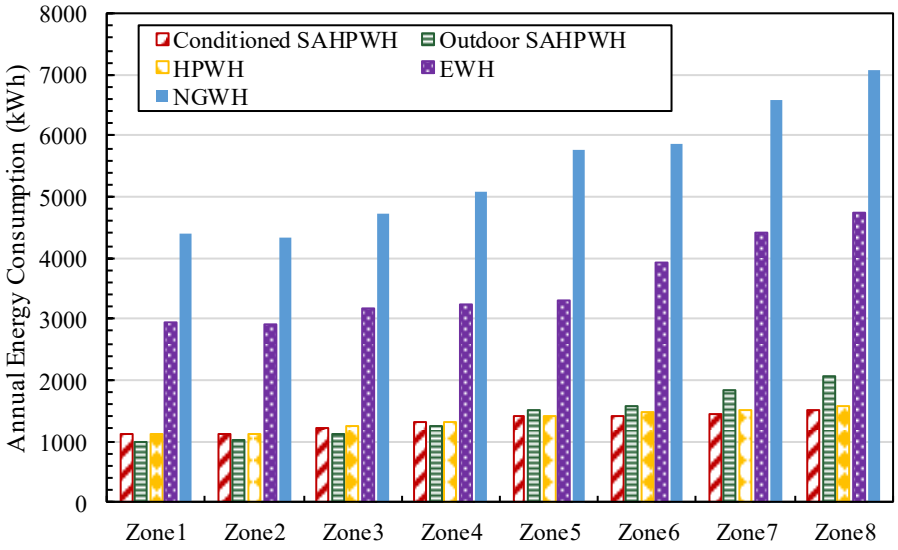

Figure 5.3: Energy consumption with various water heating methods

Although electricity consumption was reduced from the EWH or NGWH to the HPWH, a lower difference in electricity reduction was observed between the HPWH and SAHPWHs. The conditioned SAHPWH and HPWH had similar energy performance in all locations due to the low variation in inlet air temperatures between the two configurations. Because the solar collector increased inlet HPWH air temperatures above room temperature (20°C)

during periods of sufficient insolation, the conditioned SAHPWH had slightly lower electricity consumption than the HPWH which had constant 20°C inlet air temperatures.

A larger variation occurred between the outdoor and closed loop SAHPWH configurations and the HPWH due to the variation in outdoor temperatures among the climate zones. In climate zones 1 through 4, temperatures were warmer than 20°C during a significant portion of the year, and the solar collector increased temperatures further to reduce electricity consumption compared to the HPWH or conditioned SAHPWH. In colder climate zones such as 5 through 8, ambient temperatures were often sub-zero so the solar collector was insufficient to heat the air above the operating limit of 5°C in some cases, and the outdoor and closed loop SAHPWHs relied heavily on the backup electric element.

The electricity offsets between the EWH and the SAHPWH and HPWH configurations were also quantified to determine the savings realizable when transitioning to a new system. The greatest electricity offsets occurred for configurations that consumed the least energy in the chart shown in Figure 5.3. The offsets for all locations and configurations are shown in Figure 5.4. It was found that despite usage of the electric element in some cases, colder climate zones achieved higher electricity offsets due to the greater absolute electricity savings realized when transitioning to the more efficient HPWH from the EWH.

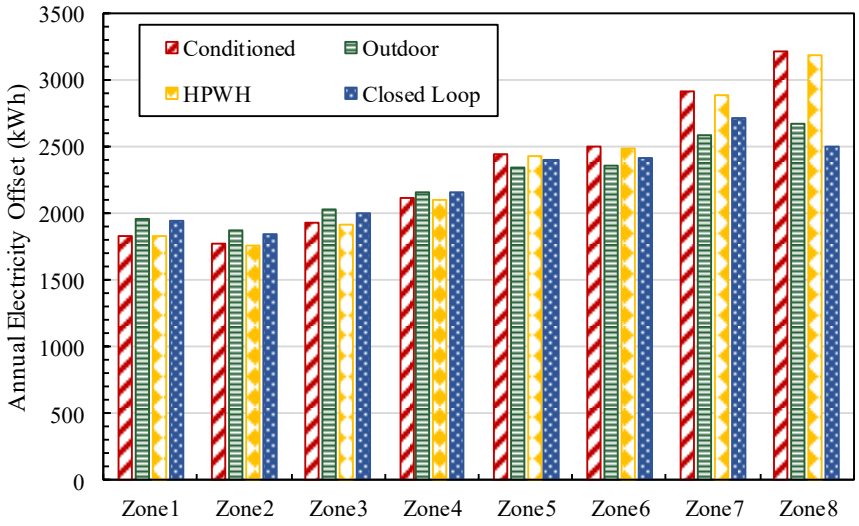

Figure 5.4: Electricity offsets realizable from an EWH to HPWH and SAHPWHs

The electricity consumption shown in Figure 5.2 through Figure 5.4 is for water heating alone and does not account for the energy impacts on space heating of the systems. Because the HPWH and conditioned SAHPWH systems both have an impact on the space conditioning of the system, the impact must be quantified to determine the benefits and load increases caused by the systems.

5.2.2 Energy for space conditioning

HPWHs have an impact on the space conditioning loads which, while valuable in reducing cooling loads in warmer locations, increases cooling loads in colder climates. The purpose of the SAHPWH was to reduce space cooling throughout winter in colder locations and increase performance year-round. In the closed loop and outdoor SAHPWHs, the water heating system operated independently of the space conditioning systems and had no impact on conditioning loads, but the HPWH and the conditioned SAHPWH both had an impact on space conditioning. The conditioned SAHPWH was designed to reduce the heating load increase that occurred as a result of the HPWH and thus allow the electricity

savings for water heating to be realized. The space heating load increase due to the HPWH and space heating decrease due to the conditioned SAHPWH are shown in Figure 5.5.

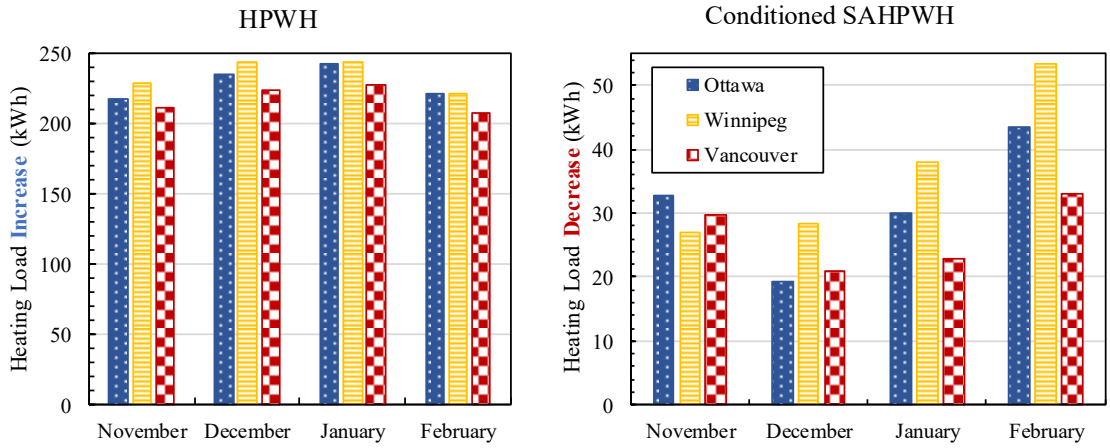

Figure 5.5: Cooling by HPWH (left) and heating by conditioned SAHPWH (right) during winter in Canadian cities

The main challenge of HPWH only systems in cold climates is secondary space cooling which increases space heating throughout winter and decreases room air temperatures. The HPWH increased space heating loads by 207 to 244 kWh per month throughout winter in various Canadian cities. The slight variation in HPWH space cooling among the Canadian cities was the result of variations in the mains water temperature which caused the HPWH to operate for different total durations in each of the cities. Cities with cooler mains water temperatures such as Winnipeg required a greater amount of HPWH operating time to heat the water, during which time additional space cooling occurred. The conditioned space configuration of SAHPWH had net heating for the space throughout winter in the Canadian cities, as opposed to the HPWH alone which had significant space cooling. When the HPWH was coupled with a solar collector in conditioned configuration, the cooling was fully offset and about 20 to 54 kWh per month of additional heat was provided to the space in locations across Canada thus reducing monthly space heating loads.

The impact of the HPWH and conditioned SAHPWH configurations on the annual heating and cooling loads across the climate zones were also quantified. If space cooling due to the HPWH or SAHPWH occurred during the cooling season, there was a space cooling decrease, whereas if space cooling occurred due to one of the systems during the heating season, there was a space heating increase. The impact of the systems on the space conditioning loads for all climate zones is shown in Figure 5.6.

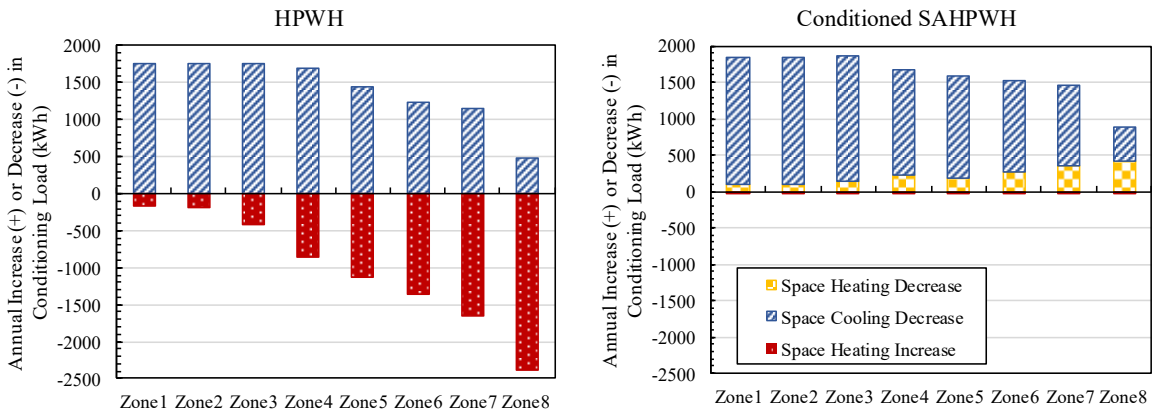

Figure 5.6: Impact of HPWH (left) and conditioned SAHPWH (right) on annual space conditioning loads

As Figure 5.6 shows, adding the solar collector in conditioned configuration nearly eliminated the annual space heating increase in all climate zones. A 2 to 32 kWh space heating increase remained in all climate zones with the solar collector, but this space heating increase was relatively insignificant compared to the space heating increase of 177 to 2394 kWh that occurred due to the HPWH alone.

The space heating increase did not reach zero for the SAHPWH because although most of the water tank charging time occurred during the day, the SAHPWH occasionally operated during periods of low solar insolation, such as evenings or cloudy days. During periods of

low solar insolation, the energy gain by the air inside the solar collector was lower than the energy removed by the HPWH, thus causing space cooling.

There was a variation in conditioning load increases and decreases between the climate zones that was largely caused by the heating and cooling seasons. Locations such as climate zone 1 and 2 with long cooling seasons realized the greatest space cooling benefits, whereas locations such as zone 8 with the longest heating season realized the greatest space heating benefits from the SAHPWH. Although there was little change in the conditioning load impact with the HPWH and conditioned SAHPWH in warm climate zones, there was significant impact of adding the solar collector in cold climate zones. In colder climates which had a considerable space heating increase with the HPWH, the effect of the solar collector was significant in reducing the space cooling caused by HPWHs during the long heating season, while also decreasing the heating load.

5.2.3 Total energy impact of systems

The total energy impact of the HPWH and SAHPWH configurations was analyzed to determine the net effect of the systems. The results showing the net energy balance for the HPWH and conditioned SAHPWH systems are provided in Figure 5.7.

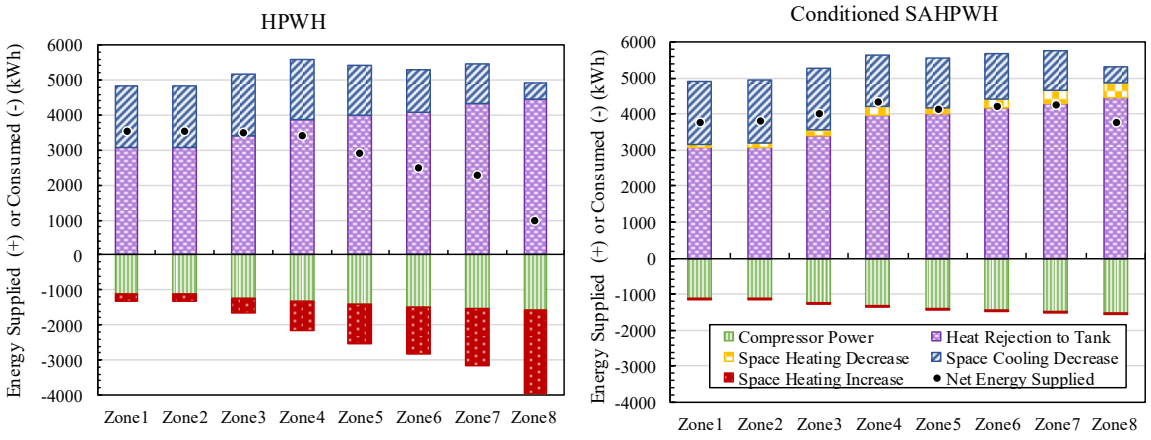

Figure 5.7: Energy balance for HPWH (left) and conditioned SAHPWH (right)

Although there was significant negative space cooling in the colder climate zones with the HPWH, even zone 8 still had a net amount of energy supplied, thus meaning that the HPWH reduced net energy consumption regardless of climate zone. However, Figure 5.7 shows that the net useful energy supply was greater in all climate zones for the SAHPWH than the HPWH. This is because the solar collector had the triple benefit of reducing the electricity for water heating due to higher inlet air temperatures, reducing annual space heating increase due to the HPWH to near zero, while also providing space heating to reduce the space heating load during winter.

The zone with the maximum energy supplied shifted from zone 3 for the HPWH to zone 4 when the solar collector was added. In the HPWH case, zone 3 had the maximum energy supplied due to a balance of the slightly colder mains water temperatures than zones 1 and 2 and the relatively long cooling season which increased cooling benefits beyond those realized in zones 5 through 8. Zones with colder mains water temperatures required more energy to heat the water, meaning that the compressor was on for longer durations and there was additional space cooling. In zone 3, mains water temperatures were slightly

cooler than those in zones 1 or 2, and thus zone 3 realized additional space cooling benefits for a smaller increase in compressor power.

For the SAHPWH, zone 4 had the maximum energy supplied because the solar collector nearly eliminated the space heating increase, while the slightly colder mains water temperatures than zones 1 through 3 increased the energy required for water heating, as well as the useful space cooling. Zone 4 also has higher insolation than some of the colder-temperature zones, which resulted in additional space heating benefits due to the solar collector. For conditioned SAHPWH, maximum energy supply occurred in locations which have an optimal balance of low mains water temperatures and high solar insolation levels.

5.2.4 Analysis with house model

The HPWH and conditioned SAHPWH were analyzed within a house model to determine the heating and cooling seasons used for the standalone model and to compare trends between the system performance in the house and standalone models. The closed loop and outdoor configurations were not analyzed within the house model because they were designed to be independent of the space conditioning loads.

In the house model, the impact of the HPWH on the space conditioning was the difference of the performance with and without the HPWH. In the standalone models, as discussed in Chapter 4, the impact on space conditioning was calculated based on the season and the temperature differential of the air entering and exiting the HPWH. The impacts on the heating and cooling loads in the house model and standalone model were compared for the HPWH in Figure 5.8 and the SAHPWH in Figure 5.9.

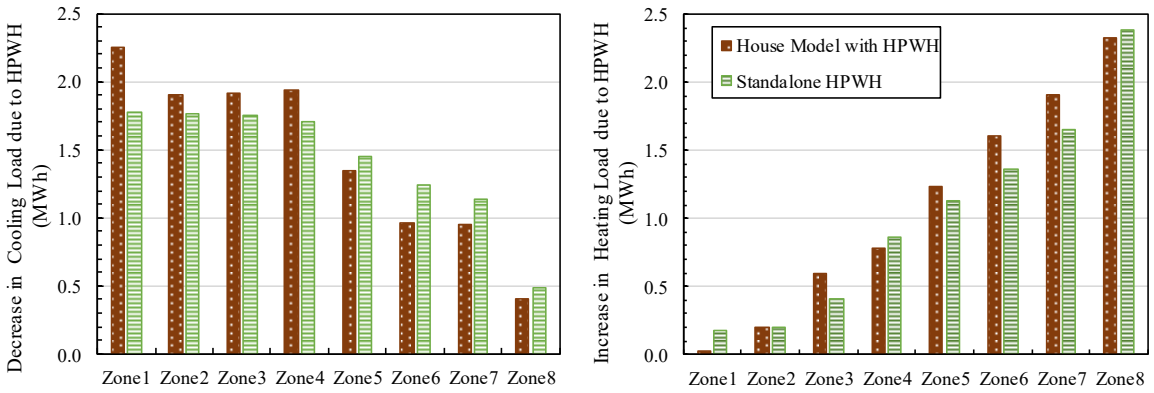

Figure 5.8: Impact of HPWH in decreasing cooling load (left) and increasing heating load (right)

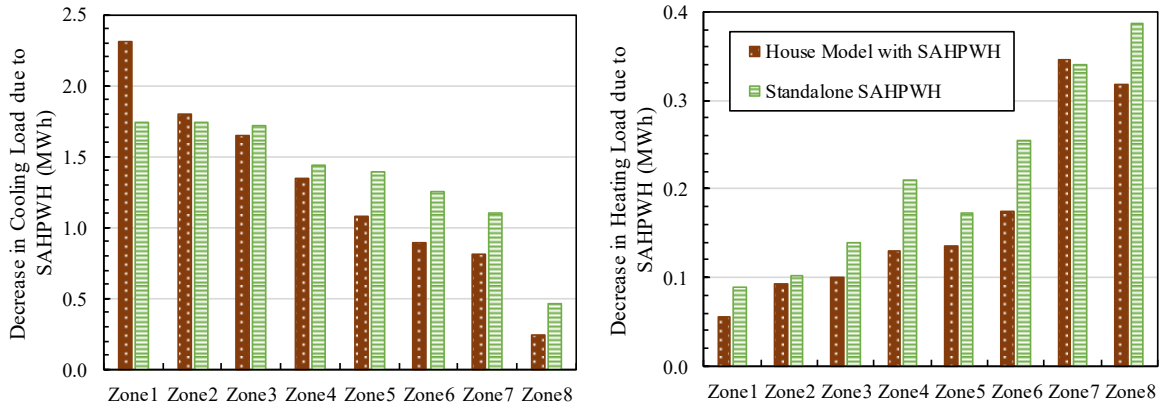

Figure 5.9: Impact of SAHPWH in decreasing cooling load (left) and decreasing heating load (right)

For the HPWH, there was a 14% average difference in cooling decrease between the house model and the standalone model, and there was a 21% average difference in the impact on heating load between the house model and standalone model. The SAHPWH had similar results; there was a 14% average difference in cooling decrease between the models, and a 23% average difference on the heating decrease between the models. When these differences between the house and standalone models were considered as a proportion of the total heating and cooling load consumed annually, it was found that there would be less than a 2% variation in annual heating or cooling load if one modelling method was used

instead of another. This means that the disagreement between the house model and standalone model had an impact of less than 2% annually on either conditioning load.

Variations between models such as what was observed in this study are common when using different modelling techniques. For example, changing assumptions for modelling methods and parameters such as air infiltration, ground contact, thermal bridging, ambient temperatures, and ground reflected radiation have been shown to have a significant impact on the heat loads of a house model [86], and differences caused by these highly sensitive parameters may be greater than the variations observed between the house model and standalone model in this study.

The slight disagreement in the house model and standalone models was caused by a few factors. Firstly, the air temperature range in the house model was set to be 20°C for heating and 23°C for cooling, and had some fluctuation outside of the setpoint range, whereas the air temperature for the standalone model was assumed to be at a constant 20°C. At higher air temperatures, the HPWH caused a greater amount of space cooling based on the performance map that was developed. These high temperatures occurred for a larger portion of time in warm climate zones 1 to 4 with long cooling seasons, thus causing the house model to predict slightly higher decreases in cooling load than the standalone model which did not account for variation in air temperatures, as shown in Figure 5.8 and Figure 5.9. The house model predicted a lower decrease in cooling load for cooler climate zones 5 to 8 for the opposite reason; lower air temperatures within the house model resulted in the HPWH providing a lower amount of space cooling than the standalone model. Another factor that was not captured in the standalone model was the increase or decrease in heat

transfer to or from outdoors due to changes in air temperature. For greater temperature differences, greater heat transfer would occur thus increasing the result predicted by the house model, in which air temperatures fluctuate.

The impact of the HPWH and SAHPWH in the house and standalone models on the annual space conditioning loads was also analyzed. A summary of the impacts of the SAHPWH and HPWH on space heating and cooling loads is shown in Table 5.4.

Table 5.4: Space conditioning changes due to SAHPWH and HPWH operation

	Base Conditioning Loads (MWh)		**Percent of total space conditioning by SAHPWH**		**Percent of total space conditioning by HPWH**	
	Cooling	Heating	Cooling Decrease	Heating Decrease	Cooling Decrease	Heating Increase
Zone1	25.77	0.33	7%	27%	7%	53%
Zone2	23.01	1.14	8%	9%	7%	17%
Zone3	20.16	4.71	9%	3%	9%	9%
Zone4	14.77	6.81	10%	3%	12%	13%
Zone5	9.51	11.69	15%	1%	15%	10%
Zone6	9.80	13.56	13%	2%	13%	10%
Zone7	9.19	20.31	12%	2%	12%	8%
Zone8	4.52	24.32	10%	2%	11%	10%

It was found that the HPWH provided 7% to 15% of the total space cooling load throughout the climate zones, and increased the space heating load by 8% to 17% (excluding zone 1 which had only a 0.33 MWh space heating load and saw a space heating increase of 53% due to the small base heating load). For the SAHPWH, between 7% and 15% of the total space cooling load was supplied (the same as the HPWH). A 1 to 3% reduction in space heating loads occurred with the SAHPWH, with the exception of zones 1 and 2 which have

small base heating loads so the SAHPWH was therefore able to provide 27% and 9% of the space heating load, respectively.

The temperatures within the house were also analyzed to determine the impact the HPWH and SAHPWH have on maintaining comfortable temperatures with the house model. The temperatures in the house model with and without the HPWH and SAHPWH systems were compared. Because the HPWH had a cooling effect on the space, the temperatures of the house shifted to lower temperatures throughout the study. It was found that the HPWH caused a 4.1% increase in time throughout the year that temperatures were below 19°C and a 0.9% decrease in time that temperatures were greater than 25°C. With the SAHPWH, there was a 2.2% increase in time that temperatures were less than 19°C and a 0.2% increase in time that the temperatures were greater than 25°C compared to the house model without any HPWH or SAHPWH. The SAHPWH was successful in reducing the duration of lower temperatures that occurred with the HPWH and was able to half the amount of time that the temperatures were below 19°C from the HPWH model. However, it should be noted that the SAHPWH decreased the time that the house was within the 19°C to 25°C comfortable range by 210 hours throughout the year.

Both the house model and the standalone model provided results regarding the performance of HPWH and SAHPWH systems in various climates. Both modelling methods were based on different sets of assumptions, yet the models yielded agreement within 2% of the annual space conditioning loads. Given the inherent assumptions with both the house model and the standalone model, as well as the low difference in space conditioning impact between the models, the standalone HPWH model was used for the other analyses. Further,

analyzing the HPWH and conditioned SAHPWH without the house model ridded the analysis of the house model assumptions and prevented additional variations in compressor power, heat delivery, and space conditioning. This allowed for clearer comparison of trends caused by the closed loop, outdoor, and conditioned SAHPWHs that all encompassed the assumptions of the standalone model, without adding the assumptions on space conditioning loads that were imposed by the house model in the conditioned configuration.

5.3 Greenhouse gas emissions of configurations analyzed

The GHG analysis was conducted to determine the GHG offsets possible for a HPWH and SAHPWH offsetting an EWH or a NGWH with either electric or natural gas space heating. This analysis included GHGs due to the natural gas consumption for space and water heating, the HPWH refrigerant leakage, as well as GHGs due to electricity generation. Figure 5.10 and Figure 5.11 show the annual GHG reduction possible, excluding refrigerant leakage, as a function of the GHG intensity of the electricity grid when transitioning to a HPWH and a SAHPWH, respectively, from a certain alternative water heater (EWH or NGWH) with a certain space heating method (electric, natural gas, or none). Because the HPWH always had an impact on the space heating loads, there was not a “none” space heating option included, whereas the closed loop and outdoor SAHPWH configurations had no impact on space heating loads and a “none” option was possible.

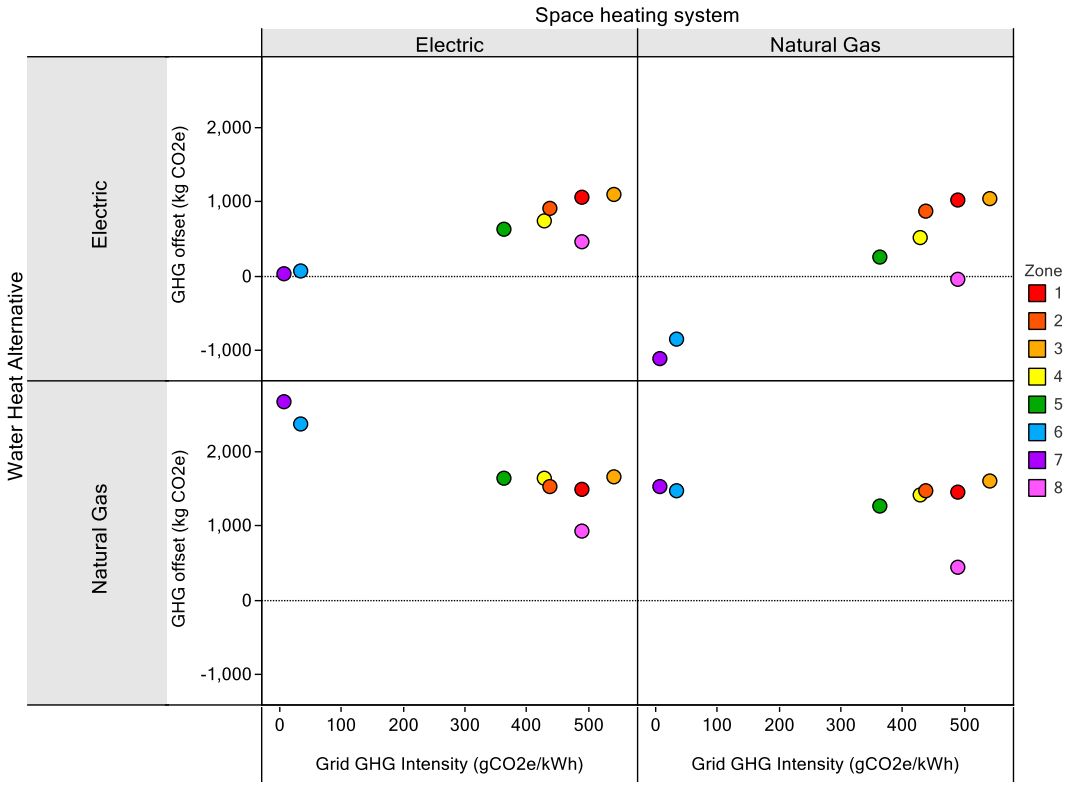

Figure 5.10: GHG offsets for HPWH compared to EWH and NGWH with electric and natural gas heating systems

Figure 5.10 shows the GHG reductions possible for various scenarios when transitioning to a HPWH. It shows that the GHG reduction values were more sensitive to the water heating alternative than to the space heating system because there was a greater difference in GHG offsets between EWH and NGWH for one single space heating system than there was between the electric and natural gas space heating systems for one single water heating alternative.

It was found that GHG offsets from EWH to HPWH increased with grid GHG intensity, whereas GHG offsets from NGWH to HPWH decreased with grid GHG intensity. This is because HPWHs in cleaner electricity grids nearly eliminate GHG emissions compared to NGWHs, whereas electricity grids that are highly reliant on fossil fuels still produce

significant GHGs with a HPWH. Similarly, EWHs in cleaner electricity grids already produced very little GHGs so switching to a HPWH had a low GHG offset.

In zone 6 and 7, which have cleaner electricity grids than the other locations, the transition from EWH to HPWH did not have a significant impact on reducing the GHG emissions because very little GHGs were produced with the EWH. Further, due to the low GHG reductions between the EWH and the HPWH coupled with the high space heating increase with the HPWH in zones 6 and 7, there was a net increase in GHG emissions when using natural gas for space heating in these locations. Other locations within zones 6 and 7 with fossil fuel dominant electricity generation would result in a net GHG reduction for all cases, rather than the result observed in Figure 5.10.

The greatest GHG reductions were realized when transitioning from a NGWH to a HPWH regardless of the space heating system used. In all climate zones studied, the greatest GHG reductions occurred for the NGWH with electric heat case. This is because the HPWH increased space heating loads, so cleaner space heating systems resulted in greater GHG reduction because less GHGs were released for this supplemental space heating. Locations with electricity grids that were cleaner than natural gas produced less GHG emissions for electric space heating than natural gas space heating, thus creating a larger total offset.

The trend for the HPWH case was that there were, in general, greater GHG reductions for colder climate zones. The significant amount of additional space heating required throughout the year in zone 8, however, prevented zone 8 from realizing the greatest GHG reductions. The results in Figure 5.10, particularly for climate zones 6, 7, and 8 indicate that there may be a method to increase the GHG reductions of HPWHs further if space

heating increases did not occur. The GHG offsets for SAHPWHs, which mitigated this issue are shown in Figure 5.11. The results for the electric and natural gas space heating systems are for the conditioned SAHPWH, which was the only SAHPWH with an impact on space conditioning. The results shown that had no heat impact are the closed loop configuration, which was independent of space heating and had similar trends to the outdoor configuration.

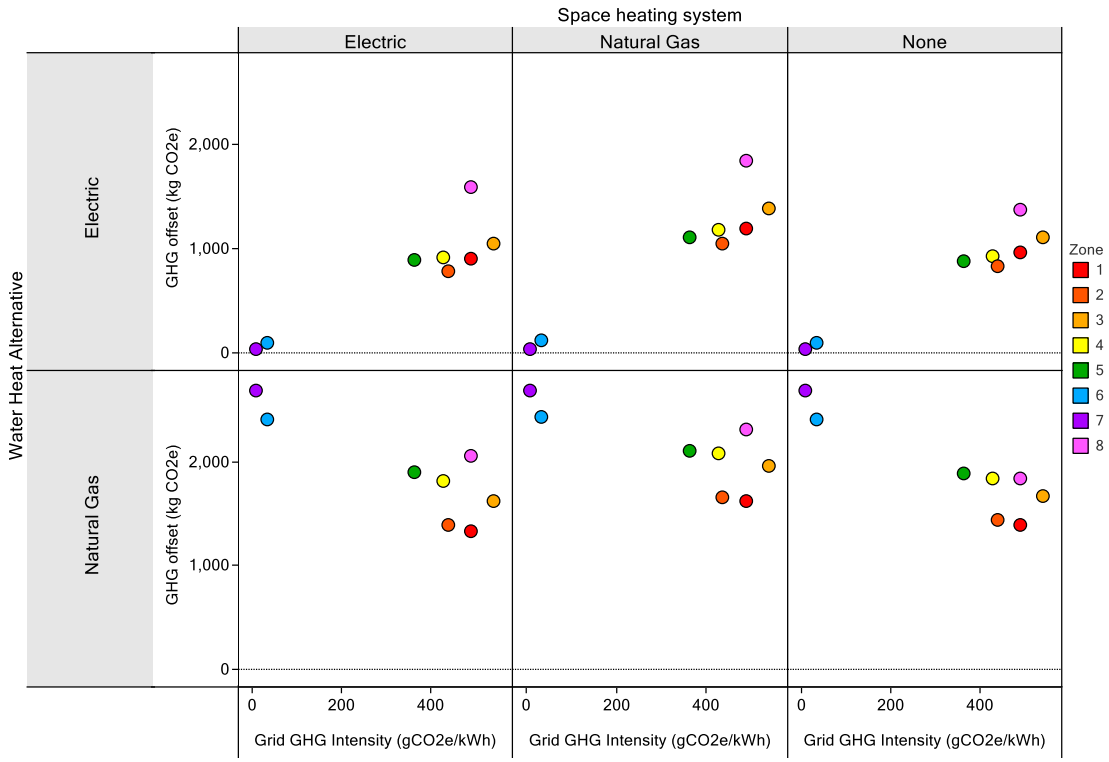

Figure 5.11: GHG offsets for SAHPWH compared to EWH and NGWH with electric and natural gas heating systems

The GHG offsets from EWH to SAHPWH increased with grid GHG intensity, whereas GHG offsets from NGWH to SAHPWH decreased with grid GHG intensity, similar to the results shown for HPWHs. The GHG reduction that occurred from an EWH to a SAHWPH was related to the GHGs released for electricity generation; cleaner grids like Ontario in zone 6 and Manitoba in zone 7 had less GHG reductions because the water heating source

was relatively clean with the EWH. In contrast, grids that were largely dominated by natural gas, such as zone 8, had larger GHG reductions between EWHs and HPWHs because the amount of greenhouse gas emitting electricity was significantly reduced.

For any given water heating alternative and space heating system, the relationship between electricity makeup and GHG offsets appeared nearly linear. The variation from a linear relationship was caused by two main factors: energy required for water heating in each zone was not the same (there was variation in mains water temperatures between zones) and space heating and cooling seasons were different for all zones (there were different amounts of space heating and cooling offsets).

The trends show that the SAHPWH caused a net space heating decrease because there was a slightly greater GHG reduction for the cases with natural gas heat than electric or no heat impact. Because the SAHPWH provided some space heating reduction and the natural gas for space heating was reduced, the GHGs were also reduced. This result shows that the SAHPWH with no heat impact, the closed loop (or outdoor) configurations, had less GHG reductions than the conditioned SAHPWH which had an impact on space heating loads.

When comparing the results for the HPWH and SAHPWH in Figure 5.10 and Figure 5.11, it can be seen that the SAHPWH has potential to offset more GHGs than the HPWH. In addition, the HPWH was more sensitive to the space heating method than the SAHPWH. That is, there was more variation in GHG reductions for different space heating methods and water heating alternatives for the HPWH than the SAHPWH because the HPWH had a greater impact on space conditioning loads. Although the SAHPWH did have an impact, it was much less than the HPWH.

5.4 Economic performance of configurations analyzed

The economic performance was analyzed in terms of PBP, LCC, breakeven costs, possible subsidies, and potential effects of carbon pricing. Because the HPWH and SAHPWH have high capital costs yet provide savings throughout their lifetime, it is important to study the economics of the systems using metrics that capture the full lifecycle savings.

5.4.1 Operating costs

The annual operating costs of the water heating methods included both the cost to heat water and the cost impact of the space heating and cooling impact in offsetting or increasing space conditioning loads. The annual operating costs for a location in each climate zone are shown in Figure 5.12. Costs are not shown for NGWH in zone 8 because there was no natural gas supply in the Canadian territories.

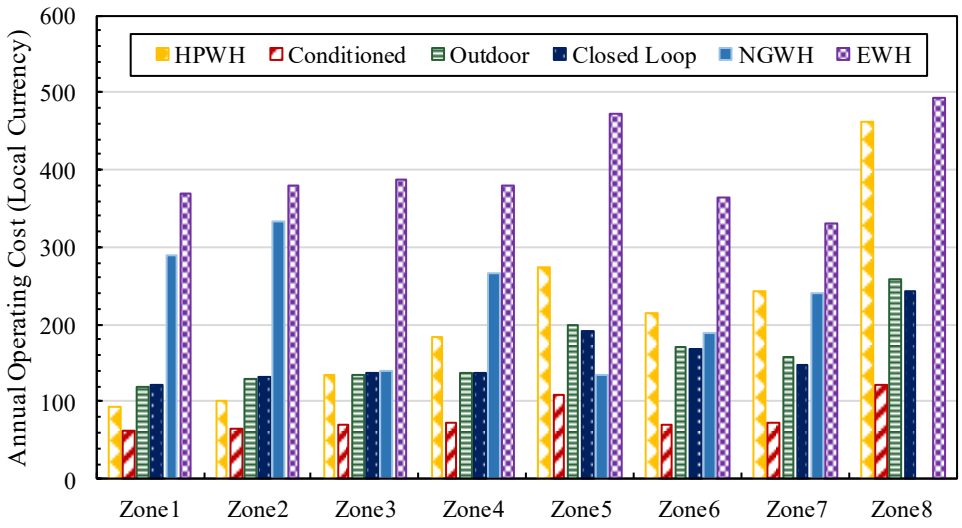

Figure 5.12: Annual operating costs of various water heating methods

Although energy consumption for water heating alone increased from climate zone 1 to climate zone 8, the annual operating costs were also dependent upon the electricity and natural gas costs in each location, so operating costs did not necessarily increase

sequentially between zones 1 through 8. However, costs for operating an EWH or a NGWH were consistently higher than operating costs of HPWHs or SAHPWHs.

For all climate zones, the conditioned configuration of SAHPWH resulted in the lowest operating costs because the conditioned SAHPWH provided space heating benefits in the winter to reduce heating costs and space cooling in the summer to reduce space cooling costs. HPWHs, which caused a decrease in space cooling loads and an increase in space heating, had low operating costs in locations with short heating seasons such as zone 1, but high operating costs in zone 8. EWH and NGWH operating costs fluctuated significantly between climate zones because they were highly dependent upon local fuel prices.

There was the greatest variation in the operating costs for the HPWH across the climate zones than other water heating methods due to the impact of the space cooling caused by the HPWH. In climate zone 1, the space cooling was beneficial during most of the year, whereas it increased space heating costs during most of the year in climate zone 8. In addition, the colder mains water temperature in zone 8 also contributed to the increased costs as compared to the warmer climate zones.

In all climate zones, an operating cost decrease occurred between an EWH and a HPWH or SAHPWH, even when the impact on space conditioning is considered. Most locations also had an operating cost decrease from a NGWH to a HPWH or SAHPWH, but this decrease was less than that of the EWH to HPWH or SAHPWH due to the cheaper cost of natural gas in many locations. The greater the annual operating cost savings from an alternative water heating method to a HPWH or SAHPWH, the shorter the time would be to pay off the high capital cost of the HPWH or SAHPWH. However, in locations where

the annual operating cost of the NGWH was cheaper than that of the HPWH or a SAHPWH configuration, the high capital cost of the HPWH or SAHPWH would not be overcome over the lifetime.

5.4.2 Payback period

Payback period was used to calculate the number of years of operating cost savings required to offset the higher capital cost of the HPWH or SAHPWH as compared to electric or natural water heating systems. The PBPs of the conditioned SAHPWH and the HPWH compared to EWH and NGWH systems are shown in Figure 5.13. The outdoor and closed loop configurations were omitted from this graph because their operating cost performance was between the HPWH and conditioned SAHPWH.

The PBP of the SAHPWH and HPWH systems compared to NGWH had a nonuniform trend across the climate zones due to the significant variation in natural gas prices between locations. Further, because natural gas was a cheaper water heating method in terms of annual operating costs than the HPWH or SAHPWH in some cases, the PBP period for a SAHPWH or HPWH in some locations was negative. Negative PBP values indicated that operating costs of the NGWH were cheaper than the HPWH or SAHPWH, thus there was no period within which the HPWH or SAHPWH would pay for itself compared to a NGWH. Negative PBPs and PBPs greater than 100 years were not included in Figure 5.13.

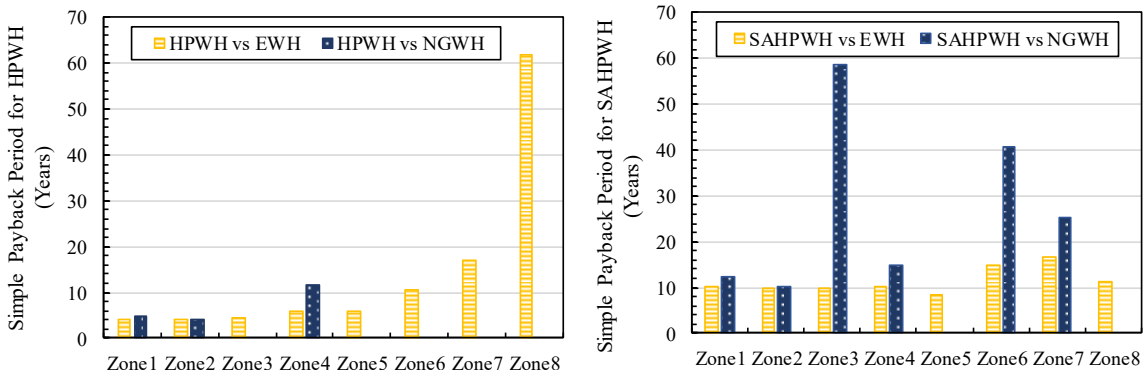

Figure 5.13: Payback period for HPWH (left) and SAHPWH (right) compared to other water heating methods

Figure 5.13 shows that a longer PBP occurred when comparing a HPWH or SAHPWH to a NGWH than to an EWH in all locations, due to the low fuel cost of natural gas. When comparing the PBP of the HPWH systems to the EWH, Figure 5.13 shows a trend of increasing PBP from climate zone 1 through 8, because both systems are electricity driven, and because of the increase in space heating load that occurred in colder climate zones. However, for the SAHPWH compared to the EWH, the maximum PBP occurred in zones 6 and 7, while climate zone 8 had a lower PBP due to the space heating benefits of the SAHPWH. In warmer climates (zone 1 through 6), the HPWH had a lower PBP than the SAHPWH, despite the lower operating cost of the SAHPWH. This is because the SAHPWH nearly doubled the capital cost of the system, so the difference in EWH operating cost and SAHPWH cost had to be much greater than the difference between EWH and HPWH to result in the SAHPWH having a lower PBP. In climate zones 7 and 8, the significant annual operating cost savings of the conditioned SAHPWH caused the SAHPWH to overcome the high capital costs and have a lower PBP.

In the PBP analysis, it was important to note that the expected lifetime of the HPWH and SAHPWH were 15 years, so PBPs of longer than 15 years would result in the system being

economically infeasible. In addition, the sample PBP analysis for each climate zone provided general trends, but PBP values are highly sensitive to electricity and natural gas costs, so analysis for all desired locations must be conducted separately, rather than garnering specific values for each climate zone from Figure 5.13.

5.4.3 Lifecycle cost

The lifecycle costs of the HPWH and SAHPWHs encompassed full operating, maintenance, and capital costs of the systems. Instead of comparing the HPWH or SAHPWH to an alternative technology, the LCC calculation considered only the HPWH or SAHPWH. The LCC for the HPWHs and SAHPWHs is shown in Figure 5.14. LCC had less variability than the PBP calculation because LCC was not dependent upon multiple fuel sources and technology options in each calculation.

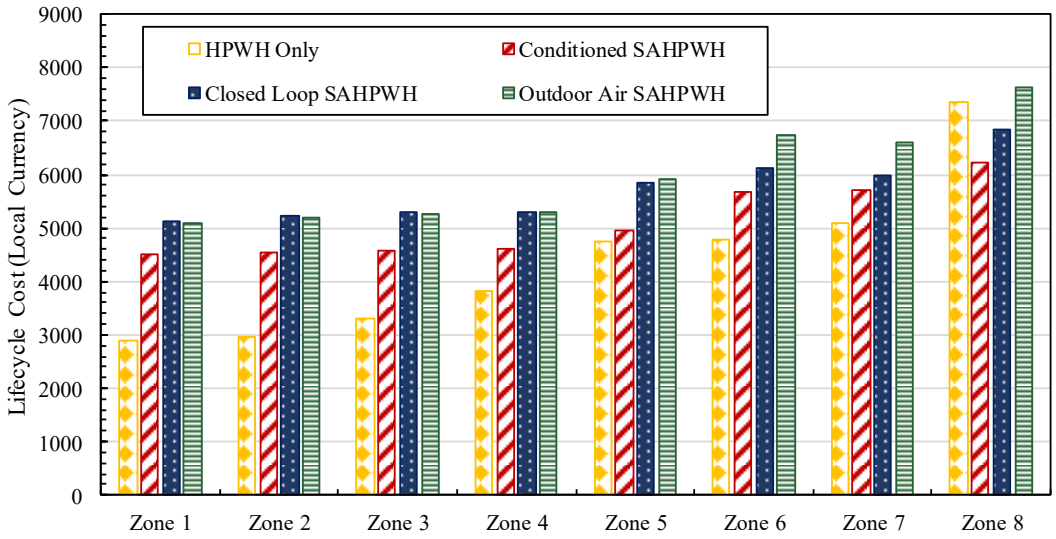

Figure 5.14: Lifecycle Costs of HPWH and SAHPWH systems

HPWHs have significantly lower capital costs than SAHPWHs, so the HPWH typically also had a lower LCC. The exception was the SAHPWH in zone 8 which provided significant space heating load reduction and therefore the conditioned SAHPWH had the

lowest LCC. In the colder climate zones with ambient temperatures that were often below 5°C, such as zones 6 through 8, the outdoor configuration had the highest LCC due to the high operating costs caused by reliance of the SAHPWH on the electric backup element in these colder locations.

The SAHPWHs had more uniform LCC values across zones 1 through 8 than the HPWH LCC values. This is because the SAHPWH had higher capital costs which increased the LCC particularly in warm climate zones, while adding the solar collector decreased the LCC in cold climate zones due to the space heating benefits. The HPWH had a larger variation in LCC across climate zones than the SAHPWH because the HPWH decreased costs by offsetting space cooling in warm climate zones but added to the LCC in cold climate zones by increasing space heating costs throughout the long heating season.

5.4.4 Cost breakeven

The breakeven capital cost for a HPWH or SAHPWH was the capital cost required to have the same LCC as an EWH or NGWH. If the calculated breakeven capital cost was greater than the actual capital cost, the actual HPWH or SAHPWH had a lower LCC than the alternative water heating system. If the calculated breakeven cost was less than the actual capital cost, the capital cost of the HPWH or SAHPWH would need to be cheaper in order to have the same LCC as an alternative water heating system. If the breakeven was lower than the actual capital cost, one method to decrease the actual capital cost of the HPWH or SAHPWH such that the HPWH or SAHPWH would have the same LCC as an electric or natural gas water heater would be to introduce financial incentives. The incentives could be valued at an amount that is difference between the actual capital cost and the calculated

breakeven cost, thus allowing the LCC paid for the HPWH or SAHPWH system to be equal to that of an electric or natural gas water heater.

The breakeven costs, which are the capital cost of the HPWH and SAHPWH required to have the same LCC as alternative methods of water heating, are shown in Figure 5.16 and Figure 5.16, respectively. The subsidy values shown are the subsidy that would have to be introduced for a HPWH or SAHPWH to have the same LCC as the alternative water heating methods given the current capital costs of HPWHs or SAHPWHs.

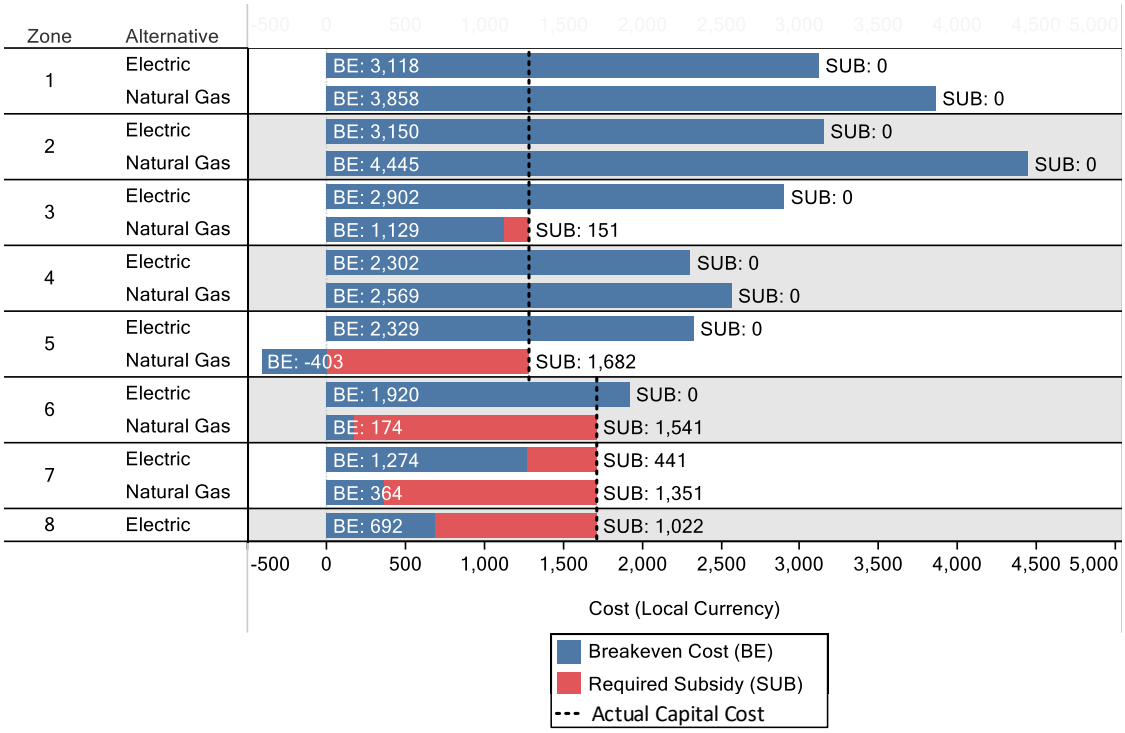

Figure 5.15: Breakeven cost of HPWHs compared to EWH and NGWH and actual capital costs

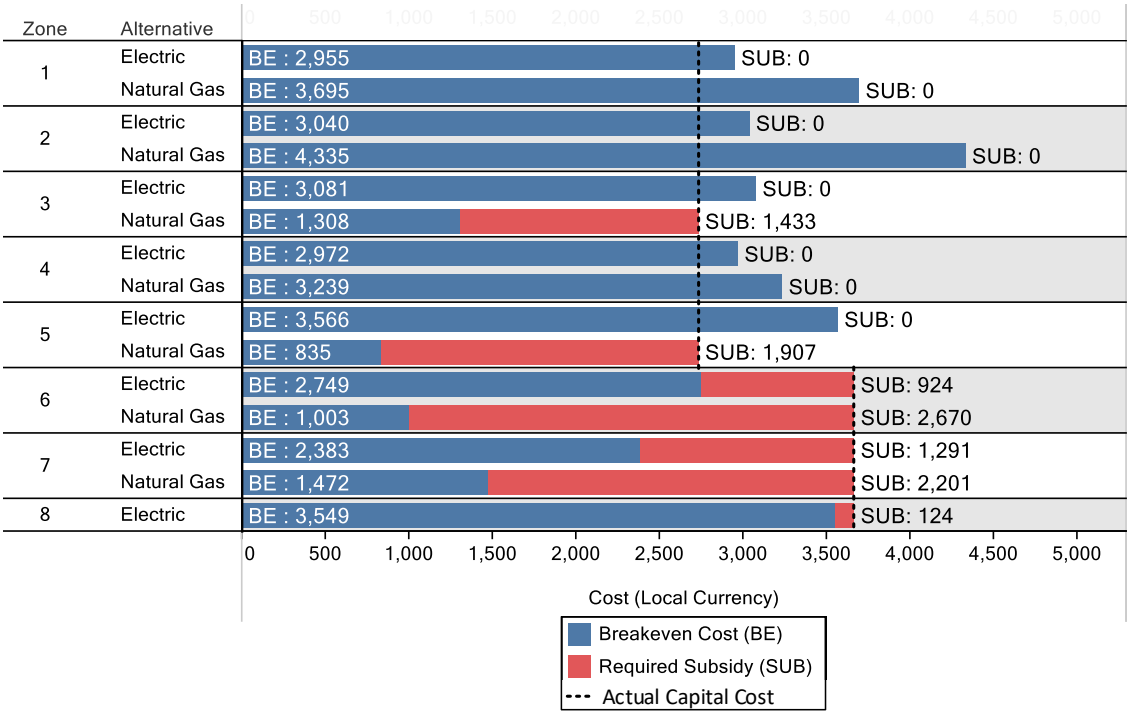

Figure 5.16: Breakeven cost of SAHPWHs compared to EWH and NGWH and actual capital costs

Zones 1 through 5 are located in the United States and therefore have different actual capital costs (in USD) than zones 6 through 8 which are located in Canada (in CAD). The subsidies are the amount that would be required for the calculated breakeven cost in Figure 5.16 to reach the actual capital cost of the systems. These subsidies could be introduced by governments to promote increased uptake of HPWHs or SAHPWHs. As can be seen from the sample locations studied, higher subsidies would be required in Canada than in the United States.

The increased feasibility in the United States occurred based on two main factors, which are the high electricity prices in the United States and low capital costs. Firstly, electricity prices (in local currency) in the United States were often greater than those in Canada. As

such, there were significant operating cost savings realized with the HPWH or SAHPWH compared to the alternative systems, which resulted in a greater breakeven capital cost. Secondly, the lower actual capital cost of the HPWH and SAHPWH in the United States was easier to overcome than in Canada.

In Figure 5.16, bars without subsidy values indicate that the breakeven capital cost calculated was greater than the actual capital cost of the system, and therefore the system was presently feasible. For locations in which subsidies would be required for HPWH or SAPHWH to have the same LCC as alternative water heating methods, the sum of the required subsidy and the calculated breakeven cost was equal to the actual capital cost of the HPWH or SAHPWH.

When comparing the results for the HPWH and SAHPWH, the subsidy values were greater for the SAHPWH in all locations except zone 8. This is due to the higher capital costs of the SAHPWH that provided a relatively low benefit in terms of operating costs. In zone 8, however, the solar collector prevented a significant amount of cooling and added space heating benefits and thus a lower subsidy was required for the SAHPWH than the HPWH.

5.4.5 Inclusion of greenhouse gas emissions in economics

The GHG offsets from a NGWH to the HPWH and SAHPWH options had a sample carbon price associated with them to indicate what could occur as the carbon tax increases and quantify the environmental and economic footprint together for the HPWH and SAHPWHs. Further, it can be used to illustrate the relative impact that an increasing carbon price may have on the economic feasibility of a HPWH or SAHPWH. The impact of a $50/kg carbon tax on the LCC, breakeven costs, and subsidies were determined, with the

GHG offset possible using HPWHs or SAHPWHs. The carbon offsets for a HPWH or SAHPWH compared to a NGWH were considered for this analysis. The LCC values for a HPWH and SAHPWH with and without carbon pricing are shown in Figure 5.17.

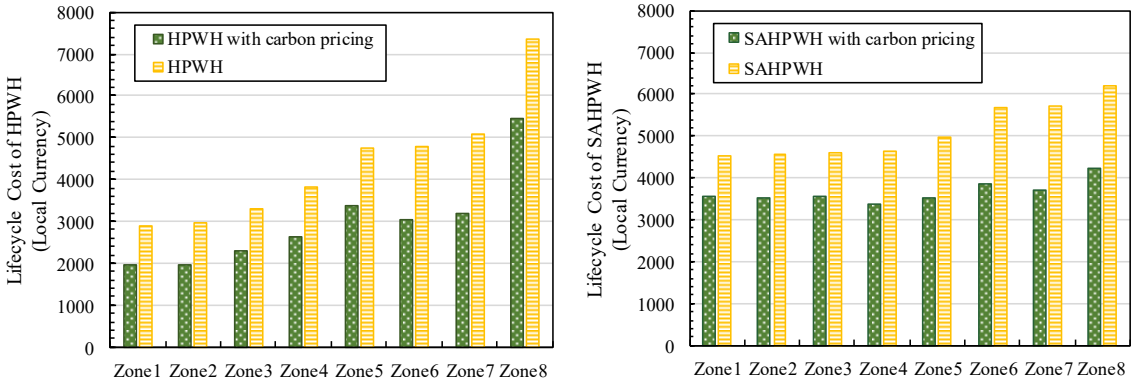

Figure 5.17: Comparison of LCC with and without carbon pricing for HPWH (left) and SAHPWH (right)

The LCC with carbon pricing put a price on the GHG offset possible with HPWHs or SAHPWHs when offsetting a NGWH in all climate zones. The LCC with carbon pricing was less than the LCC without carbon pricing in all zones for both the HPWH and the SAHPWH because there were significant GHG reductions realized with HPWHs or SAHPWHs from the large GHGs produced using NGWHs. In the method including carbon pricing, the LCC decreased because a credit was put on the GHG offsets achieved using a HPWH or SAHPWH. From the base case to the LCC with carbon pricing, there was an average of a 32% and 28% decrease in LCC for the HPWH and SAHPWH, respectively.

The breakeven cost with and without carbon pricing was also compared for the HPWH and SAHPWH against natural gas water heaters. The calculated breakeven costs are shown in Figure 5.18 and Figure 5.19 for a HPWH and SAHPWH, respectively.

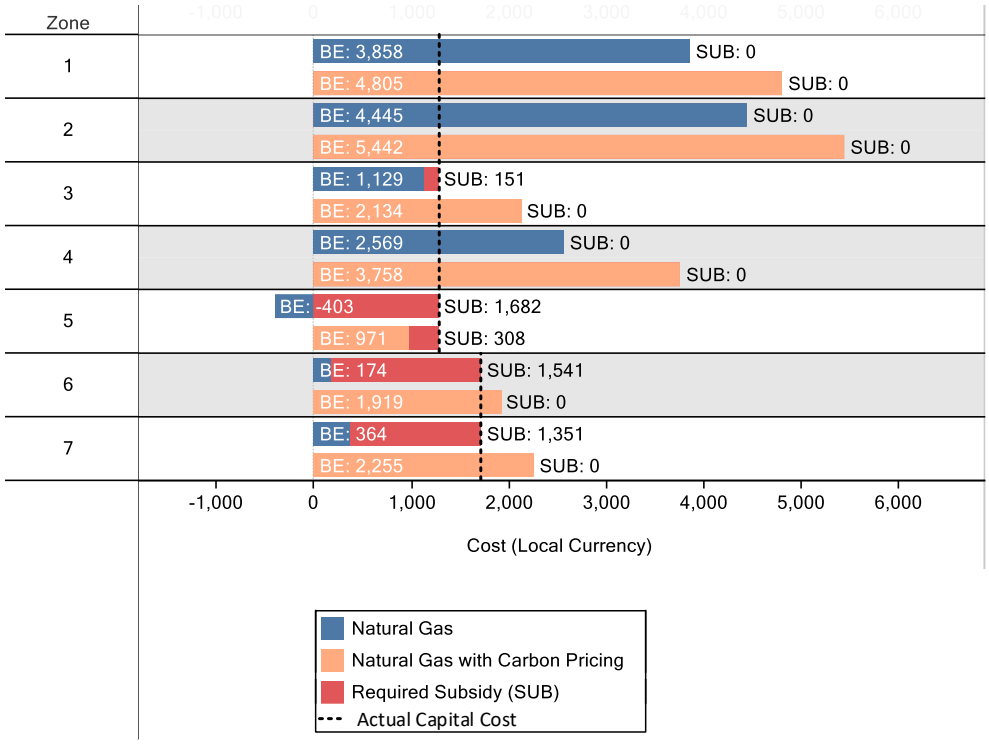

Figure 5.18: Breakeven cost with and without carbon pricing of HPWH compared to NGWH

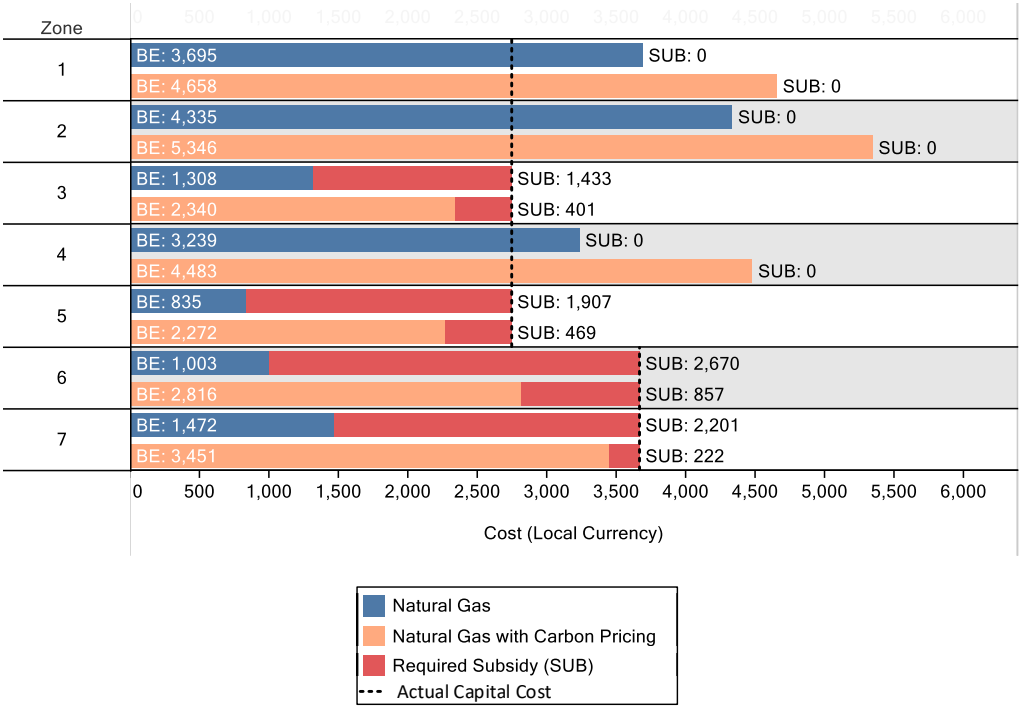

Figure 5.19: Breakeven cost with and without carbon pricing of SAHPWH compared to NGWH

When carbon pricing was included in the breakeven analysis, the calculated breakeven cost for the HPWH and SAHPWH increased, and thus the feasibility also increased. This is because the LCC of the NGWH significantly increased when carbon pricing was included, which increased the allowable capital cost of the HPWH or SAHPWH. For the HPWH, including carbon pricing increased the breakeven capital cost value to above the actual capital cost in all locations studied except zone 5. Figure 5.19 indicates this, showing that most locations did not require subsidies for the case with carbon pricing. For the SAHPWH, however, adding carbon pricing did not cause the breakeven cost to exceed the high capital cost in most sample cities studied. Although it reduced the subsidy required, all locations that required subsidies without carbon pricing also required subsidies with carbon pricing.

5.5 Summary of results

The results and trends shown in this section aid in understanding the broader findings provided in the discussion section. The results for the energy, GHG, and economic analysis were analyzed within this section, using the validated TRNSYS model. In the energy analysis, the energy required to heat water increased between climate zones 1 through 8 due to cooler mains water temperatures in colder climate zones. The energy balance of all climate zones was analyzed including the impact on space heating and cooling, and the standalone HPWH and SAHPWH models were compared to a HPWH or SAHPWH performance within a house model. For a HPWH alone, the greatest net energy supply occurred in climate zone 3 due to a high need for space cooling and a slightly cooler mains water temperatures than zones 1 or 2. For a SAHPWH, however, the greatest net energy

supply occurred in climate zone 4 due to the added space heating benefits provided by the SAHPWH.

The GHG offsets were studied for all climate zones, all of which are highly dependent upon the fuel sources used to generate electricity. The GHG offsets increased with increasing grid GHG intensity for EWHs to HPWHs or SAHPWHs, but GHG offsets decreased with increasing grid GHG intensity for NGWHs to HPWHs or SAHPWHs. The least GHG offsets occurred between an EWH and a HPWH in locations with cleaner electricity grids, and the least GHG offsets occurred between a NGWH and a HPWH in locations where the HPWH had little impact on the space heating load (such as warm locations in zones 1 through 3).

In the economic analysis, it was found that operating cost savings could be realized with HPWHs or SAHPWHs compared to EWHs. However, particularly when the high capital cost of the HPWH or SAHPWH was considered, the HPWH and SAHPWH were not economically feasible in some locations compared to NGWHs. When a carbon price was applied to the GHG offset in the economic analysis, however, the feasibility of the HPWH and SAHPWH increased significantly; with a carbon price, the HPWH had a lower LCC than NGWH in nearly all sample locations studied, but the SAHPWH remained infeasible in most locations due to the high capital cost. The trends for economic analysis shown in this section are highly sensitive to local energy prices. As such, other locations within each climate zone will not necessarily have a similar result to the sample location studied in said climate zone.

Chapter 6: Discussion

There are several implications of the results for the HPWH and SAHPWH performance in terms of energy consumption, economics, and GHG reductions. Expansion of the results beyond the sample locations is necessary to establish further trends and outcomes for a broader range of locations in each climate zone studied. The implications of the results are discussed in this chapter for additional locations across Canada and the United States.

6.1 Energy performance of configurations analyzed

The energy performance of the HPWH and SAHPWH configurations had a similar result across the climate zones to the trend which occurred for the sample locations. The results for the configurations of HPWH or SAHPWH with the lowest electricity consumption across Canada and the United States are shown in Figure 6.1.

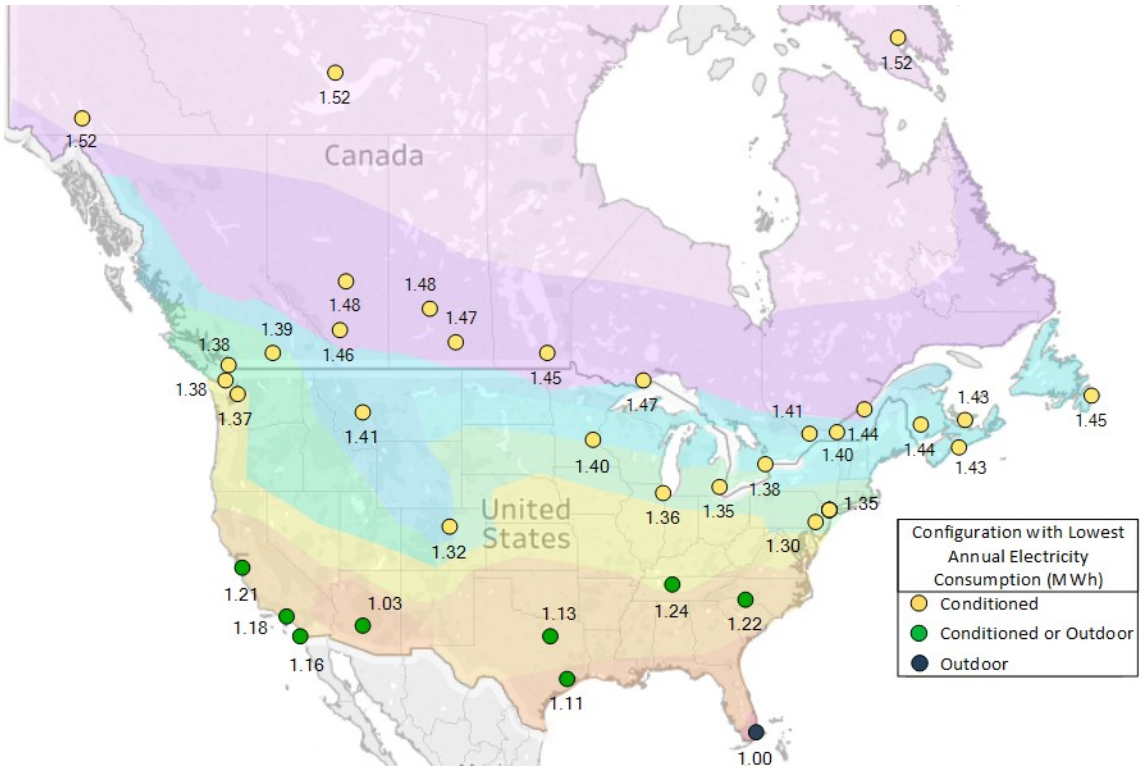

Figure 6.1: SAHPWH configuration with lowest annual electricity consumption

In climate zone 1, the outdoor and closed loop configurations had similar performance and resulted in the lowest annual electricity consumption, whereas in colder climate zones, the conditioned configuration resulted in the lowest annual electricity consumption, as shown in Figure 6.1. In climate zones 2 and 3, there was less than a 10% difference in electricity consumption between the outdoor and conditioned configurations.

In each city, the configuration of SAHPWH with the lowest energy consumption was the one with the greatest inlet air temperatures to the HPWH; for warm climates, this was the outdoor configuration and for cold climates, this was the conditioned configuration. The climate zone with the least annual electricity consumption across Canada and the United States was climate zone 1 which had the greatest mains water temperatures and inlet HPWH air temperatures. Colder climate zones had higher annual electricity consumption with all configurations due to the lower mains water temperatures, but because the conditioned SAHPWH had highest inlet air temperatures to the HPWH, the conditioned SAHPWH performance increased above the outdoor and closed loop SAHPWHs. Further, frigid inlet air temperatures for the outdoor and closed loop SAHPWHs caused a heavy reliance on the electric backup element. Although greatest electricity consumption occurred for SAHPWHs in northern regions, greatest electricity savings did not occur in the far north for an EWH to SAHPWH transition, as shown in Figure 6.2. Instead, there was found to be a correlation between the climate zone in which a city is located and the electricity offset.

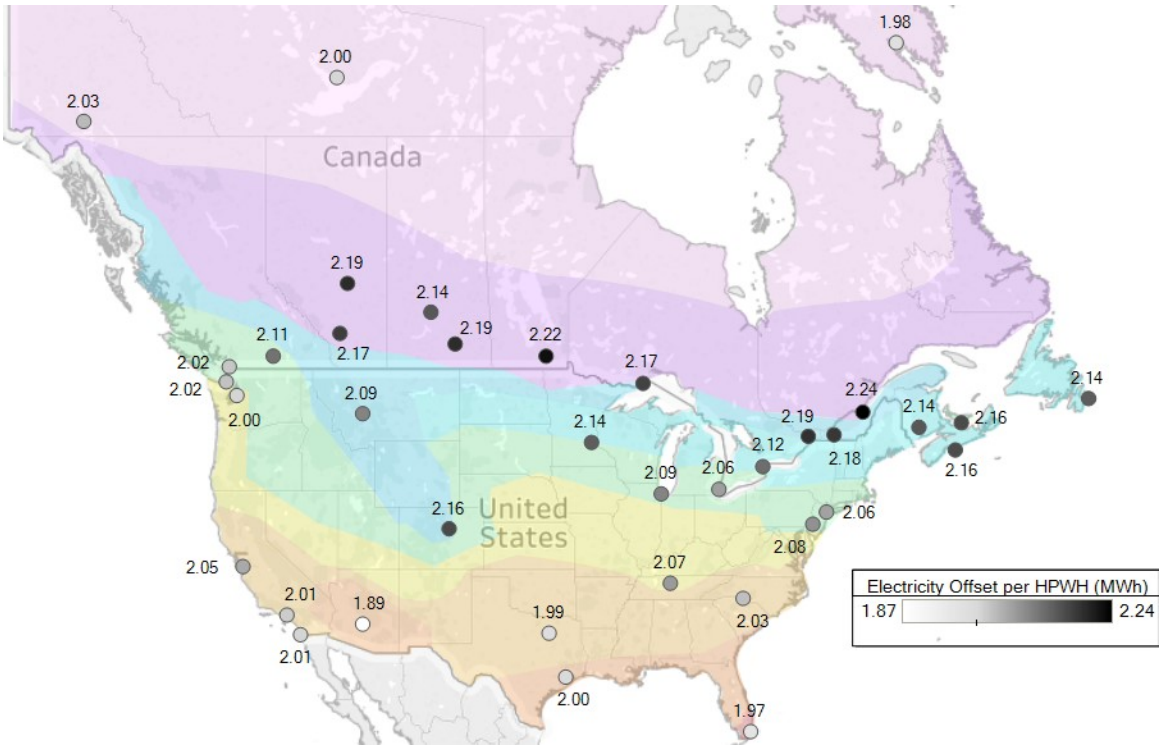

Figure 6.2: Annual electricity offset of SAHPWH compared to EWH

Greatest electricity savings occurred near the Canada and United States border due to the low mains water temperatures and high solar insolation. In cool mains temperature regions, such as northern Canada, a greater amount of energy was required for water heating, so implementing a HPWH with a COP of 2 to 3 had a high absolute energy reduction. However, it was found that far northern cities did not have the greatest electricity reduction with a SAHPWH due to lower inlet air temperatures from the solar collector than higher insolation regions. The balance of high solar insolation to improve HPWH performance with low mains water temperature to increase base electricity consumption occurred near the Canada and United States border, where electricity savings were maximized.

The electricity savings due to the SAHPWH in each location were scaled based on population to determine the electricity reduction that would occur if 5% of existing water

heaters were replaced by SAHPWHs. This represents the electricity reduction possible if 5% of households with an average occupancy of 2.7 persons per dwelling transitioned from an EWH to a SAHPWH based on local populations for each city studied [87], [88]. The results for population-scaled electricity offsets are shown in Figure 6.3.

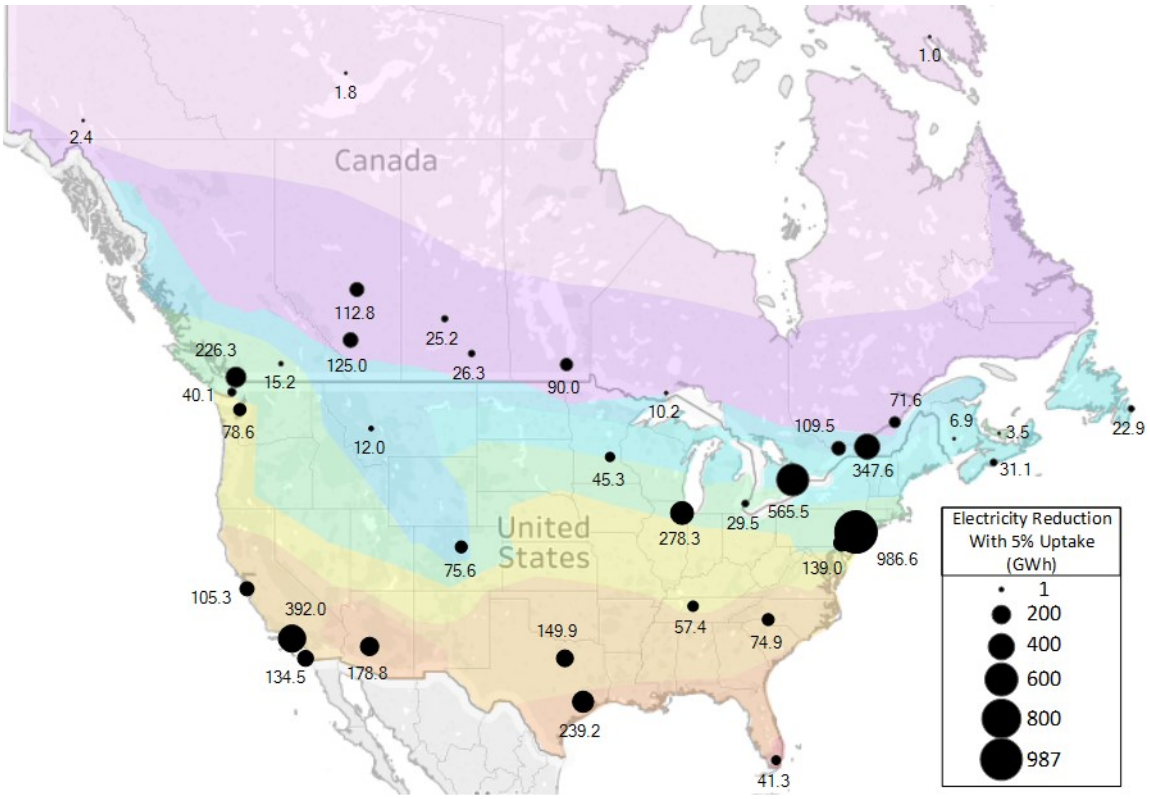

Figure 6.3: Electricity reduction with 5% technology uptake in Canadian and American cities

When scaled by population, large cities such as New York, Toronto, and Los Angeles achieved the largest energy savings due to large populations, whereas northern Canada had the least savings due to their lower populations. It was found that if 5% of households in Canada switched from their existing EWH or NGWH to a SAHPWH, the national energy reduction would be 2.46 TWh annually, which translates to an energy reduction of 3.1% for residential water heating energy consumption.

6.2 Greenhouse gas emissions of configurations analyzed

Quantifying the carbon footprint of water heaters is important given the ongoing GHG reduction goals at international, national, and regional levels. As such, water heating options were analyzed in terms of their equivalent lifecycle GHGs, which included GHGs due to the natural gas or electricity fuel consumed for an alternative water heater and the footprint of the HPWH refrigerant leakage which was assumed to have a leakage rate of 6% per year of the 15-year lifetime. The GHG offsets when transitioning from an EWH to a HPWH are shown in Figure 6.4. The GHG offsets for HPWHs and SAHPWHs varied very little due to their low difference in electricity consumption which translated to even less difference in GHG offsets.

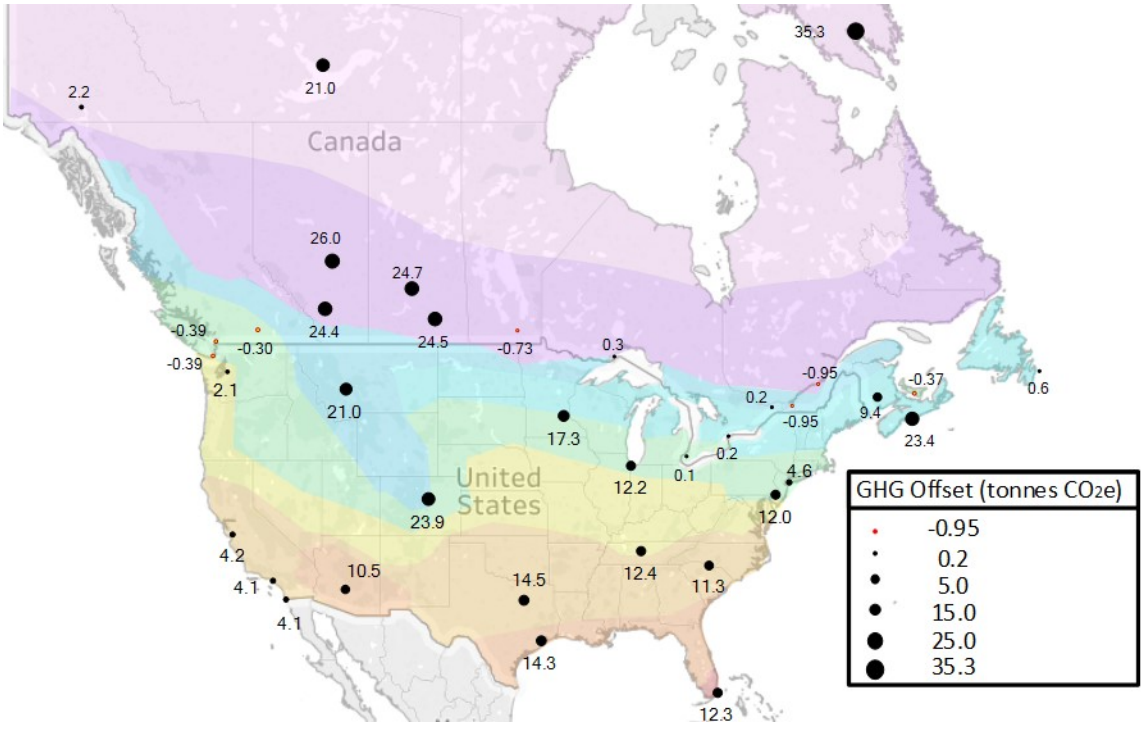

Figure 6.4: GHG offset of HPWH over the lifetime compared to EWH

The GHG offsets over the lifetime of a HPWH were greatest in locations with electricity grids that were highly reliant on fossil fuels such as Alberta, Saskatchewan, and Nova

Scotia. In locations such as Ontario with moderately clean electricity grids, there was a very small lifetime GHG reduction when transitioning from an EWH to a HPWH, because there were low emissions with an EWH to begin with. Further, in locations with grids that have near zero emissions such as British Columbia, Manitoba, PEI, and Quebec, the refrigerant leakage of the HPWH over its lifetime produced more GHGs than the HPWH could offset from an EWH, leading to a negative GHG offset, or a GHG increase, in these locations. When transitioning from a NGWH, more significant GHG savings can be realized in locations with clean electricity grids, as shown in Figure 6.5.

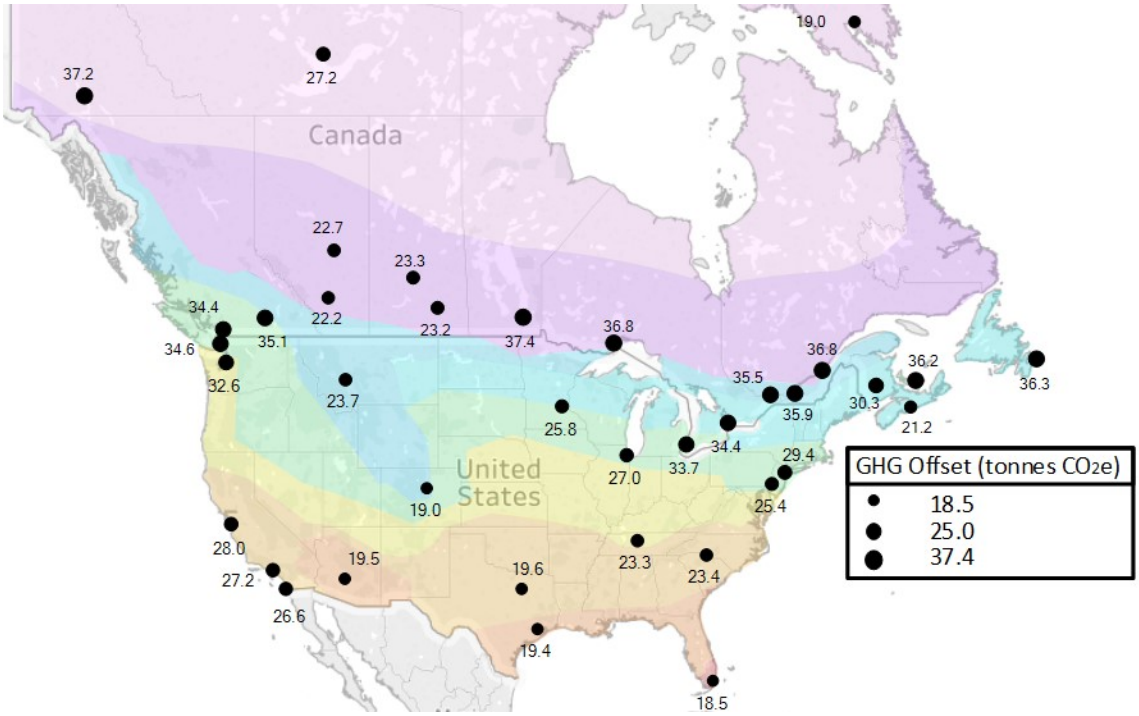

Figure 6.5: GHG emissions offset of HPWH over the lifetime compared to NGWH

The GHG offsets that were found to occur when switching from a NGWH to a HPWH were more similar across Canada and the United States than the GHG offsets from an EWH to a HPWH. The uniformity in GHG offsets from a NGWH to a HPWH was caused by the decrease in natural gas fuel consumption that occurred across the two countries and

dominated the GHG reductions. It is important to note that NGWHs are not present in the Canadian territories, PEI, or Newfoundland due to the lack of natural gas supply in these locations, but they are provided on the graph for insight into the trends and behavior that could occur in the studied cities.

When the results from Figure 6.4 and Figure 6.5 are compared, it can be seen that locations with clean electricity grids were more sensitive to the alternative technology (EWH or NGWH) than locations with fossil fuel-dependent grids, in terms of GHG reduction. In British Columbia, Manitoba, PEI, and Quebec, there was a far greater difference in GHG offset between the EWH to HPWH and NGWH to HPWH cases than the difference in offsets in Alberta or Saskatchewan. Further, in Alberta and Saskatchewan which are reliant upon coal for electricity generation, there was a lower GHG offset when comparing a HPWH to a NGWH than when comparing a HPWH to an EWH. This is because coal has almost three times the global warming potential than natural gas, meaning EWHs produce more GHGs than NGWHs in coal-dominant locations. As such, switching to a HPWH from an EWH had a greater GHG reduction than from a NGWH in fossil fuel dominant locations.

6.3 Economic performance of configurations analyzed

The economic parameters were functions of geographically specific conditions such as mains water temperatures and space heating and cooling seasons but were also of electricity and natural gas rates in each location. As such, the results for PBP and LCC did not necessarily follow the same trends as those for the energy consumption analysis.

6.3.1 Payback period

The PBP values for the HPWH and SAHPWH were compared for each of the Canadian and American locations studied to determine the locations in which each configuration resulted in a lower PBP, as shown in Figure 6.6.

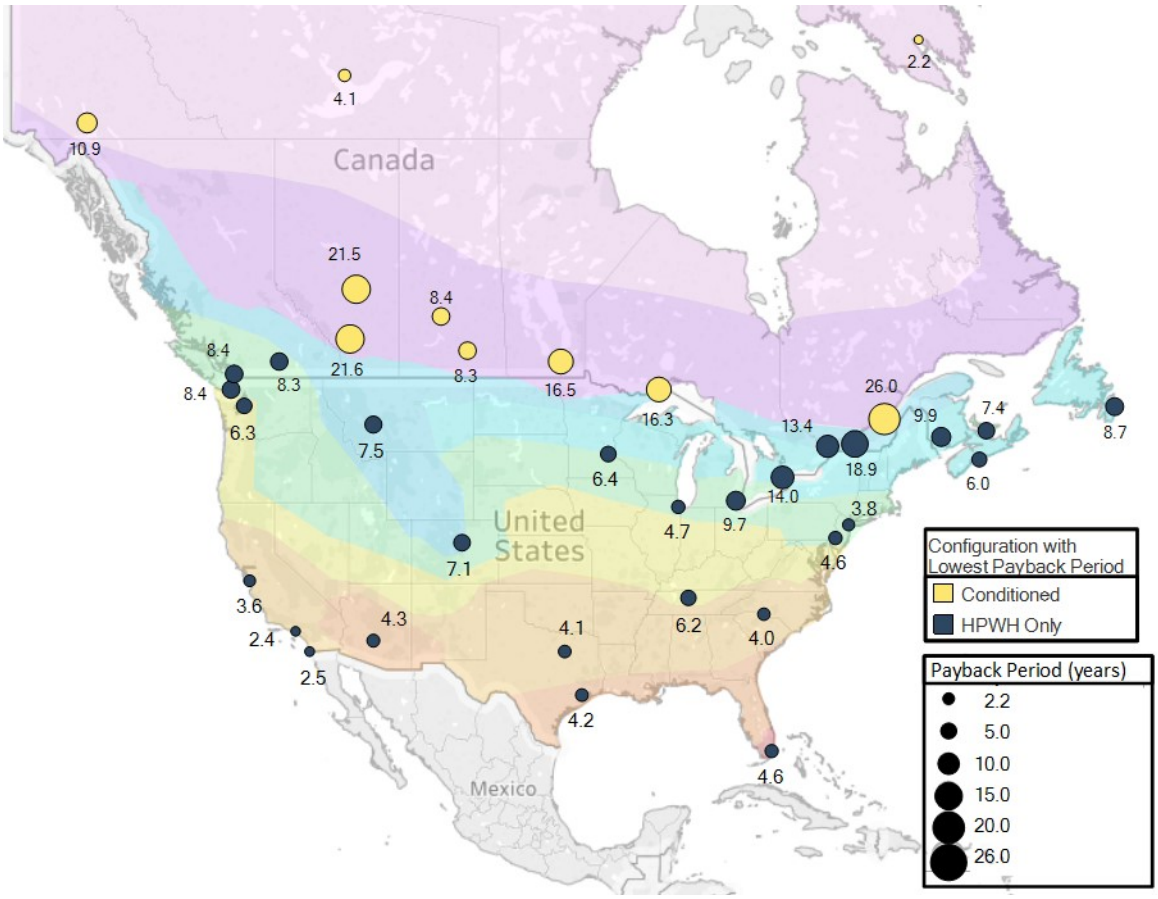

Figure 6.6: Configuration of water heater with the lowest PBP compared to an EWH

The configuration of HPWH or SAHPWH with the lowest PBP was highly correlated to the climate zone in which a city was located; in zones 7 and 8, the conditioned SAHPWH had the lowest PBP, while in climate zones 6 and lower, the HPWH had the lowest PBP. In the cooling-dominant southern United States, the HPWH which provided cooling benefits throughout a significant portion of the year resulted in lower PBPs, while in

heating-dominant northern Canada, the SAHPWH which provided heating benefits resulted in lowest PBPs. The locations which were in colder climate zones had the greatest negative impact due to the HPWH space cooling and thus the SAHPWH which mitigated the space cooling effect decreased the PBP.

Although the energy analysis showed that greatest electricity offsets for water heating occurred near the Canada and United States border, these offsets did not translate to a lower PBP. This was caused by two major factors. Firstly, locations near the Canada and United States border which had nearly equal heating and cooling seasons had longer PBP than the southern-most locations due to their relatively high energy consumption for water heating (due to lower mains water temperatures than the south). Secondly, many locations that happen to be near the Canada and United States border had low electricity prices, which reduced the yearly savings that occurred; this did not cause a geographical impact on the HPWH or SAHPWH system despite that it seemed like a geographical factor.

The PBPs were highly dependent upon local electricity prices: locations such as Quebec with low electricity prices had significantly lower operating costs for the EWH so annual savings by the HPWH or SAHPWH were relatively low, and thus PBP was over 20 years. In contrast, Iqaluit had high electricity prices which translated to high operating costs, high savings with a SAHPWH, and thus a low PBP.

The PBP was also analyzed against a NGWH, and the results are shown in Figure 6.7. In some locations, NGWH was not an option due to the lack of natural gas supply, and in some places the PBP compared to a NGWH was either negative indicating that the operating cost of the NGWH was cheaper than that of the HPWH or SAHPWHs or the

PBP was greater than 50 years. For any of these three cases, there was deemed to be no configuration with a lowest PBP compared to a NGWH.

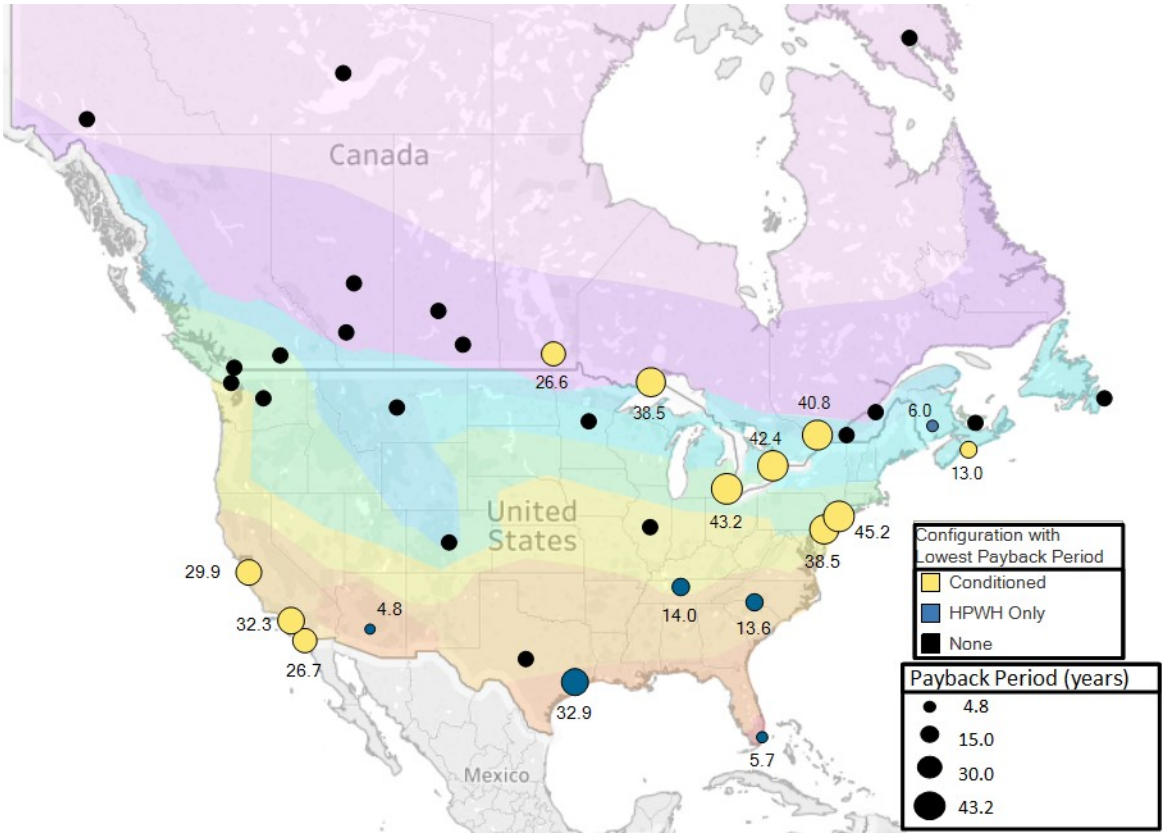

Figure 6.7: Configuration of water heater with the lowest PBP compared to a NGWH

The configuration with the lowest PBP compared to a NGWH did not appear to have any correlation to the climate zone. Rather, there was a stronger correlation to local electricity and natural gas rates than to the climate zone. In locations such as Miami, Houston, Nashville, and Fredericton, there were high natural gas rates and moderate electricity rates. The high natural gas rates lead to both the HPWH and SAHPWH having lower operating costs than the NGWH on an annual basis, while the moderate electricity prices did not cause the SAHPWH to have annual operating cost savings that were sufficiently greater than the HPWH to overcome the additional costs of the solar collector. In locations with

higher electricity rates and relatively high natural gas rates such as California, New York, Philadelphia, Ontario, the SAHPWH provided sufficiently higher operating cost savings than the HPWH thus allowing the high capital cost of the solar collector to be overcome.

In locations such as Alberta and Saskatchewan which had low natural gas rates and therefore low operating costs for a NGWH, the electricity rates did not have a significant impact on the PBP. Due to the low natural gas rates, neither Alberta, which has low electricity rates, nor Saskatchewan, which has high electricity rates were able to overcome the high capital cost of the HPWH or SAHPWH. In both locations, the operating cost of the NGWH was cheaper than that of the HPWH and SAHPWH.

Because the values used to calculate PBP and the other economic parameters may have a high degree of variability, the sensitivity of the PBP to variation in input values was tested. The results of this PBP sensitivity analysis are shown in Appendix E.

6.3.2 Lifecycle cost

The LCC of the HPWH and SAHPWHs were compared across Canada and the United States to determine the configuration with the lowest LCC in each location. The results are shown in Figure 6.8, with the LCC values provided in local currency for each location.

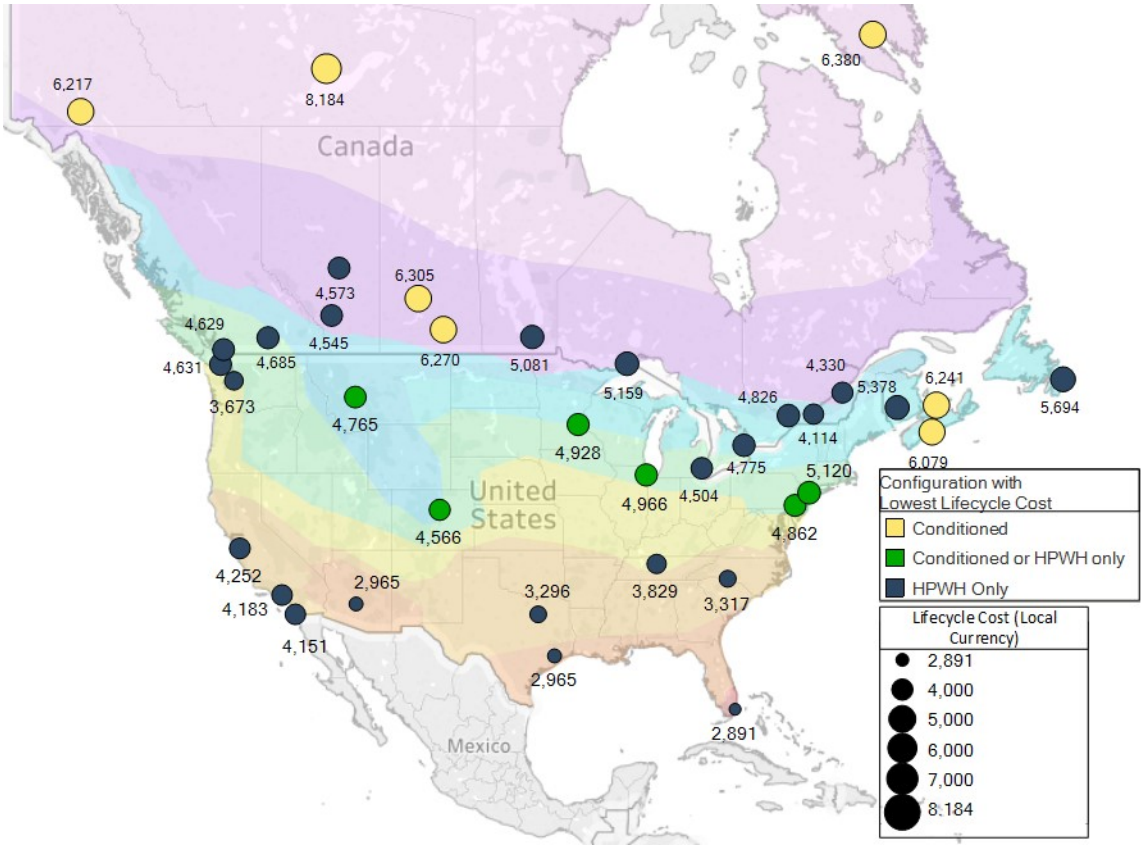

Figure 6.8: Configuration with lowest lifecycle cost

The configuration with the lowest LCC in each location was not necessarily the same as the configuration with the lowest PBP. This is because LCC is based only upon a the HPWH or SAHPWH technology option, whereas the PBP encompassed an alternative option as well (an EWH or NGWH). Some locations which moderately benefitted from the space heating of the SAHPWH, such as those in zone 7, had a different configuration with lowest PBP than configuration with lowest LCC. For example, in Manitoba, the conditioned SAHPWH had the lowest PBP, but the HPWH had the lowest LCC. This difference in Manitoba and other Canadian locations was caused by their relatively cheap electricity rates. If electricity rates were cheap, there was a lower absolute cost savings between an EWH and a HPWH or SAHPWH, and thus the PBP calculation which

compared the EWH to the HPWH or SAHPWH was less influenced by direct water heating costs and more influenced by space conditioning benefits. The SAHPWH which provided greater space heating benefits in zone 7 therefore had a lower PBP in locations with low electricity rates. However, due to the low electricity rates and the high solar collector cost, the HPWH had a lower LCC than the SAHPWH.

The high capital cost of the solar collector caused the SAHPWH to have a higher LCC in locations with low electricity rates. However, in locations with high electricity rates the higher electricity rates translated to a higher savings for space conditioning costs with the SAHPWH, thus leading to lower LCC values with the SAHPWH than the HPWH in locations such as Saskatchewan.

6.3.3 Breakeven capital costs

The breakeven capital cost is a comparison of the LCC of the HPWH or SAHPWH compared to an alternative such as the EWH or NGWH. If the breakeven capital cost was greater than the actual capital cost of the HPWH or SAHPWH, the technology was said to have a lower LCC than the EWH or NGWH to which it was compared. A summary of the configurations of HPWH or SAHPWH with a lower LCC than an EWH are shown in Figure 6.9.

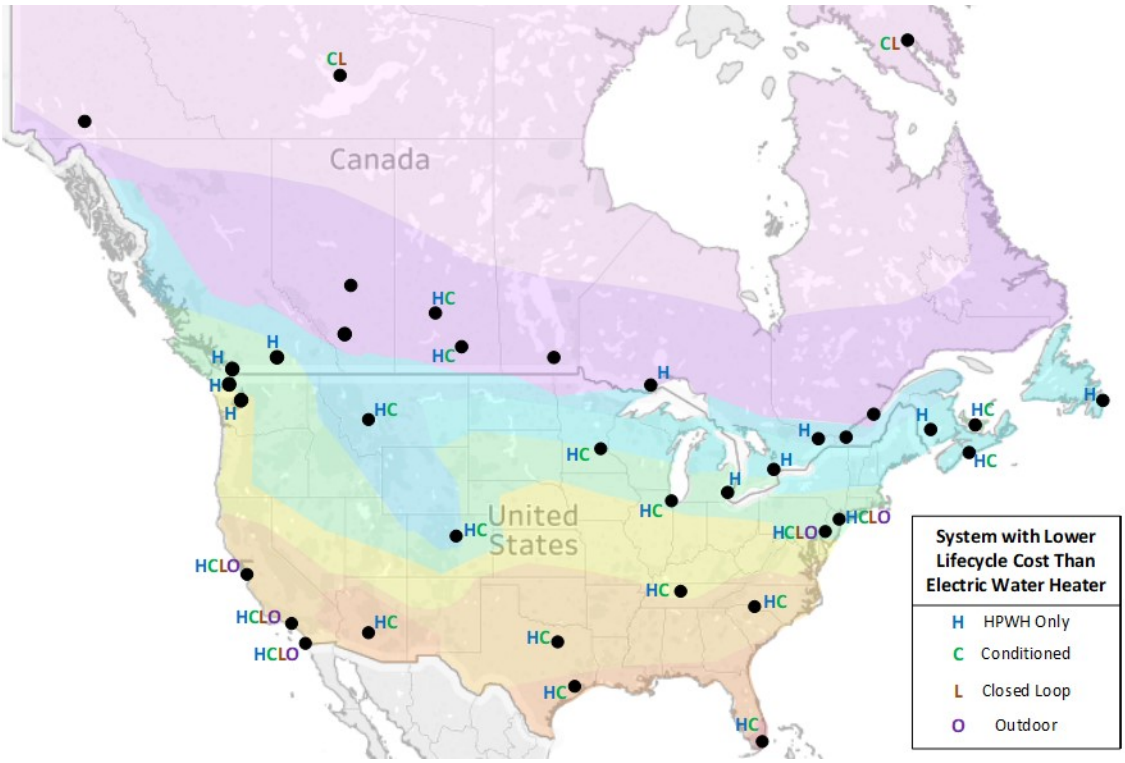

Figure 6.9: Configurations with lower LCC than an EWH

In general, the locations with the highest electricity prices were the locations in which the most configurations of HPWH and SAHPWH were found to be economically feasible in terms of breakeven costs. For example, California which had high electricity rates had a lower LCC for all configurations of HPWH and SAHPWH than the EWH. The Canadian territories had high electricity rates but were an exception to the high electricity rate and increased system feasibility correlation. In the territories, only the conditioned and closed loop configurations were feasible because the outdoor SAHPWH relied heavily on the electric backup element which significantly increased energy consumption and costs, and the HPWH added high amounts of harmful space cooling throughout the year.

When considering the HPWH and SAHPWH against a NGWH, the SAHPWH was infeasible in that the breakeven cost calculated was always less than the actual capital cost

across Canada and the United States. Compared to the NGWH, the HPWH only had a breakeven capital cost that was greater than the actual capital cost in Phoenix, Miami, and Fredericton, all of which have high natural gas rates. Because the low cost of natural gas was an economic barrier for HPWH and SAHPWHs and the future cost of natural gas is relatively unknown, an analysis was conducted to determine the difference in feasibility if the natural gas rate increased by 50%, as shown in Figure 6.10.

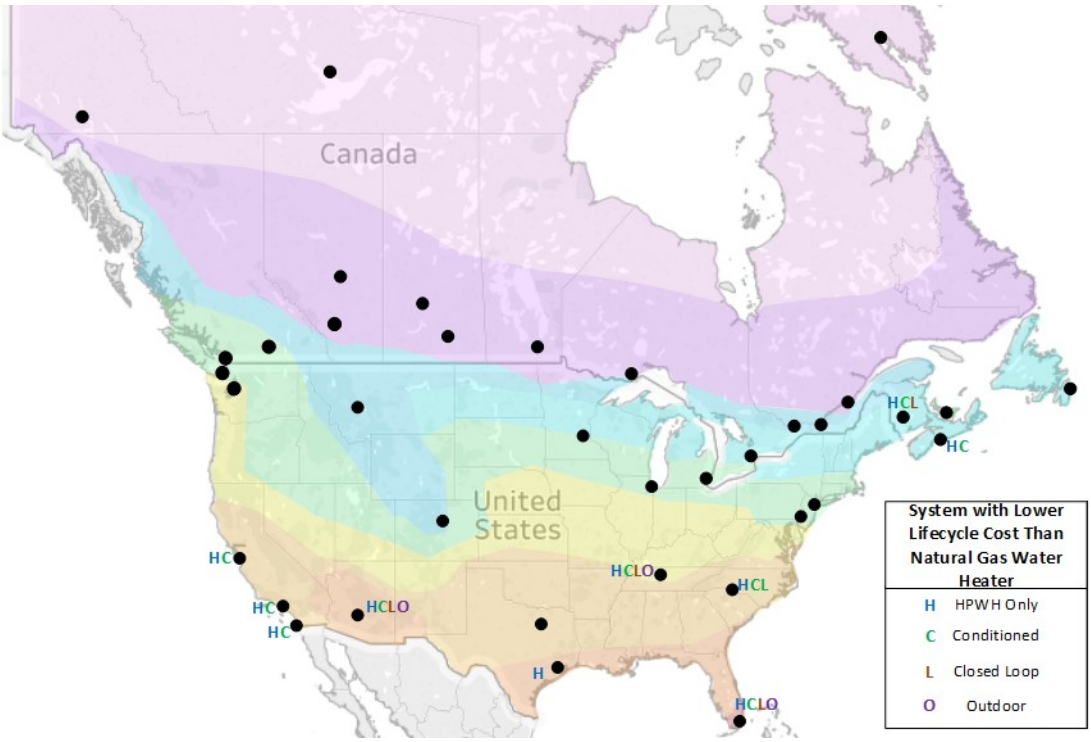

Figure 6.10: Configurations with lower LCC than a NGWH with a 50% increase in natural gas rates

Even with a 50% increase in natural gas rates across Canada and the United States, HPWHs and SAHPWHs were not found to be economically feasible in many locations. However, they were most feasible in the southern United States and the maritime provinces of Canada which have high natural gas rates. In general, it was difficult to overcome the high capital costs of the HPWHs and SAHPWHs in terms of breakeven costs in locations that had cheap

fuel rates for the NGWH or EWH. To increase the feasibility of HPWHs and SAHPWHs, subsidies could be introduced which would decrease the capital cost of HWPHs and SAHPWHs and thus decrease the overall LCC. The subsidies required for the LCC of the HPWH and SAHPWH to have the same LCC as the EWH in local currency are shown in Figure 6.11 and Figure 6.12, respectively.

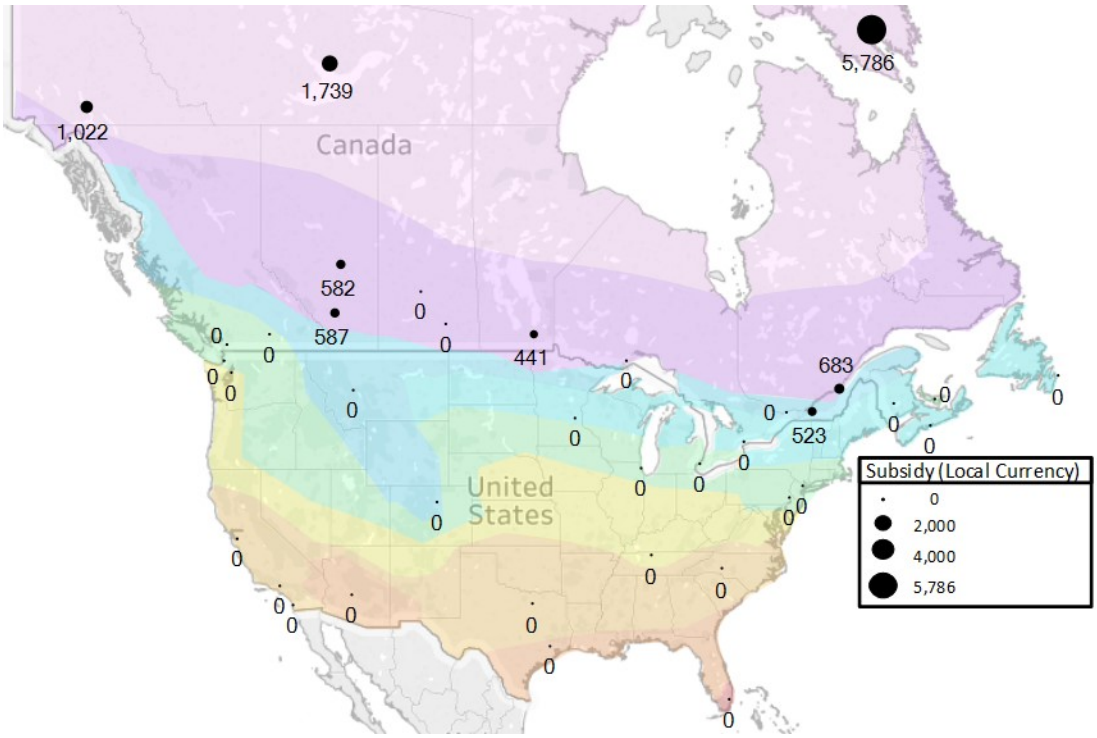

Figure 6.11: Subsidies for a HPWH to have the same LCC as an EWH

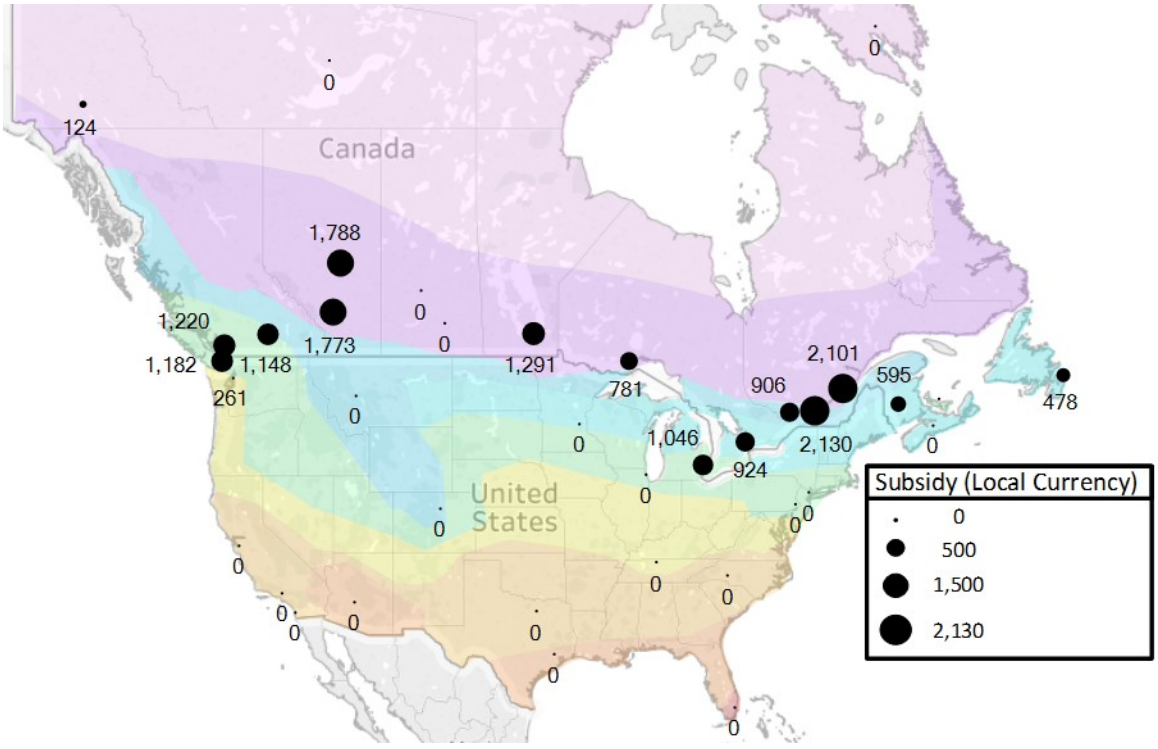

Figure 6.12: Subsidies for a conditioned SAHPWH to have the same LCC as an EWH

The subsidies for the HPWH and SAHPWH compared to the EWH were highly dependent upon the climate zone in which each city was located. For the EWH to HPWH transition, there was no subsidy required across the United States and in warm Canadian locations, but the subsidy amount increased further north within Canada. This is because the HPWH provided greatest space cooling benefits in the southernmost locations, whereas the space cooling increased space heating loads in northern locations that were heating dominant.

For the EWH to SAHPWH, the lowest subsidies were required in the southern United States and the Canadian territories. In the southern United States, a high amount of space cooling allowed even the capital cost of the solar collector to be overcome in the LCC calculation, while in the Canadian territories, the space heating benefits provided by the SAHPWH reduced the LCC to below that of the EWH. In climates near the Canada and

United States border, the highest subsidies were required for the SAHPWH. The cheap cost of electricity in southern Canada compared to other locations which reduced the value of the operating cost savings between the EWH and SAHPWH was a primary reason for this.

The trend for subsidies for a HPWH and SAHPWH against a NGWH in local currency, as shown in Figure 6.13 and Figure 6.14, were similar to that of the HPWH and SAHPWH against an EWH. In general, the subsidies were greater when the HPWH and SAHPWH were compared to a NGWH than when compared to an EWH due to the low cost of natural gas fuel which caused the NGWH to have low annual operating costs. This indicates the difficulty to increase uptake of HPWHs or SAHPWHs when comparing these technology options to a NGWH; the increased cost over the lifecycle and large subsidies that would need to be implemented to decrease the cost to that of the NGWH may prevent the HPWH or SAHPWH from becoming mainstream technology options in many locations.

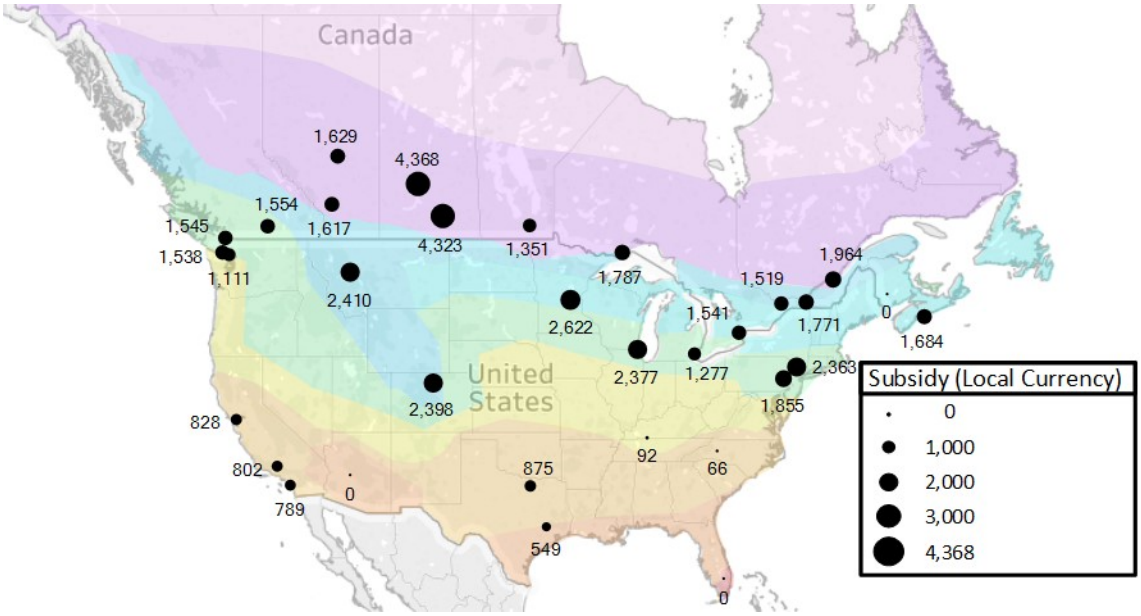

Figure 6.13: Subsidies for a HPWH to have the same LCC as a NGWH

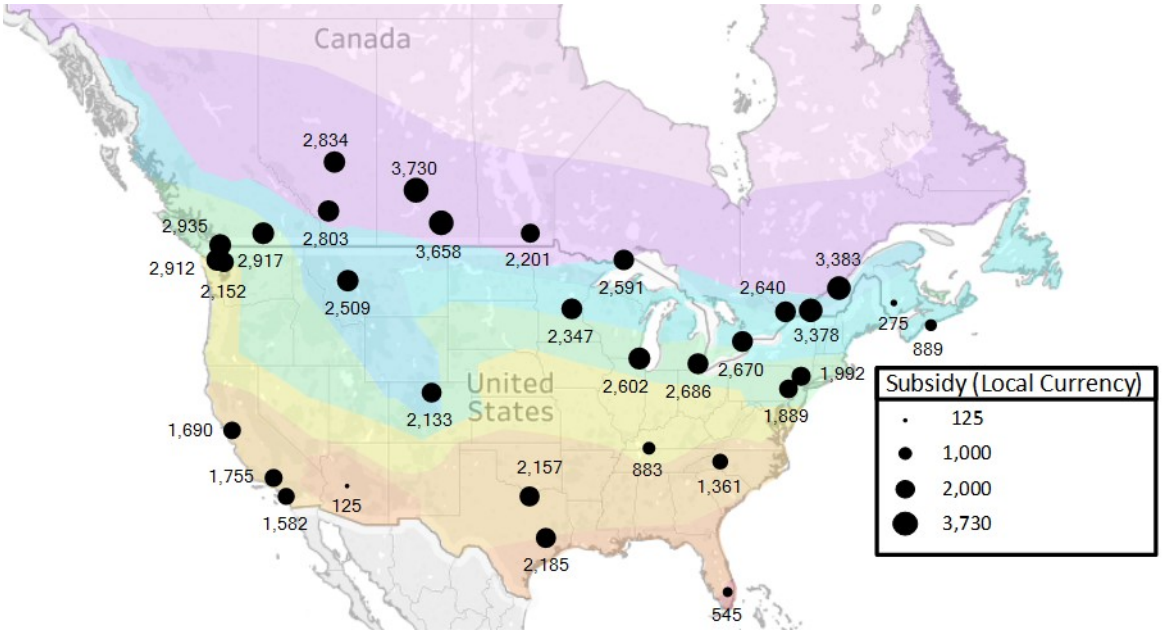

Figure 6.14: Subsidies for a conditioned SAHPWH to have the same LCC as a NGWH

In many locations, the LCC, breakeven costs, and subsidies to bring the LCC of a HPWH or SAHPWH down to that of an EWH or NGWH were found to be prohibitively high and may thus limit uptake of the HPWH and SAHPWHs. It is possible that the subsidies could be reduced, particularly compared to the NGWH, if GHG reductions were valued.

6.3.4 Inclusion of greenhouse gas emissions

An analysis was conducted to determine if valuing the GHGs from HPWHs, SAHPWHs, and alternative water heaters increased the economic feasibility of HPWHs and SAHPWHs. Although future carbon prices are highly unknown, this analysis provided a potential scenario for the impact that carbon pricing could have on the technology options. The impacts from this analysis could be scalable between the carbon price selected and the no carbon price scenarios described previously. The carbon price analyzed in this study was \$50 per metric ton of CO_2e. The results for the subsidies required to make the LCC of

HPWHs and SAHPWHs equal to that of a NGWH when considering carbon pricing are shown in Figure 6.15 and Figure 6.16, respectively.

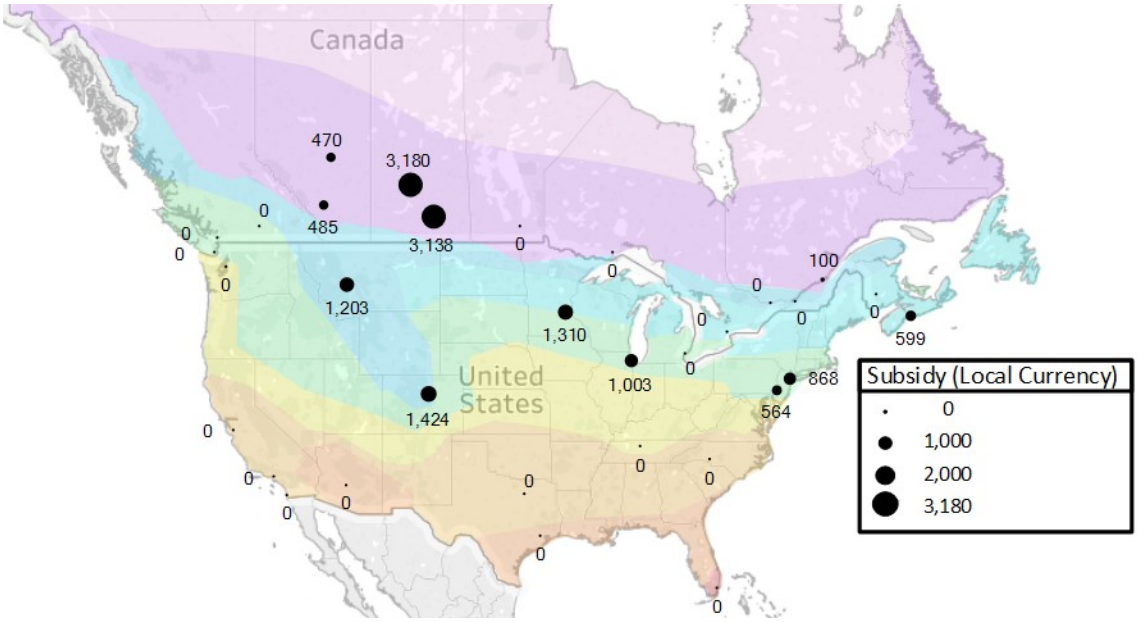

Figure 6.15: Subsidies for a HPWH to have the same LCC as a NGWH with a $50 carbon price

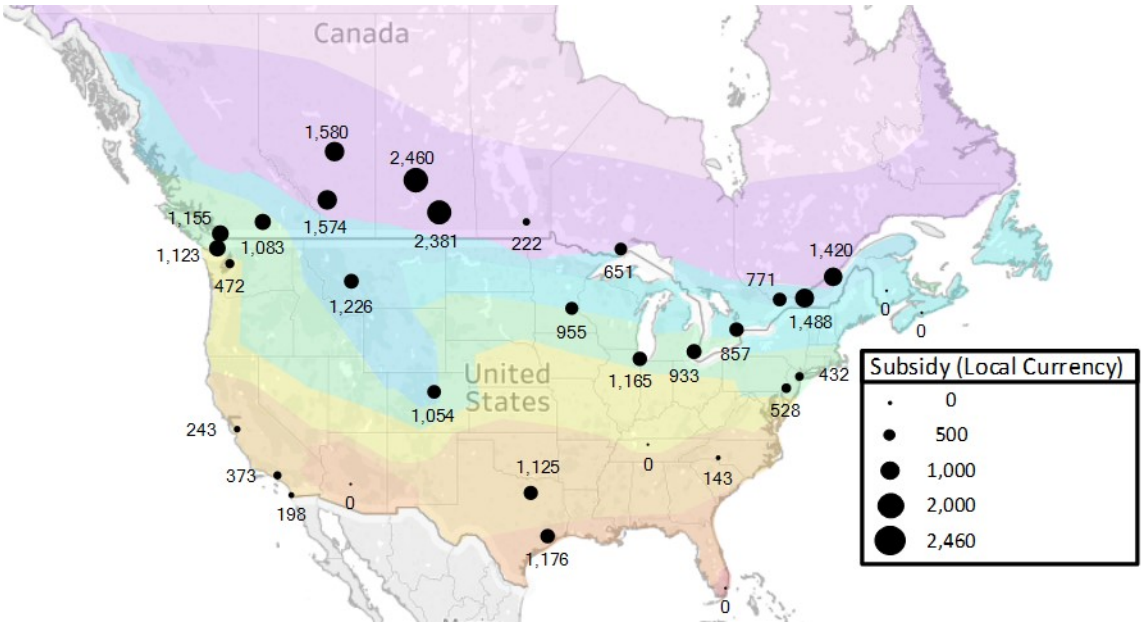

Figure 6.16: Subsidies for a conditioned SAHPWH to have the same LCC as a NGWH with a $50 carbon price

In most locations the subsidy required for a HPWH was less than that required for a SAHPWH, except locations that were highly reliant upon coal for electricity generation, such as Nova Scotia and Saskatchewan. In these locations, the high GHGs produced by the coal electricity generation caused the HPWH to be more expensive than the SAHPWH due to its extra electricity consumption. Locations with cleaner electricity grids had cheaper subsidy values for the HPWH because less savings were realized between the HPWH and SAHPWH, so the high capital cost of the solar collector could not be overcome.

For both the HPWH and the SAHPWH, a significant reduction in subsidy value occurred when carbon pricing of $50 per ton was introduced. The HPWH and SAHPWH had a reduction in subsidy value of at least 27% and 34%, respectively when carbon pricing was considered. However, in many locations across Canada and the United States, the subsidy value was reduced to zero when carbon pricing was considered. This illustrates that there may be significant value of adding a carbon price in terms of the economic feasibility.

6.4 Summary of key findings

In this study, there were several findings for the energy, GHG, and economic analyses. For energy consumption, it was found that the HPWH greatly reduced energy consumption compared to the EWH and NGWH options, but from the HPWH to the SAHPWH there was not a significant decrease in energy consumption. However, it was determined that the greatest electricity offsets occurred for EWHs to SAHPWHs near the Canada and United States border due to the balance of low mains water temperatures and high solar insolation.

The GHG analysis showed that the greatest emissions reduction occurred when transitioning from a NGWH to a SAHPWH in a location with a clean electricity grid and

with a natural gas space heating system in place. However, when transitioning from an EWH to a HPWH, there was an increase in GHG emissions in locations with clean electricity grids when the refrigerant leakage was considered.

The economic analysis showed that although HPWHs and SAHPWHs may be viable when compared to EWHs, the low cost of natural gas fuel was a barrier for HWPHs and SAHPWHs and prevented the systems from being highly viable in many locations when compared to a NGWH. When a price was put on the GHG reductions that could be realized with HPWHs and SAHPWHs, the economic feasibility of the systems against a NGWH increased significantly.

Chapter 7: Conclusions and Future Work

Several conclusions can be drawn from the research presented within this thesis. These conclusions are presented first within this chapter and are followed by future research options that build upon the current project.

7.1 Conclusions

This study included experimental and simulated analyses of a HPWH with the objective of determining the energy, GHG, and economic performance of HPWHs and SAHPWHs across Canada and the United States. Experiments were used to characterize the performance of a commercially available HPWH, and a model was created and validated based on the experimental results. The HPWH model was expanded to include a solar collector in three configurations of SAHPWH: conditioned, outdoor, and closed loop. All configurations were analyzed in selected cities across Canada and the United States to determine which had the best performance based on the energy consumption and reduction, GHG reduction, and economic parameters studied.

Both the HPWH and SAHPWHs were found to significantly decrease energy consumption compared to an EWH or NGWH across Canada and the United States, and although the conditioned SAHPWH decreased energy consumption compared to the HPWH, it was a significantly less decrease than that from an EWH or NGWH to a HPWH. The variations in performance of HPWHs and SAHPWHs across Canada and the United States were largely due to the differences in mains water temperature and inlet air temperatures to the HPWHs. In lower mains temperature locations, greater electricity consumption was required to heat the water, and thus a greater absolute electricity decrease occurred between

the EWH and HPWH or SAHPWH in these locations. An increase or decrease in inlet air temperature to the HPWH corresponded to an increase or decrease in performance, respectively, so the warmer inlet air temperatures of the conditioned SAHPWH increased performance compared to the HPWH. Additionally, locations with cold outdoor temperatures required a high amount of electricity consumption and had a high reliance upon the electric resistance backup element for the outdoor SAHPWH. Due to the balance of low mains water temperature and high insolation (and therefore inlet air temperatures), the greatest electricity offset between an EWH and SAHPWH was realized near the Canada and United States border. It was found that if 5% of existing water heaters in Canada were replaced by a HPWH, there would be a 3.1% decrease in energy consumption for water heating in the country.

The GHG analysis showed that the greatest GHG offsets from an EWH to a HPWH or SAHPWH could be realized in locations with electricity grids that were dominant on fossil fuels, while the greatest GHG offsets from a NGWH to a HPWH or SAHPWH could be realized in locations with clean electricity grids. Further, if a transition was made from an EWH to a HPWH in a location with a clean electricity grid, an increase in GHGs occurred when the HPWH refrigerant leakage was considered, or when a natural gas space heating system was used in cold climate locations. These increases occurred because in locations with clean electricity grids the GHG reductions due to operation of a HPWH instead of an EWH were low, therefore factors that contributed more to the GHGs such as the natural gas space heating increase or refrigerant leakage were greater than the GHG reduction from an EWH to a HPWH.

In the economic analysis, it was found that the HPWHs and SAHPWHs were more feasible when compared to EWHs than NGWHs due to the inexpensive cost of natural gas fuel. However, when a price was added to the GHGs produced by NGWH, it was found that the subsidies required to make the HPWH or SAHPWH have the same LCC as the NGWH were reduced by at least 27% in all locations and were completely eliminated in others, and thus the feasibility of the HPWHs and SAHPWHs increased. Further, increases in natural gas fuel costs would increase the feasibility of HPWHs and SAHPWHs as well.

The calculated subsidy values were the amounts that the capital cost of a HPWH or SAHPWH would have to decrease to have the same LCC as an EWH or NGWH. In locations with low electricity and natural gas rates, the subsidy values were greater than locations with high utility rates. In most locations, the subsidies were less for a HPWH than a SAHPWH and for an EWH than a NGWH.

When considering the feasibility of HPWHs and SAHPWHs in terms of PBP, it was found that the PBP would be minimized for a HPWH with an inefficient space cooling system and an efficient space heating system, because this scenario maximized the benefits provided to the space by the HPWH. For the SAHPWH, the PBP was found to be minimized with an inefficient space heating and cooling system because the SAHPWH provides both space cooling and space heating benefits. This did not consider the increased total operating cost of using the space conditioning systems, and instead only included the economic impact of the existing space conditioning systems.

In general, it was found that HPWHs were often cheaper than SAHPWHs across Canada and the United States. There were three main factors which caused an exception to this:

- locations with high electricity prices had greater absolute energy savings for the SAHPWH compared to the HPWH thus making the SAHPWH cheaper over the lifetime than the HPWH,
- when a price was put on the GHGs, locations which were highly reliant upon fossil fuels for electricity generation had a high cost associated with electricity consumption and therefore the SAHPWH which reduced electricity consumption were cheaper over the lifetime than the HPWH, and
- locations with long heating seasons such as zone 8 had a significant increase in space heating costs throughout the year with the HPWH which was offset by the SAHPWH.

This study provided insight into the performance of HPWHs and SAHPWHs across Canada and the United States and showed the value of implementing the systems for energy and GHG reductions. Although it was difficult to overcome the high capital costs of the systems in many locations, adding a value to the GHGs increased the economic feasibility. HPWHs and SAHPWHs could be implemented as a clean and efficient technology for water heating that will help reduce GHGs of the building sector and meet climate goals, but to date the cost barrier of the systems remains present in many locations.

7.2 Future Work

Additional work should be conducted on this project to determine the behavior of the HPWH and SAHPWH systems under different conditions and for different applications. In this study, CSA Schedule A draw profile was studied, but it is important to study the impacts of different draw profiles such as ones that have larger or more irregular daily

draws. Different draw events could significantly change the results obtained within this study, particularly if there were large draw events that would require use of the electric backup elements in the HPWH.

Future studies should include experiments on a commercially available solar thermal collector to determine performance variations from the measurements provided by the manufacturer that occur in colder climate locations or under less ideal conditions. Further, including experimental analysis of a solar collector would help to quantify heat losses and temperature decreases that may occur between the solar collector and the HPWH in a house, thus providing a more accurate representation of SAHPWH performance.

Future analysis should also include the power consumed by the fan at the solar collector inlet. The fan would increase the overall energy consumption of the SAHPWH systems and this energy should be quantified to fully analyze the system performance. During periods when the HPWH was operating, the built-in HPWH fan would run and the solar collector fan would not be required. However, during periods of high solar insolation when the refrigeration cycle was not on and drawing air using the built-in fan, an external fan would be required to use the solar to heat the home. The increase in energy consumption may decrease the feasibility of the SAHPWH systems.

Since the SAHPWH system is a new, upcoming water heating technology option, further comparison should be done on newer methods of water heating with other fuel types. This includes natural gas tankless water heaters which achieve higher energy factors than the tank-type natural gas water heaters studied in this project. The capital cost of tankless water heaters is often greater than that of tank-type systems, but their higher efficiency would

decrease fuel costs throughout the lifetime. As such, a full lifecycle comparison should be done on tankless systems in comparison with the SAHPWHs and HPWHs analyzed in this study.

A HPWH or SAHPWH could be used for demand-side management to reduce peak electricity loads and decrease fossil fuel consumption for electricity generation. HPWHs and SAHPWHs could be programmed to operate as much as possible at off-peak times with thermal storage for use during on-peak times. This could then be expanded to consider a HPWH or SAHPWH to meet all space heating and cooling loads. Increasing the operation time of a HPWH would provide additional space cooling, and the excess heated water produced could be stored in a larger tank to meet DHW requirements at other times. In the heating season, a SAHPWH could be used to heat water during off-peak times which could be stored and used in a radiant floor heating loop. Using a HPWH or SAHPWH for space and water heating could help significantly reduce GHGs for the two largest energy end use categories in Canada.

References

[1] NRCAN, “Comprehensive Energy Use Database,” 2016. [Online]. Available: http://oee.nrcan.gc.ca/corporate/statistics/neud/dpa/menus/trends/comprehensive_tables/list.cfm. [Accessed: 30-Sep-2019].

[2] Government of Canada, “The Paris Agreement,” 2016. [Online]. Available: https://www.canada.ca/en/environment-climate-change/services/climate-change/paris-agreement.html. [Accessed: 17-Dec-2019].

[3] Energy Star, “Water Heater Key Product Criteria.” [Online]. Available: https://www.energystar.gov/products/water_heaters/residential_water_heaters_key_product_criteria. [Accessed: 14-Jan-2020].

[4] VHK for European Commission, “WH Water Heaters Ecodesign and Energy Label Review,” 2019.

[5] Government of Canada, “Water temperature and burns/scalds,” 2011. [Online]. Available: https://www.canada.ca/en/public-health/services/water-temperature-burns-scalds.html. [Accessed: 01-Oct-2019].

[6] K. Khalaf, “Experimental Characterization and Modelling of a Heat Pump Water Heater,” Carleton University, 2017.

[7] GE Appliances, “GE Hybrid Water Heater GEH50DEED Technical Service Guide,” Louisville KY, 2012.

[8] Waide Strategic Efficiency, “Policy Opportunities for More Efficient Residential Water Heating,” 2015.

[9] H. Zhao, Y. Gao, and Z. Song, “Strategic outlook of Heat pump development in China,” in *12th IEA Heat Pump Conference*, 2017.

[10] D. Ryan, R. Long, D. Lauf, M. Ledbetter, and A. Reeves, “Water Heater Market Profile,” Silver Spring, MD, 2010.

[11] NRCAN, “Paving the Road to 2030 and Beyond: Market transformation road map for energy efficient equipment in the building sector,” *Energy Mines Minist. Conf.*, 2018.

[12] CADMUS, “Heat Pump Advantage – Water Heater Rebate Pilot Evaluation,” Toronto, ON, 2018.

[13] K. J. Chua, S. K. Chou, and W. M. Yang, “Advances in heat pump systems: A review,” *Applied Energy*, vol. 87, no. 12. Elsevier Ltd, pp. 3611–3624, 2010.

[14] J. A. Pietsch, “The Unitary Heat Pump Industry: 25 Years of Progress,” *ASHRAE J.*, vol. 19, no. 7, 1977.

[15] J. Bursill and C. A. Cruickshank, “Heat Pump Water Heater Control Strategy Optimization for Cold Climates,” *J. Sol. Energy Eng.*, vol. 138, no. 1, p. 011011, Dec. 2015.

[16] M. Lei, H. Zhang, F. Wang, and X. You, “Experimental study of an instantaneous-heating air source heat pump water heater with a temperature stratified water tank,” *Adv. Mech. Eng.*, vol. 8, no. 9, pp. 1–9, Sep. 2016.

[17] J. Ji, T. T. Chow, G. Pei, J. Dong, and W. He, “Domestic air-conditioner and integrated water heater for subtropical climate,” *Appl. Therm. Eng.*, vol. 23, no. 5, pp. 581–592, Apr. 2003.

[18] K. Hudon, B. Sparn, D. Christensen, and J. Maguire, “Heat pump water heater technology assessment based on laboratory research and energy simulation models,” *ASHRAE Trans.*, pp. 683–704, 2012.

[19] J. Maguire, X. Fang, and E. Wilson, “Comparison of Advanced Residential Water Heating Technologies in the United States,” Golden, Colorado, 2013.

[20] B. Sparn, K. Hudon, and D. Christensen, “Laboratory Performance Evaluation of Residential Integrated Heat Pump Water Heaters,” Golden, Colorado, 2014.

[21] A. Amirirad, R. Kumar, and A. S. Fung, “Performance characterization of an indoor air source heat pump water heater for residential applications in Canada,” *Int. J. Energy Res.*, vol. 42, no. 3, pp. 1316–1327, Mar. 2018.

[22] P. J. A. Smith, “Analyzing the Performance of a Heat Pump Water Heater when Coupled with a Heat Recovery Ventilator for Heating Applications in Canada,” Carleton University, 2018.

[23] M. Song, J. Dong, C. Wu, Y. Jiang, and M. Qu, “Improving the frosting and defrosting performance of air source heat pump units: review and outlook,” *HKIE Trans. Hong Kong Inst. Eng.*, vol. 24, no. 2, pp. 88–98, Apr. 2017.

[24] K. Kwak and C. Bai, “A study on the performance enhancement of heat pump using electric heater under the frosting condition: Heat pump under frosting condition,” *Appl. Therm. Eng.*, 2010.

[25] X. Q. Kong, Y. Li, L. Lin, and Y. G. Yang, “Modeling evaluation of a direct-expansion solar- assisted heat pump water heater using R410A,” *Int. J. Refrig.*, vol. 76, pp. 136–146, Apr. 2017.

[26] W. Deng and J. Yu, “Simulation analysis on dynamic performance of a combined solar/air dual source heat pump water heater,” *Energy Convers. Manag.*, vol. 120, pp. 378–387, Jul. 2016.

[27] A. S. Vieira, R. A. Stewart, and C. D. Beal, “Air source heat pump water heaters in residential buildings in Australia: Identification of key performance parameters,” *Energy Build.*, vol. 91, pp. 148–162, Mar. 2015.

[28] S. Poppi, N. Sommerfeldt, C. Bales, H. Madani, and P. Lundqvist, “Techno-economic review of solar heat pump systems for residential heating applications,” *Renewable and Sustainable Energy Reviews*, vol. 81. Elsevier Ltd, pp. 22–32, 2018.

[29] R. S. Kamel, A. S. Fung, and P. R. H. Dash, “Solar systems and their integration with heat pumps: A review,” *Energy and Buildings*, vol. 87. Elsevier Ltd, pp. 395–412, 01-Jan-2015.

[30] D. Carbonell, M. Y. Haller, and E. Frank, “Potential benefit of combining heat pumps with solar thermal for heating and domestic hot water preparation,” in *Energy Procedia*, 2014, vol. 57, pp. 2656–2665.

[31] J. Cai, J. Ji, Y. Wang, and W. Huang, “Operation characteristics of a novel dual source multi-functional heat pump system under various working modes,” *Appl. Energy*, vol. 194, pp. 236–246, Nov. 2016.

[32] J. Chu, “Evaluation of a Dual Tank Indirect Solar-Assisted Heat Pump System for a High Performance House,” Carleton University, 2014.

[33] H. Li, L. Sun, and Y. Zhang, “Performance investigation of a combined solar thermal heat pump heating system,” *Appl. Therm. Eng.*, vol. 71, no. 1, pp. 460–468, Oct. 2014.

[34] M. Kegel, J. Tamasauskas, R. Sunye, and A. Langlois, “Assessment of a solar assisted air source and a solar assisted water source heat pump system in a Canadian household,” in *Energy Procedia*, 2012, vol. 30, pp. 654–663.

[35] M. Kegel, R. Sunye, and J. Tamasauskas, “Life Cycle Cost Comparison and Optimisation of Different Heat Pump Systems in the Canadian Climate,” *Proc. eSim*, pp. 492–505, 2012.

[36] S. K. Chaturvedi, V. D. Gagrani, and T. M. Abdel-Salam, “Solar-assisted heat pump - A sustainable system for low-temperature water heating applications,” *Energy Convers. Manag.*, 2014.

[37] A. Amirirad, “Heat pump water heater for cold climate - Canada,” Ryerson University, 2016.

[38] M. Kegel, J. Tamasauskas, R. Sunye, and D. Giguere, “Heat Pump Water Heaters in the Canadian Residential Market,” in *IEA Heat Pump Conference*, 2017.

[39] M. S. Buker and S. B. Riffat, “Solar assisted heat pump systems for low temperature water heating applications: A systematic review,” *Renewable and Sustainable Energy Reviews*, vol. 55. Elsevier Ltd, pp. 399–413, 01-Mar-2016.

[40] S. Marinelli, F. Lolli, R. Gamberini, and B. Rimini, “Life Cycle Thinking (LCT) applied to residential heat pump systems: A critical review,” *Energy and Buildings*. 2019.

[41] C. Baldwin and C. A. Cruickshank, “Using TRNSYS Types 4, 60, and 534 to model residential cold thermal storage using water and water/glycol solutions,” in *IBPSA eSim Conference*, 2016.

[42] C. A. Cruickshank and S. J. Harrison, “Heat loss characteristics for a typical solar domestic hot water storage,” *Energy Build.*, vol. 42, no. 10, pp. 1703–1710, Oct. 2010.

[43] Continental Control Systems, “WattNode Pulse Installation and Operation Manual,” Boulder, CO, 2011.

[44] Standards Council of Canada - Conseil canadien des normes, “CAN/CSA-F379.1-09 ,” 2018. [Online]. Available: https://www.scc.ca/en/standardsdb/standards/25191. [Accessed: 10-Dec-2019].

[45] NRCan, “Chapter 2: Legionella risk and hazard assessment,” 2019. [Online]. Available: https://www.tpsgc-pwgsc.gc.ca/biens-property/legionella/chapitre-chapter-2-eng.html. [Accessed: 10-Dec-2019].

[46] J. Burch and C. Christensen, “Towards development of an algorithm for mains water temperature,” Golden, Colorado, 2009.

[47] R. Bitter, T. Mohiuddin, and M. Nawrocki, “LabVIEW: Advanced Programming Techniques.” Crc Press, 2006.

[48] F. C. McQuiston, J. D. Parker, and J. D. Spitler, *Heating, Ventilating, and Air Conditioning*, 6th ed. John Wiley & Sons, Inc, 2005.

[49] R. S. Figiola and D. E. Beasley, *Theory and Design for Mechanical Measurements*, Fifth. John Wiley & Sons, Inc, 2011.

[50] C. Baldwin, “Design and Construction of an Experimental Apparatus to Assess the Performance of a Solar Absorption Chiller with Integrated Thermal Storage,” Carleton University, 2013.

[51] National Instruments, “NI 9214 and TB-9214 Datasheet,” 2016. [Online]. Available: http://www.ni.com/pdf/manuals/375138a_02.pdf. [Accessed: 07-Oct-2019].

[52] University of Wisconsin-Madison. Solar Energy Laboratory, “TRNSYS, a Transient Simulation Program.” The Laboratory, Madison, Wis, 1975.

[53] Fraunhofer, “Report of measurement on the basis of EN 12975-1,2:2006,” Freiburg, Germany, 2012.

[54] C. Baldwin and C. A. Cruickshank, “Assessing the Potential for Reduction in Peak Residential Electrical Loads Using a Heat Pump and Thermal Storage Systems,” in *International High Performance Buildings Conference* , 2016.

[55] K. Seyboth *et al.*, “IPCC Renewable Energy Sources and Climate Change Mitigation,” New York, NY, 2012.

[56] NEB, “Provincial and Territorial Energy Profiles,” 2019. [Online]. Available: https://www.cer-rec.gc.ca/nrg/ntgrtd/mrkt/nrgsstmprfls/index-eng.html. [Accessed: 25-Nov-2019].

[57] R. Yokoyama, T. Shimizu, K. Ito, and K. Takemura, “Influence of ambient temperatures on performance of a CO2 heat pump water heating system,” *Energy*, 2007.

[58] Alberta Utilities Commission, “Residential regulated rate option at a glance,” 2019. [Online]. Available: http://www.auc.ab.ca/Pages/current-rates-electric.aspx. [Accessed: 08-Oct-2019].

[59] Gas Alberta Inc, “Gas Rates in Alberta.” [Online]. Available: https://www.gasalberta.com/gas-market/gas-rates-in-alberta. [Accessed: 30-Apr-2019].

[60] BC Hydro, “Residential Rates,” 2019. [Online]. Available: https://app.bchydro.com/accounts-billing/rates-energy-use/electricity-rates/residential-rates.html. [Accessed: 08-Oct-2019].

[61] Fortis BC, “Natural gas rates - residential.” [Online]. Available: https://www.fortisbc.com/accounts-billing/billing-rates/natural-gas-rates/residential-rates. [Accessed: 24-Oct-2019].

[62] Manitoba Hydro, “Residential rates,” 2019. [Online]. Available: https://www.hydro.mb.ca/accounts_and_services/rates/residential_rates/. [Accessed: 08-Oct-2019].

[63] NB Power, “NB Power Rate Schedules and Policies,” 2018. [Online]. Available: https://www.nbpower.com/media/827983/rsp-manual-1-august-2018.pdf. [Accessed: 08-Oct-2019].

[64] Liberty Utilities, “Gas Supply Price Update,” 2019. [Online]. Available: https://naturalgasnb.com/en/for-home/accounts-billing/gas-price-update/. [Accessed: 30-Apr-2019].

[65] Newfoundland and Labrador Hydro, “Current Rates | Newfoundland & Labrador Hydro,” 2019. [Online]. Available: https://nlhydro.com/electricity-rates/current-rates/. [Accessed: 08-Oct-2019].

[66] Northwest Territories Power Corporation, “Residential Electrical Rates,” 2019. [Online]. Available: https://www.ntpc.com/customer-service/residential-service/what-is-my-power-rate. [Accessed: 08-Oct-2019].

[67] Nova Scotia Power, “Time-of-Day Rates | Nova Scotia Power,” 2019. [Online]. Available: https://www.nspower.ca/en/home/for-my-home/heating-solutions/electric-thermal-storage/tod-rates/default.aspx. [Accessed: 08-Oct-2019].

[68] Efficiency Nova Scotia, “Heating Comparisons .” [Online]. Available: https://www.efficiencyns.ca/guide/heating-comparisons/. [Accessed: 24-Oct-2019].

[69] Qulliq Energy Corporation, “Customer Rates | Qulliq Energy Corporation,” 2019. [Online]. Available: https://www.qec.nu.ca/customer-care/accounts-and-billing/customer-rates. [Accessed: 08-Oct-2019].

[70] Ontario Energy Board, “Electricity rates | Ontario Energy Board,” 2019. [Online]. Available: https://www.oeb.ca/rates-and-your-bill/electricity-rates. [Accessed: 08-Oct-2019].

[71] Union Gas, “Southern Ontario Residential Rates,” 2019. [Online]. Available: https://www.uniongas.com/residential/rates/current-rates/rate-m1. [Accessed: 24-Oct-2019].

[72] Maritime Electric, “Maritime Electric - Rates and General Rules and Regulations,” 2018. [Online]. Available: https://www.maritimeelectric.com/about-us/regulatory/rates-and-general-rules-and-regulations/. [Accessed: 08-Oct-2019].

[73] Hydro Quebec, “Rate D | Hydro-Québec,” 2019. [Online]. Available: http://www.hydroquebec.com/residential/customer-space/rates/rate-d.html. [Accessed: 08-Oct-2019].

[74] Energir, “Price of Natural Gas,” 2019. [Online]. Available: https://www.energir.com/en/business/price/natural-gas-price/. [Accessed: 30-Apr-2019].

[75] “Explaining Your Saskatchewan Electricity & Natural Gas Rates - EnergyRates.ca,” 2019. [Online]. Available: https://energyrates.ca/saskatchewan/explaining-your-saskatchewan-electricity-natural-gas-rates/. [Accessed: 08-Oct-2019].

[76] The Yukon Electrical Company Limited, “Yukon Electrical Company Limited & Yukon Energy,” 2011.

[77] National Energy Board, “What is in a Canadian residential natural gas bill?,” 2019. [Online]. Available: https://www.cer-rec.gc.ca/ l. [Accessed: 24-Oct-2019].

[78] Enbridge Gas, “Federal Carbon Charge.” [Online]. Available: https://www.enbridgegas.com/Natural-Gas-and-the-Environment/Enbridge-A-Green-Future/Federal-Carbon-Pricing-Program. [Accessed: 30-Apr-2019].

[79] Bank of Canada, “Monthly Exchange Rates,” 2019. [Online]. Available: https://www.bankofcanada.ca/rates/exchange/monthly-exchange-rates/. [Accessed: 17-Oct-2019].

[80] “Historic inflation Canada,” 2019. [Online]. Available: https://www.inflation.eu/inflation-rates/canada/historic-inflation/cpi-inflation-canada.aspx. [Accessed: 17-Oct-2019].

[81] C. Weisflogg, “Solar panel pricing information.” Personal Communication, 2019.

[82] T. Wong and J. Leber, “Analysis of Various Water Heating Systems,” California, 1996.

[83] A. S. Rushing, J. D. Kneifel, and P. Lavappa, “Energy Price Indices and Discount Factors for Life-Cycle Cost Analysis - 2014,” 2014.

[84] Treasury Board of Canada Secretariat, *Canadian Cost-Benefit Analysis Guide Regulatory Proposals*. 2007.

[85] P. Bagnoli, C. Matier, and M. Askari, “The Impact of a Pan-Canadian Carbon Pricing Levy on PBO’s GDP Projection,” Ottawa, Canada, 2018.

[86] J. Purdy and I. Beausoleil-Morrison, “The significant factors in modelling residential buildings,” in *Seventh International IBPSA Conference*, 2001, pp. 207–214.

[87] US DOC, “United States Census Bureau,” 2019. [Online]. Available: https://data.census.gov/. [Accessed: 26-Nov-2019].

[88] “Population and Dwelling Count Highlight Tables, 2016 Census – Population centres.” [Online]. Available: https://www12.statcan.gc.ca. [Accessed: 26-Nov-2019].

[89] US EIA, “Electric Power Sector Consumption Estimates,” 2017. .

[90] US EIA, “Electric Power Monthly,” 2019. [Online]. Available: https://www.eia.gov/electricity/monthly/current_month/epm.pdf. [Accessed: 08-Oct-2019].

[91] US EIA, “Natural Gas Prices,” 2019. [Online]. Available: https://www.eia.gov/dnav/ng/ng_pri_sum_a_EPG0_PRS_DMcf_m.htm. [Accessed: 21-Nov-2019].

Appendix A: HPWH Performance Map

The experimental performance map included compressor power, heat rejection to the water tank, total air cooling capacity, and sensible air cooling capacity shown in Table A. 1 through Table A. 4, respectively. These were used in an external file that was read in by the HPWH in using TRNSYS. Using the performance map, the modelled HPWH closely followed the behavior of the experimental system.

Table A. 1: Compressor power for performance map (W)

Relative Humidity (%)	Inlet Air Temperature (°C)	Water Temperature (°C)						
		10	20	30	40	50	60	70
20	10	358.8	364.0	379.3	394.5	409.7	414.9	420.1
	20	270.0	311.5	351.8	409.1	458.2	555.0	651.8
	30	356.0	400.7	455.5	500.3	555.1	609.8	664.6
	40	360.0	450.0	540.0	630.0	774.0	822.9	871.7
30	10	348.6	361.2	373.8	396.3	418.9	431.5	444.1
	20	270.0	311.5	351.8	409.1	458.2	555.0	651.8
	30	507.6	549.2	580.8	622.4	664.0	675.6	687.2
	40	320.8	446.9	599.5	612.9	776.0	825.9	875.8

Table A. 2: Heat rejection for performance map (W)

Relative Humidity (%)	Inlet Air Temperature (°C)	Water Temperature (°C)						
		10	20	30	40	50	60	70
20	10	1314.9	1299.5	1244.2	1198.8	1153.4	1088.1	1022.7
	20	1629.7	1536.1	1442.5	1348.9	1255.3	1161.7	1068.1
	30	2324.8	2175.1	2025.5	1975.8	1826.1	1776.4	1726.8
	40	2306.6	2206.4	2106.2	2006.0	1905.8	1805.6	1705.4
30	10	1340.4	1292.7	1247.0	1190.3	1153.6	1056.9	960.2
	20	1583.9	1494.5	1405.1	1315.7	1226.3	1136.9	1047.5
	30	2165.5	2043.1	1920.8	1998.5	1876.1	1753.8	1631.5
	40	2782.1	2666.1	2550.1	2343.1	2318.1	2202.1	2086.1

Table A. 3: Total cooling capacity for performance map (W)

Relative Humidity (%)	Inlet Air Temperature (°C)	Water Temperature (°C)						
		10	20	30	40	50	60	70
20	10	569.6	674.0	632.8	590.6	548.5	506.4	464.3
	20	565.9	701.5	818.3	917.1	870.8	884.1	897.5
	30	668.0	852.0	877.2	913.3	930.9	959.2	987.6
	40	1399.4	1500.8	1653.0	1551.6	1450.1	1348.6	1247.2
30	10	671.9	637.0	689.4	654.4	619.5	584.5	549.5
	20	598.0	712.6	824.3	934.0	884.8	883.2	881.6
	30	668.3	833.4	905.5	930.2	948.6	964.5	980.5
	40	1654.5	1836.8	2015.1	2159.4	1997.4	1627.1	1256.7

Table A. 4: Sensible cooling capacity for performance map (W)

Relative Humidity (%)	Inlet Air Temperature (°C)	Water Temperature (°C)						
		10	20	30	40	50	60	70
20	10	776.0	722.0	702.8	660.6	576.4	534.3	492.2
	20	2380.8	2296.5	2212.3	2128.0	1877.0	1299.4	721.7
	30	2619.6	2980.8	3050.5	3133.5	3013.1	3091.1	3169.1
	40	2349.6	2377.8	2415.4	2509.3	2353.5	2179.1	2004.6
30	10	776.0	722.0	702.8	660.6	576.4	534.3	492.2
	20	2127.9	2334.1	2465.7	2425.7	2418.7	2031.2	1643.6
	30	2619.6	2980.8	3050.5	3133.5	3013.1	3091.1	3169.1
	40	2516.9	2607.6	2743.8	2653.0	2562.3	2471.5	2380.7

Appendix B: TRNSYS project image

The TRNSYS projects used within this study all used the same subroutines to model the HPWHs and SAHPWHs. A sample of the TRNSYS project used for the HPWH is shown in Figure B. 1. A full description of the subroutines that were used within the project is provided in Chapter 4.

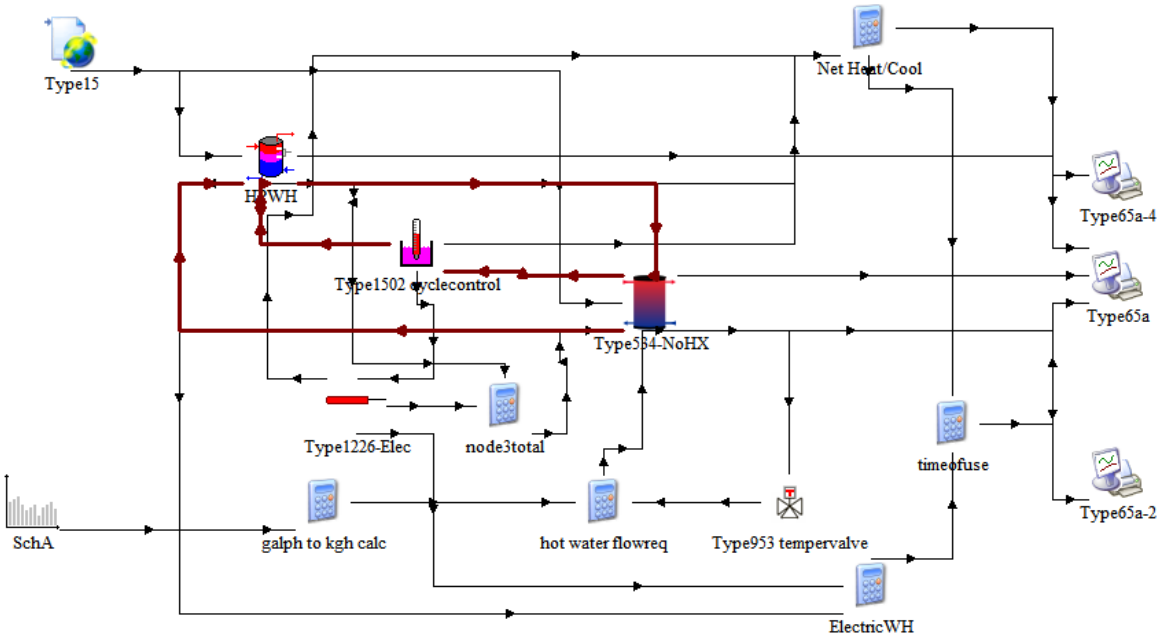

Figure B. 1: TRNSYS project used for HPWH modelling

Appendix C: American utility rates and electricity grid emissions

The importance of the electricity rates and GHGs values used for this study were stressed within Chapter 6, so it is important to note the numbers used for the GHG and economic analysis. To calculate the GHG intensity values, the breakdown of electricity generation fuels was obtained from the US Energy Information Administration [89], and the GHG intensity calculation methodology from Chapter 4 was followed. The GHG intensity values for each location are shown in Table C. 1.

Table C. 1: GHG intensity of electricity grids in American locations

Location	GHG Intensity (gCO2e/kWh)
Arizona	439.43
California	184.02
Colorado	710.41
Florida	490.99
Illinois	365.04
Minnesota	461.03
Montana	565.66
New York	172.35
North Carolina	410.59
Pennsylvania	385.78
Tennessee	429.16
Texas	541.82
Washington	100.46

The utility rates used for the analysis were obtained from the US Energy Information Administration. The electricity rates [90] and natural gas rates [91] are shown in Table C. 2. Average electricity rate values, rather than on- and off-peak values were used for the United States after the analysis in Chapter 4 which showed little difference between

average and peak methods. Additionally, in many American locations, electricity is privatized, so using average values provided by the US IEA gives an average over the state of all providers rather than selecting one arbitrary provider to use in each location.

Table C. 2: Utility rates in American locations

Location	Electricity Rate ($/kWh)	Natural Gas Rate ($/kWh)
Arizona	0.1235	0.0402
California	0.193	0.0463
Colorado	0.121	0.0259
Florida	0.1184	0.0626
Illinois	0.01281	0.0248
Minnesota	0.01291	0.028
Montana	0.1078	0.0225
New York	0.1686	0.0396
North Carolina	0.1141	0.0432
Pennsylvania	0.1363	0.0363
Tennessee	0.1082	0.0289
Texas	0.1167	0.0285
Washington	0.0946	0.0288

Appendix D: Time of use GHGs compared to annually averaged GHGs

A comparison was made for Toronto, ON between using the total electricity generation on an annual basis and by considering the variations in GHG intensity between seasons and on-, mid-, and off-peak times of day. The Independent Electricity Systems Operator (IESO) publishes hourly data on the emissions intensity of the Ontario electricity grid, which was plotted by Baldwin and Cruickshank [54] to calculate the intensity values based on the time of use electricity billing periods for 2015, as shown in Table D. 1. The greatest difference occurred between off-peak winter and on-peak summer, and there was a 38% difference in GHG intensity between these times.

Table D. 1: Time of use GHG intensity ($kgCO_2e$ /MWh)

	Off-Peak	**Mid-Peak**	**On-Peak**
Summer	54.9	70.5	76.0
Winter	51.8	59.9	60.2

The GHGs for a HPWH were determined throughout the year using the time of use method and an annual average GHG value (60.02 $kgCO_2e$ /MWh) for 2015. It was found that the GHG reduction using the annual averaged GHG intensity and time-of-use GHG intensity resulted in 2% difference for the HPWH operation. The low difference in averaged GHG offset and time-of-use GHG offset occurs because HPWH operation is relatively uniform throughout the seasons and on- and off-peak times. For this reason, and because the HPWH was not analyzed for reducing peak consumption in this study, the annual averaged GHG intensity values were used for other locations.

Appendix E: Sensitivity study of payback period

The PBP was studied in a sensitivity analysis to determine the impact of the dependent parameters on the calculation. The EWH capital cost, space cooling COP, and space heating system parameters were varied to determine their average impact on the PBP for the HPWH and the SAHPWH across the climate zones. The values studied as well as the base case value are shown in Table E. 1.

Table E. 1: Sensitivity analysis of PBP parameters

Parameter	Base Case Value	Sensitivity Value	Average Effect on SAHPWH PBP	Average Effect on HPWH PBP
Capital Cost EWH (CAD)	415.06	629.76	-4.1%	-14.4%
Space Cooling COP	3.5	3	-2.1%	-5.0%
Space Cooling COP	3.5	4	2.4%	3.9%
Space Heating EF and Fuel Type	1, electric	2, electric	4.7%	-28.0%
Space Heating EF and Fuel Type	1, electric	0.67 natural gas	4.4%	-27.1%
Space Heating EF and Fuel Type	1, electric	0.67, natural gas*	3.4%	-23.3%

*with a 20% natural gas fuel cost increase

The analysis of PBP variation shows that HPWH was more sensitive than SAHPWH to all dependent parameters. This is due to the higher capital and installation costs of the SAHPWH as opposed to the HPWH which dominated the PBP calculation.

The analysis shows that both HPWH and SAHPWH had a decreased PBP when the space cooling COP decreased and an increased PBP for a higher space cooling COP. The base space cooling COP value of 3.5 indicates that 3.5 times more energy was delivered than

input, whereas a COP of three indicates that three times more energy was delivered than input. This means that for lower COP values, more electricity and therefore more cost was required to provide the same space cooling, thus the space cooling offset provided by the HPWH had a higher cost value for a lower COP.

When the space heating system was changed to a lower cost system than the electric base case, such as a heat pump with an energy factor of two or to a natural gas system, similar trends occurred. Both the electric heating system and the natural gas heating system would have lower annual space heating costs than an electric system with an EF of one. For the HPWH alone, which caused an increase in space heating, cheaper heating costs mean that the impact of the HPWH had a lower cost impact on space heating and thus the PBP decreased. The opposite occurred for the SAHPWH; because the SAHPWH caused a net decrease in space heating costs, the value of the space heating offset due to the SAHPWH was greater when the efficiency of the system was lower. Increasing the efficiency of the system decreased the overall operating cost and thus the value of the space heating benefit from the SAHPWH. The trends for space conditioning system efficiency for the SAHPWH and HPWH are shown in Table E. 2.

Table E. 2: Space conditioning systems that minimize HPWH and SAHPWH payback periods

		Space Heating System	
		Efficient	**Inefficient**
Space Cooling System	**Efficient**	Max SAHPWH PBP	Max HPWH PBP
	Inefficient	Min HPWH PBP	Min SAHPWH PBP

The trends from the sensitivity analysis show that more efficient space conditioning systems reduced PBP when negative space cooling externalities occurred, while more efficient space conditioning systems increased PBP when positive externalities occurred. Thus, for the HPWH alone, PBP was reduced for less efficient space cooling systems and more efficient space heating systems, while for SAHPWHs, PBP was reduced for less efficient space heating and cooling systems.